Encapsulation of desmopressin into hydrophobic nanoparticles and hydrophilic microparticles for pulmonary drug delivery

Dissertation

zur

Erlangung des Doktorgrades

der Naturwissenschaften

(Dr. rer. nat.)

dem

Fachbereich Pharmazie der

Philipps-Universität Marburg

vorgelegt von

Daniel Andreas Addi Primaveßy

aus **Mainz**

Marburg/Lahn **Jahr 2017**

Erstgutachter: **Professor Dr. Marc Schneider**

Zweitgutachter: **Professor Dr. Udo Bakowsky**

Eingereicht am **28.03.2017**

Tag der mündlichen Prüfung am **19.05.2017**

Hochschulkennziffer: 1180

ERKLÄRUNG

Ich versichere, dass ich meine Dissertation

„Encapsulation of desmopressin into hydrophobic nanoparticles and hydrophilic microparticles for pulmonary drug delivery“

selbständig ohne unerlaubte Hilfe angefertigt und mich dabei keiner anderen als der von mir ausdrücklich bezeichneten Quellen bedient habe. Alle vollständig oder sinngemäß übernommenen sind Zitate als solche gekennzeichnet.

Die Dissertation wurde in der jetzigen oder einer ähnlichen Form noch bei keiner anderen Hochschule eingereicht und hat noch keinen sonstigen Prüfungszwecken gedient.

Marburg, den 28.03.2017

.....

(Unterschrift mit Vor- und Zuname)

Akademische Danksagung

Bedanken möchte ich mich insbesondere bei meinem Doktorvater Prof. Dr. Marc Schneider, der mir nicht nur die Möglichkeit zur Promotion gegeben hat, sondern sich auch sehr viel Zeit genommen hat, um mich bei Versuchen, Planungen, dem Schreiben von Anträgen, Abstracts und der Dissertation zu unterstützen. Auch bedanken möchte ich mich bei ihm für das große Maß an Freiheit, das er mir beim Entwickeln und Ausprobieren von eigenen Ideen gewährt hat.

Des Weiteren möchte ich mich bei meinem Zweitkorrektor Prof. Dr. Udo Bakowsky für die Übernahme der Zweitkorrektur, die freundlichen Unterhaltungen nach seinen Vorlesungen, die reibungslose Zusammenarbeit und die gute Stimmung im Institut bedanken.

Bei Prof. Dr. Gerhard Wenz möchte ich mich dafür bedanken, dass er gleich zweimal bereit war, mein wissenschaftlicher Begleiter zu werden, obwohl die Universität beim zweiten Mal in Marburg ein gutes Stück von seinem Dienstort, der Universität des Saarlandes, entfernt lag.

Neben den rein akademischen Personen ist noch die Firma Evonik Industries zu nennen, deren Zusammenarbeit ich es verdanke, diese Promotion anfertigen zu können. Hier sticht insbesondere Dr. Silko Grimm heraus, der uns stets unterstützt hat und der auf sehr freundliche Art und Weise für uns zum Gesicht seiner Firma wurde. Nicht vergessen möchte ich aber auch Dr. Rosario Lizio und Dr. Jessica Müller-Albers, die für die Projektleitung bei Evonik zuständig waren.

Ferner möchte ich mich auch bei allen weiteren Mitgliedern des PeTrA-Konsortiums bedanken, für ihre Anstrengungen, das sehr große Konsortium zu führen, um eine sinnvolle Durchführung zu ermöglichen, und für ihre Arbeit am Projekt.

Ich danke all denen, die mir bei der Erstellung dieser Dissertation mit Rat und Tat zur Seite standen, insbesondere sind zu nennen: Frau Dr. Sarah Barthold, Herr Michael Möhwald und Frau Johanna Wawrzik.

Auch den anderen Doktoranden im PeTrA-Projekt, insbesondere Marius Hittinger, René Rietscher, Rike Wallbrecher und Andreas Kirchner, möchte ich für ihre Zusammenarbeit und die gemeinsame Zeit danken.

Persönliche Danksagung

Persönlich möchte ich mich zuallererst bei meinen Eltern bedanken, denn ohne ihre fortwährende Unterstützung von Kindheit an wäre nichts von alledem hier zustande gekommen. Meine Eltern haben meine wissenschaftliche Neugier geweckt (auch wenn Bücher mit ausziehbaren Vulkanen thematisch nicht in der Pharmazie verortet sind). Sie haben mich damit bereits in der Grundschule unterstützt. Sie haben mich in den eher schwierigen Phasen der Jugendzeit unterstützt, und schlussendlich haben sie mir mein Studium finanziert und damit diese wissenschaftliche Arbeit möglich gemacht: Vielen Dank!

Ich möchte mich des Weiteren auch bei meinen Kollegen bedanken, insbesondere bei meinen direkten Kollegen am Lehrstuhl, die mir über die Zeit hinweg auch zu Freunden wurden, sowie auch bei den Kollegen der Lehrstühle Lehr und Bakowsky für die gute Zusammenarbeit und ein freundschaftliches Verhältnis (die Professoren eingeschlossen).

Diese Arbeit konnte ich schreiben dank derer, die mich Dinge gelehrt haben. Sie sollte, auch wenn sie letztlich mein Werk ist, als das gesehen werden, was sie ist: Eine Erweiterung unseres Wissensschatzes als Gesellschaft durch die Anstrengungen Vieler. Daher möchte ich allen, die mich gelehrt haben, dafür danken. Danke!

Noch schlimmer? Was kann denn noch schlimmer sein? Hä?

Jehova, Jehova, Jehova…

- Monty Pythons „Das Leben des Brian“

1 Introduction

1.1 Drug Delivery

Drug Delivery, i.e. bringing a drug to its site of action, is a core discipline of pharmaceutical technology. The drug has to be delivered from the outside of the body to the blood stream and from there to its target site.

In principle, two different types of application exist: *Local application* in which the drug is directly applied to the site of action, like zinc paste to an area of sore skin, and *systemic application* in which the drug is distributed throughout the whole body, as for example in case of painkillers. The main difference between both ways of application is that in the latter way the drug passes the blood stream as systemic compartment before reaching its target. There are other compartments, like the lymphatic system, [1, 2] that are also aspects of systemic drug delivery, but for matters of simplicity these are not considered in this context.

If possible, local delivery is favored, as only the site of action is exposed to the drug and thus side effects are diminished; however, in many cases the site of action is not easily accessible so that systemic delivery is the only option. In most cases, systemic delivery is realized by oral delivery of tablets and capsules, being the most convenient way. The parenteral route of application, though of invasive character, also shows its advantage as the drug is directly applied to the blood stream with no biological barrier that has to be crossed. In rare cases, rectal (*e.g.* paracetamol suppositories) and pulmonary (*e.g.* inhalable insulin and dihydroergotamine mesylate[3]) applications are also possible. These cases usually have the problem that patient compliance is rather bad. For rectal application, many people feel uneasy with the application itself. In case of the pulmonary medicines, the inhalation process is demanding, such that patients fail to deliver the drug into their lungs. Often, most of it is deposited in the throat or the upper bronchus instead of the alveolus. However, both have an important advantage over oral application as there is no first pass effect and thus drug concentrations applied can be lower. For the lungs: despite having several clearance mechanisms such as alveolar macrophages and efflux drug resistance proteins, there is no restrain to a quick uptake of drugs into the blood.[4] For systemic drug delivery, the oral route of application is usually the option of choice. In contrast to the parenteral application, formulating and storing the medicinal product is rather easy and economical. Furthermore, it can easily be applied by the patient himself and thus shows a good compliance. Therefore, only drugs that cannot be administered orally are usually available as parenteral medicines. Whether a drug can be administered orally or not, depends on its physical and chemical properties: mainly on solubility in water and permeability through cell membranes. Therefore, it is common to classify drugs by these two characteristics, according to the BCS (Biopharmaceutical Classification System)). The (four) classes of the BCS roughly indicate how hard or easy it is to deliver

drugs orally. While for BCS class I drugs it is sufficient to bring the drug just to the intestine (high solubility and high permeability), it is different for the classes II (high permeability, low solubility), III (low permeability, high solubility), or even class IV where both parameters are low.

The problem with drug delivery systems for parenteral application is that they have to be produced and kept sterile and that they have to be applied by trained personnel, which makes them very expensive. Furthermore, parenteral applications are mostly injections and infusions. Since a dislike of needles is quite common among the population, parenteral application is minimized to absolutely necessary applications.

In recent years, biological drugs (biologicals), like DNA-, RNA-, peptide-, or protein-based drugs, started to play a major role in therapy. Thanks to recent progress in biotechnology, many different biologicals are now available in therapeutic quantities.[5-7] The disadvantage of biologicals is that they are, in contrast to simple chemical compounds, comparatively large and susceptible to degradation. The size of the molecule greatly reduces the permeation through cell membranes.[8] Furthermore, these biological molecules are by default objects of operation to biological lifeforms, therefore the body has countermeasures to defend itself against those molecules coming from the outside. Especially deoxyribonucleases and ribonucleases are widely spread in the body and disintegrate DNA[9] and RNA[10] rapidly. Proteases exist in the gastric intestinal tract, not only with the function of countermeasure but mainly as enzymes for digestion of food proteins. It is an unfortunate but evolutionary expectable coincidence that the easiest route of administration is blocked for this kind of drugs. In order to provide them as drugs, an advanced technological approach is necessary.

The position of micro- and nanoparticles in pharmaceutical technology

The conservative dosage forms of pharmaceutical technology, like tablets, capsules, creams and powders, have been sufficient to provide patients with functional medicines for a long time; however, the newer biological therapeutic agents are not only more powerful, but they also are more demanding in terms of storage and delivery; therefore, new dosage forms had to be identified. Microparticles and subsequently nanoparticles including liposomes were the answer to that problem.[11] This seems reasonable, as very small structures can be equipped with all necessary properties for being delivered right to the spot.[12-14] Core requirements of this delivery system is the protection of the active pharmaceutical ingredient (API), delivery over biological barriers to the site of action and proper release (kinetics) from the particle. To meet all these requirements is not an easy task, and thus for every API an own dosage form has to be constructed, specifically tailored to its needs.

1.2 Polymeric particle preparation

There are numerous ways of preparing polymeric particles for pharmaceutical application. In general, all polymeric particles can be divided into two different groups: particles made of hydrophilic polymers and particles made of hydrophobic polymers. For most applications, hydrophobic particles are used as their preparation is rather simple, but many new drugs (including biologicals) are hydrophilic and the encapsulation of the compounds into hydrophobic polymers is difficult, such that hydrophilic particles are favored for this kind of application.

1.2.1 Preparation of hydrophobic PLGA particles

One of the mostly used substances for preparing hydrophobic particles is PLGA (Polylactic-co-glycolic acid). It is a co-polymer made of lactic acid and glycolic acid monomers and thus similar to poly lactic acid and poly glycolic acid. As lactic acid is more hydrophobic than glycolic acid, it is assumed that the hydrophobicity of the PLGA polymer can be adjusted by the ratio of the two monomers along with its swelling and degradation behaviors.[15, 16] It is biocompatible and biodegradable, as it is turned into lactic acid and glycolic acid monomers by hydrolysis.[17, 18] Lactic acid is further degraded to water and carbon dioxide [19] and glycolic acid is mainly metabolized to oxalate in the liver, as experiments by Brady and Farinelli in rats indicated.[20] Furthermore, there exist [21] FDA and EMA approved implants made of PLGA, and therefore PLGA is a suitable candidate for particle preparation.

The two most common ways of preparing PLGA nanoparticles (and microparticles) are the emulsion method [22-29] or the precipitation method.[30-33] For the latter one, PLGA is dissolved in an organic solvent that is miscible with water such as acetone. The solution is then dropped or injected into stirred water. The acetone directly mixes with water, so that PLGA, unable to mix with water, precipitates as nanoparticles. For matters of drug encapsulation, the drug can be dissolved in the organic solvent together with the PLGA and should then, during particle formation, be encapsulated. These methods work especially well for rather hydrophobic drugs. Hydrophilic drugs are more difficult to encapsulate as they have more attraction to the aqueous phase.[32] For the emulsion method, PLGA is dissolved in an organic solvent that is partially miscible with water. An emulsion is formed with the organic solvent, with PLGA being in the inner phase. By increasing the water volume beyond the miscibility border of the two partially miscible solvents, the organic solvent mixes with water and PLGA precipitates as it cannot mix with water. Thus, nanoparticles are formed. In case of hydrophilic drugs, often double emulsion methods are used. Double emulsion techniques work well for microparticles, as nanodroplets can be incorporated into the microparticles.[34] This method is used as well for nanodroplets in nanoparticles;[35-37] however, it has not yet been demonstrated, that there are smaller

nanodroplets in nanoparticles. Other options include surface coatings of the nanoparticles or the use of stabilizers that increase the amount of drug inside the nanoparticles.[22, 38]

Surface modifications of PLGA nanoparticles for the purpose of functionalization are a common topic in pharmaceutical research. Usually three different purposes of surface modification exist: targeting, release modification and bioavailability (see also section 1.3.3). In case of surface modification, for example antibody coatings can be used to target nanoparticles to cancer cells.[39] In case of modifying release kinetics, often polymers are used to surface-coat particles layer-by-layer wise.[40-42] For enhancing bioavailability, for example penetration enhancers [43] can be used as coating material,[44] as it will be shown for PLGA in this thesis.

PLGA nanoparticles can be characterized in many ways. The most common characterization methods are size measurement by Dynamic Light Scattering (DLS) methods, but in some cases Nanoparticle Tracking Analysis (NTA) is used as well. The NTA usually has a better resolution, especially in case of multimodal distributions, but its preparation is less simple.[45] Zeta potential of particles is usually measured by Laser-Doppler Velocimetry (LDV). While zeta potentials are usually negative because of the carboxylic end group of commonly used PLGA types, the size of particles usually differs. Common sizes of PLGA nanoparticles are going down to 100 nm. The sizes usually depend on different parameters, such as the stabilizers used, the concentration of PLGA in the organic solvent during the preparation and the size of the emulsion that is prepared in case of a preparation by emulsion-based methods.

1.2.2 Preparation of hydrophilic dextran particles

Hydrophilic particles

Preparing hydrophilic particles is usually a much greater challenge than preparing hydrophobic particles, due to the hydrophilic nature of our environment. Prepared particles have to be kept and stored dry during the whole process of preparation and afterwards. Even air humidity can be a problematic factor as some substances are hygroscopic. The smaller the particles are, the higher is the surface to mass ration and thus hygroscopic effects are stronger.

For that reason, hydrophilic particles are often prepared as gels. The forces of the gel structure keep the particles in shape, despite the influence of surrounding water. Both, covalent [46] and non-covalent gels, are utilized for stabilization. Among the covalently bound gels, gelatin is a prominent example.[47] Due to its protein nature, gelatin particles can be crosslinked with for example glutaraldehyde to form stable particles. That also illustrates a drawback of covalent gels: peptide and protein drugs tend to be crosslinked with the polymer mesh rendering them non-functional. Non-covalent gels have less

problems with that issue. But as they are usually held together by ionic forces, they are also less stable, because the ionic bonds in water are weaker by one power of 10, compared to covalent bonds.[48] Another way to reduce the affection by water is the use of larger molecular weight polymers; however, that is not always possible as the molecular weight usually changes the viscosity, and thus the whole process of particle preparation can be affected.

Dextran and Dextran particles

Dextran is a polymer based on glucose monomers, which are connected via α-1,6 and α-1,4 connections. The dissolution of the polymer in water depends very much on its average molecular weight, but even polymers of around 40 kDa can easily be dissolved to an extent of a > 50% (m/v) solution in water.[49] Due to that strong hydrophilicity, lower molecular weight dextrans tend to be strongly hygroscopic. Dextran is non-toxic, biocompatible and biodegradable, and is FDA approved for parenteral use, for example as blood plasma expander.[50-53]

Dextrans have no groups or structures that work well for forming non-covalent gels in contrast to, for example, alginates. Many preparations of dextran particles in literature therefore use chemically modified dextran variants.[54-56] One exception to that is the gelation of dextran with potassium ions. Six hydroxyl groups of dextran can form a pocket that is usually occupied by a water molecule; however, in the presence of potassium ions the ion moves into the pocket and binds the slightly negative charge of the dipols of the hydroxyl groups to its positive charge. The effect only works with potassium, as sodium ions are too small in size, whereas e.g. rubidium ions are too large. The gels ~~that are~~ produced in that way are rather strong and inflexible, but large amounts of potassium (around 3 mol/L) are necessary, rendering them unusable for parenteral applications, as potassium ions are toxic in that concentration.[57, 58]

Examples for dextran particles exist in great number: Particles for delivery of substances like doxorubicin and cobalamin have been shown.[59, 60] Combined approaches of magnetic iron oxide and dextran nanoparticles also exist; however, here dextran is usually more used as a coating for the iron oxide nanoparticles.[61-63] In some cases, dextran microparticles are formed as gel particles, therefore modified dextrans are used. If they are smaller in size, they are often called “nanogels” in literature.[64-67]

1.3 Biologicals – Structure and setting

1.3.1 Biomolecules

The delivery of biologicals can be much more complicated, compared to the delivery of small molecule drugs. Biologicals are in most cases polymeric or at least oligomeric structures. In case of DNA and RNA they are chains of nucleosides connected with each other at their 3' or 5' end of their ribose sugar by a phosphate group. DNA and RNA are chemically very stable against heat and pH change – double strands may disconnect but will reconnect again quickly, once the conditions return to normal state, as for example in case of polymerase chain reaction. However, the human body has a lot of enzymes that cut and degrade DNA and especially RNA, serving as countermeasures against infectious organisms.[10, 68, 69] Asides from DNA and RNA, peptides and proteins are functional biomolecules used for therapeutic purposes. Proteins/peptides are chains of amino acids, which are joined by their amino and carboxyl group. Each amino acid has one out of 21 (in case of the human body) side chains at their central carbon atom. These chains fold in certain ways and thus form an active protein. Proteins can have many different functions, like catalysis (in case of enzymes), transport, signaling, structure building, storage and many more.[70] The formation of a protein depends on its primary structure (i.e. the sequence of different amino acids), as the molecule folds into its energetically most favorable position. As proteins can be very long, – more than 2000 residues are possible – the correct folding does not always occur by its own and there are biological mechanisms to help those proteins to fold properly. Proteins thus fold into secondary structures and super secondary structures which are a small set of structures of the primary chain. Secondary structures usually form between non-interchangeable groups of amino acids, such that the residue groups only have a limited, mostly sterical influence on the structure. In contrast to that, the tertiary structure is mainly shaped by the properties of the residue groups of the amino acids, like their sterical behavior but also their electrostatic properties and hydrophobic domains. More than that, such folded proteins can attach to each other forming a quaternary structure. The way these structures form, especially the tertiary structure, indicate that they are very sensitive to changes in temperature and pH as these factors may change the energetic balance which is responsible for their structure. A once deformed protein may not be able to fold itself back into its original confirmation, and thus loses its ability to pursue its task. While the beforehand mentioned DNA and RNA are very stable in this case, proteins are not. On the other hand, while degrading enzymes for DNA and RNA are found in many fluids and on the skin of the human body [9, 68, 71], proteases can mainly be found in the stomach and the intestine. Except for the case of oral application, these do not play a significant role for drug delivery. Peptides are like very short proteins. They have rarely secondary structures and their tertiary structures are usually limited to disulfide bonds, if any. While peptides are still sensitive molecules that can be degraded easily, they

are more stable to changes in temperature and pH than proteins, and in the human body there are not as many enzymes degrading them as for DNA and RNA.

1.3.2 Pharmaceutical use of biologicals

Conventional medicines rely on small molecule drugs that alter the body's chemistry. This usually happens, when for example the molecule docks to a receptor or concentrations of the molecule cause changes in the metabolic pathways. This way of treatment is often actually an intoxication, which has a positive side effect on recovery of the patient, and in best case it does not have other negative side effects. Some biologicals, on the other hand, can work in a different way. Many of the used peptides are hormones or signaling entities that do not intoxicate the body but replace the body's own substances that are missing due to a disease (e.g. insulin). If RNA is used as a biological medicine, they often have similar purposes as the peptides. Proteins again work on higher order: As proteins are the actors of the metabolism, by introducing them into an organism it is possible to directly execute certain reactions. This can be beneficial for genetic diseases, where certain proteins are missing or underexpressed. DNA again works on a higher order than proteins do, as the DNA/gene delivery is able to transfect the cells, and thus gives them the ability to produce a protein missing e.g. due to a disease.

While the possibilities of biologicals are very promising, it is also very difficult to deliver them to the right compartment within the body and preserve their functionality. Proteins and RNA are generally the most difficult biologicals, as they degrade very quickly. The delivery of biologicals is subject to a lot of current research.[72, 73]

1.3.3 Drug delivery of biologicals

Biologicals commonly serve as the therapeutic agent in a formulation; however, they can also have other tasks. Sometimes they are used as targeting molecules.[74] In this case, a modified drug delivery system can be targeted to certain places by binding a biological on its surface.[75, 76] Also the release pattern of a drug from particles can be changed by the usage of enzymes that degrade the particle.[77, 78] A third alternative is to use biologicals on the surface of particles to mediate an uptake through a biological barrier.[79] In this thesis the human lactoferrin peptide – a known penetration enhancer – is used as a particle modification.

1.3.4 Desmopressin and its medical application

Desmopressin, which is used in the thesis as therapeutic agent, is a synthetic analogue for the peptide hormone vasopressin. It has nine amino acids of which one is D-arginine. The amino group on the N-terminal side is cut off and an amino group has been attached to C-terminal side of the peptide. There are two cysteine residues that connect with a sulfur bond and form its secondary (ring) structure.

Desmopressin is an antidiuretic drug being used to treat diabetes insipidus.[80] It can also be applied to prevent nocturnal enuresis in adults and children, and has thus a broad application on the market.[81, 82] Furthermore, it has anti-coagulopathy effects that are subject of research since the late seventies.[83-85] It has been tested for uses to counter effects of acetylsalicylic acid,[86] blood loss after cardiac surgery [87, 88] or bleeding disorders.[89]

1.4 The lung

1.4.1 Anatomic key features and barrier properties of the lung

The lung is responsible for the gas exchange (carbon dioxide and oxygen) of the blood. It is divided into a right lung, consisting of three lobes, and a left lung, consisting of two lobes. Connected to the nasal region is the trachea which first breaks down to the bronchus, then the bronchioli and later the alveoli. While bronchus and bronchioli are primarily responsible for conducting the airstream, the lower part of the bronchioli and the alveoli are responsible for the gas exchange.[90] The transport of oxygen and carbon dioxide is mediated by hemoglobin and myoglobin. In both cases, the gas is bound to an iron atom of the heme complex. The exchange happens by diffusion, mainly driven by partial gas pressures of the environment and of blood. To allow an optimal exchange, the alveoli have a squamous epithelium with a thickness of around 100 – 200 nm,[91] a total inner surface of around 140 m^2, [92] and they are well-perfused because of capillary blood vessels. The conducting airways in contrast, have a much thicker tissue, and an inner surface of just 2 m^2. As larger components do not bypass the cell membrane easily, a large surface with a thin epithelium and a good perfusion is an ideal place to start for drug delivery.[91, 93] The alveoli are coated with the alveolar lining fluid which decreases the surface tension. It avoids the adherence of the tissues among each other and thus prevents the collapse of the lung.[94] The gas exchange is also supported by the fluid, and it probably passively supports the immune system by preventing adherence of bacteria. The free fatty acids in the fluid help to inhibit microbial growth.[94]

As the speed of the air stream changes through the different branches of the lung, particles are separated by their sizes. In general, the larger the particles are, the earlier they impact into the tissue of the bronchus (with exception of porous particles, as density also plays a role [95]). Particles of the

size of 10 µm and larger are stopped by the bronchus by 100%, while for particles of 5 µm only around 80% impact in the upper airways.[96] This gradually goes down to 0% for 1-2 µm particles.[96] In the deeper lungs the speed of the air stream is slower and deposition is then mainly driven by gravitational forces on the particles. Particles smaller than 1-2 µm reach the deep lungs, but they are too small to be affected by gravity, so they are rather exhaled than deposited.[96] If particles become smaller than 200 nm, diffusion effects again mediate a deposition in the deeper lungs.[96]

1.4.2 Pulmonary clearance mechanisms

Mucociliary Escalator

Around 30-65% of the cells in the airways are populated with small cilia [93] which agitate in a concentrated metachronal pattern to move the mucus up the throat where it is swallowed. This mucociliary escalator is the primary cleaning mechanism in the bronchus/bronchioles. It removes unwanted substances, primarily larger particles stuck due to impaction, from the conducting airways (see section 1.4.1). In the lower regions of the conducting airways, less cells with cilia can be found than in the upper regions. The speed of mucus movement can be measured with a method developed by Yeats et al. They obtained a geometric mean value of 3.6 mm/min from a study with 40 subjects.[97]

Alveolar Macrophages

For removing dust particles and bacteria from the deeper lung, pulmonary macrophages take up foreign objects by phagocytosis.[98, 99] Such internalized substances are then degraded in the phagosome. During the uptake process, macrophages secrete chemokines that attract neutrophil granulocytes to enhance that body's capability to remove bacteria or dust. Furthermore, the phagocytosis produces some reactive species (e.g. oxygen derivatives) that are toxic for the surrounding bacteria. Asides from phagocytosis, macrophages also serve as coordinators for the immune system by flagging spots with cytokines like TNF-α or several interleukins.[100, 101]

Macrophages in the lung can occur in three places: [102] Directly in the alveoli, in the conducting airways, where they are being transported by the mucociliary escalator, or they can sit beneath the mucus and as interstitial macrophages in the tissues of the lung. The last kind can sit in many places such as connective tissues, lymph nodes and alveolar walls. Macrophages that are being removed from the lung either move up the throat via the mucociliary escalator and are swallowed and digested or they are transported from the lung via the lymphatic system.

1.5 Pulmonary Drug Delivery

Delivery of drugs along the pulmonary route is a very old subject. Smoking tobacco, for example, or other herbs, has been common in many cultures for a long time. Also the usage of pulmonary delivered anesthetics has a long tradition,[103] especially since the discovery of chloroform.

1.5.1 Systemic Drug Delivery into the lungs

As mentioned in section 1.1, for systemic application the drug has to be delivered to the blood. To achieve this in the lungs, the drug has to pass the squamous epithelium in the alveoli. The advantage of systemic drug delivery is that the epithelium is only 100-200 nm thick and the blood vessels lie directly behind the epithelium ready to take up compounds – usually oxygen – from the environment; however, the cells of the epithelium in the alveolus are also connected by tight junctions that block compounds from passing between the cells, and alveolar macrophages remove most of the compounds – depending on their size – remaining on the cells for too long (see section 1.4.2). Drugs can reach the blood vessels either by passing between two cells (paracellular transport) or by entering the cell on one side and leaving the cell on the other side (transcellular transport). Despite the large surface of the alveolus, the thin barrier and the close blood vessels, the barrier should not be underestimated. The transport of not well-permeable molecules into the blood stream remains a challenge. To improve the uptake of drugs, absorption enhancers such as oleic acid or others can be added.[104] There are also peptidic penetration enhancers like the hLF-peptide that mediate the diffusion into the cell for transcellular transport.[105] Paracellular transport is more desirable for systemic delivery than transcellular transport, as the drug is directly moved to the blood vessels; however considering the strong clearance mechanisms of the lung, a quick transport into the cells and slower further transport to the blood vessels might be advantageous, compared to a slow paracellular transport.

1.5.2 Short historical overview of pulmonary application

Pulmonary application has been in use for as long as mankind's records go back, mostly for application of alkaloids. Around 4000 years ago, in India smoking Datura preparations and other herbs is conveyed.[106] In ancient Egypt (around 1500 BC) black henbane vapors were inhaled, and probably the first inhaler devices known were made by the Greek (around 400 BC).[107] In the middle ages, inhalation therapy can also be cited, as it appears in the "Treatise on Asthma" by Moses Maimonides.[107] However, it is only a small part of the treatment approach on asthma and also contains suggestions like to breathe clean air and live outside the city. This also might be due to the definition of asthma

back then, which does not meet with today's definition.[108] Also the smoking of tobacco (and other herbs) by Native Americans, yet not for medical purposes, is an example for inhalation of biologically active substances. Later, in the late 18th and early 19th century, inhalation again was reported in Britain and the United States.[106] Asthma cigarettes, which were made of atropine containing herbs, became a common medicine at the time.[109] The first device called inhalator was a tin vessel made by the British physician John Mudge.[110] The first pressure driven inhaler and the first dry powder inhaler were then invented roughly 70 years later in the middle of the 19th century.[110] Another hundred years later, in the middle of the 20th century, the asthma cigarettes came under criticism because in some cases they caused poisoning.[111] More advanced metered dose inhalers came up and could take the place of the cigarettes easily, as also adrenalin as therapeutic agent for asthma had been found. Successively, new and more advanced inhalators came on the market. In the 60s, ultrasound nebulizing devices were invented, the first modern dry powder inhalers came up in the 70s,[110] leading to the devices used in today's medicine. One of the first biologicals and probably the most well-known peptide drug is insulin. To treat diabetes mellitus, the patients have to inject insulin into their adipose tissue to mediate the uptake of sugar from blood into cells. However, the compliance of injections is rather low and plain oral administration is impossible, since peptides are a natural food source to human beings. The pulmonary route, having no digestion enzymes like the stomach and no first pass effect, seemed a promising target. First reports about applying insulin via the pulmonary route can be found back in 1925.[112] Even though the drug was functional, the efficiency was rather low. Around 50 years later some research groups picked up the idea again and tried to administer aerosolized insulin to patients, which was greatly summarized by Patton et al. in 1992.[91] However, there were problems to overcome. The majority of the aerosol did not reach the alveolar compartment, such that patients had to be trained to breathe the aerosol into their lungs to maximize the effect. Rapid absorption in the lungs resulted in too high peak concentrations and short effects, as well as irritations in the respiratory area.[113]

The problem of irritation can generally be solved by encapsulating the drug in a compatible host. Furthermore, in the second half of the 80s some studies in animals [114, 115] showed that the use of liposomes could result in a sustained effect which would solve the problem of rapid absorption. In 1992 Liu et al. encapsulated insulin into liposomes to investigate the effect.[116] However, the effect did not result from the release pattern of the liposomes, as pure insulin co-administered with empty liposomes yielded the same results. But nevertheless, a sustained effect and a stronger hypoglycemic effect was observed. Liposomes could also be used for targeting to specific cells in the respiratory area which has been summarized by Schreier et al. in a review on pulmonary delivery of liposomes.[113] To solve the problem of deposition, improved inhalation devices were created which made inhalation easier for patients.

Besides that, in 1997 Edwards et al. created “large porous” particles for pulmonary administration that were big enough to carry an acceptable amount of insulin with a very low density, such that the particles did not suffer from impaction in the upper airways.[95] Thus upon inhaling, a larger amount of particles reached the alveolar compartment. Large porous particles can either be prepared from a polymer that holds a drug or from the drug itself, as it was done by Vanbever et al. with insulin.[117] Further studies resulted in the first commercially available, FDA approved, inhalable insulin medicinal product called Exubera® (marketed by Pfizer Inc.).[118] However, it was only available for a short time (2006-2007) as the demand was very low. The main reason was that it was significantly more expensive than injected insulin and meant no improvement for the treatment of the disease.[119] Also effects on patients due to heavy smoking and asthma were not considered in the clinical trials.[119]

Searching for “inhaled insulin” publications in the PubMed database yields over 1000 results. Most publications have been made in the period since 2001, peaking 2006 (99 publications) and 2007 (123 publications). After 2007 the amount of publications decreased to around 30 per year. However, the topic is still subject to research and another formulation of inhalable insulin named Afrezza® by MannKind Corp. has recently been approved,[120] continuing the story. The marketing of Afrezza®, however, was done by Sanofi with only little success. The product financially never met its expectations, resulting in Sanofi dissolving its contract with MannKind in early 2016.[121] This leaves MannKind searching for a new distributor.[122]

1.5.3 Differences between Dry Powder Inhalers and Metered Dose Inhalers

Pulmonary administration has a lot of advantages and only few, but large disadvantages. The biggest disadvantage is the application itself, because patients need to be trained to inhale the formulation in a correct way. If the inhalation is not executed properly, the main amount of the drug can be stuck in the mouth, the throat or the bronchial region of the lung instead of reaching the alveolus. Newer developments of inhaling devices support the patients in this matter, and particulate formulations can further help to avoid a deposition in the wrong place.[95]

Most modern inhalers have, for example, a dose counter that allow patients to control how many doses have been taken or are yet available in the device. They have overdose protections and properly shield their loaded drugs from the environment.[123] There are two main classes to be distinguished: dry powder inhalers and metered dose inhalers that usually provide liquid aerosols. The metered dose inhalers were developed in the middle of the 20th century (see section 1.5.2). Originally, they used chlorofluorocarbons as propellant; however, in the 90s they were refitted to work with hydrofluoroalkanes for ecological reasons. An advantage of the dry power inhaler is that it will only discharge if the negative pressure is high enough, and thus the drug can directly go to the lung. In

contrast to that, in case of the metered dose inhalers, breathing in and discharging the inhaler has to be coordinated. On the other hand, dry powders can induce coughing and therefore they are not always the right choice.

1.6 Motivation and Goal

The goal of this thesis is to create a most versatile drug delivery system. The predominant route is pulmonary application, while the routes for oral, dermal and parenteral application should not be excluded a priori. For a pulmonary delivery system, its key problems, i.e. the physical structure of the lungs (see section 1.4.1 and 1.4.2) and the problems patients have with application (see section 1.1 and 1.5.3), have to be addressed. Fortunately, there are commercially available devices (see section 1.5.3) that help patients applying aerosol, such that this aspect does not have to be part of this thesis. The physical structure of the lung as a problem for pulmonary delivery can be discriminated into two problems. One being the problem of deposition in the correct area in the lungs (see section 1.4.1) and the other being the problem of absorption of API into blood stream, which often requires penetration enhancers (see sections 1.2.1, 1.3.3 and 1.5.1). The latter only occurs for systemic delivery at which this thesis aims. Besides these physiological problems, also the API has requirements for its transport. Biological APIs, such as Proteins, Peptides, DNA and RNA, are sensitive to degradation (see section 1.3.1 and 1.3.2). Since chemical properties like hydrophobicity of theses APIs have to be taken into account as well, many different methods of encapsulating exist (see section 1.2.1 and 1.2.2). If the system is supposed to be truly versatile, then it needs a certain flexibility to be adjustable to the API used. The main factor for that matter is the polymer that is used for the encapsulation. An encapsulation will only work well if the polymer and the API can be brought together. Therefore, a system where the polymer can be exchanged without changing the method of preparation, is desirable.

2 Materials and Methods

2.1 Materials

2.1.1 Polymers

The Polylactic-co-glycolic acid (PLGA) was obtained as Resomer RG 503H (50:50 ratio) from Evonik Industries (Darmstadt, Germany). Fluorescently labelled PLGA was prepared on site: briefly, fluorescein amine was coupled to 50:50 PLGA (Resomer RG 503H) by a 4-(Dimethylamino)-pyridin (DMAP) catalyzed reaction in acetonitrile, as described by.[124] Chitosan used is Novamatrix Protosan UP CL 113 obtained from FMC BioPolymer AS (Sandvika, Norway). Glucomannan (food quality) was bought from Now Foods (Bloomingdale, IL, USA). Alginate was purchased from Carl Roth GmbH + Co. KG (Karlsruhe, Germany). Lignin (alkali), dextran (150 kDa from *Leuconostoc mesenteroides*), and gelatin (from bovine skin) were obtained from Sigma Aldrich (Steinheim, Germany). 20 kDa dextran was ordered from Tdb Consultancy (Uppsala, Sweden).

2.1.2 Stabilizers

Polyvinyl alcohol (PVA) was obtained as Mowiol 4-88 from Kuraray Europe GmbH (Hattersheim am Main, Germany). Tween 21, Tween 85, Span 80, Span 85, Polyethylene glycol (PEG) 400, Pluronic F-68/Poloxamer 188 and Pluronic F-127/Poloxamer 407 were purchased from Sigma Aldrich (Steinheim, Germany), Brij O2 was bought from Croda GmbH (Nettetal Kaldenkirchen, Germany).

2.1.3 Peptides

Desmopressin acetate was a gift from Evonik Industries (Darmstadt, Germany), bought from Ferring Arzneimittel GmbH (Kiel, Germany). The human lactoferrin peptide (hLF-peptide) was obtained from EMC (Tübingen, Germany).

2.1.4 Solvents

Organic solvents for precipitations and washing were obtained from Sigma Aldrich (Steinheim, Germany) in HPLC-grade qualities. (CHROMASOLV® Plus, for HPLC ≥99.9%), acetonitrile (CHROMASOLV® Plus, for HPLC ≥99.9%) and acetone (for HPLC ≥99.9%). Ethanol was obtained as Ethanol absolute ≥99.8% from Sigma Aldrich (Steinheim, Germany) as well. Pentane was obtained in reagent grade (98% purity) and hexane in quality for HPLC ≥95%, both from Sigma Aldrich (Steinheim, Germany) as well. Liquid paraffin was obtained from Merck KGaA (Darmstadt Germany) in quality Ph. Eur., BP, NF, JP.

2.2 Methods

2.2.1 Theoretical backgrounds of methods used

Particle Size Measurement by Dynamic Light Scattering (DLS)

Dynamic Light Scattering (DLS), also called Photon Correlation Spectroscopy (PCS), is one of the most common techniques to determine the size of nanoparticles. There are different companies offering devices like HORIBA Ltd. and Wyatt Ltd.; however, most laboratories, like in our case as well, use a Zetasizer device by the company Malvern Instruments Ltd. (Worcestershire, United Kingdom).

For measuring the size of particles, a laser beam is pointed at a nanoparticle suspension in a cuvette. The light is scattered by the nanoparticles and partly reflected towards a detector. Since the scattering also results in a phase shift for some of the light waves emitted from the laser, it happens that some light waves annihilate each other by destructive interference, while others brighten up due to constructive interference. The amount of constructive and destructive interferences in a moment of measurement results in a brightness-signal on the detector. The quicker the nanoparticles move in their suspension, the quicker the brightness-signal on the detector changes. The device calculates an autocorrelation function with these brightness values. That means, it compares the value at a certain time point with a series of values before that time point, and on this basis it calculates the size of the particles (Equation 2.1). This method works, because if no energy is applied to move the nanoparticles within the suspension, the motion of the particles is only determined by the Brownian motion, which is depending on the size of the particles. The Stokes-Einstein equation (Equation 2.1) shows the relationship between the size of the particles (d) and their translational movement by Brownian motion (D).

$$d = \frac{kT}{3 * \pi * \eta * D}$$

Equation 2.1 Stokes-Einstein equation. With d being the diameter of the particle, k the Boltzmann constant, T the temperature in Kelvin, η the dynamic viscosity and D the diffusion constant representing the translational movement velocity of the Brownian motion.

Using that correlation to measure the size of particles works well in general, but can be tricky in some situations: Particles have to be spherical and temperature and viscosity of the suspension have to be known and set precisely, which can be a problem for complex solvents like cell culture media. Furthermore, if particle concentrations of suspensions are too high, scattered light from particles might hit other particles in the suspension, scattering again and producing a signal that interferes with the measurement, so that a dilution of the sample is necessary.

The size of the particles is calculated by an autocorrelation function, which is a mathematical model that has to be fed with suitable parameters. The model is built for determining the size of nanoparticles in dispersion. The size of monomodal distributions can be determined easily; however, if a particle dispersion has multimodal size distribution, it can be difficult in some cases to determine them. For example, measuring pure water will always yield a result of some size, as the mathematical model expects particles to present in the dispersion.

However, if all necessary parameters are set and all prerequisites met, the method produces reliable results on the diameter of the particles. The size resulting from DLS measurements differs from size measurements done by, for example, electron microscopy. This is due to the fact that a particle in solution moves with a husk of solvent molecules attached to it. The size of that hull depends largely on the adhesion forces between the two materials, but also on chemical stabilizers, if used. Strong interactions between solvent and particle usually result in a bigger hull, and thus the *actual* size of the particles is smaller than determined by DLS measurement, where usually the hydrodynamic diameter (particle + attached solvent molecules) is determined.[125] This hydrodynamic diameter can increase even more, if particles have hairy structures on their surfaces.[126]

Particle Size Measurement using Laser Diffraction (LD)

Laser diffraction for particle size measurements is based on the wave character of light. If a light beam is pointed towards an obstacle with a slit, then after passing the slit, light waves will propagate equally in all directions. In case there are two slits in the obstacle, this will happen from both slits. At the point where the two waves meet, they will interfere with each other (see Figure 2.1).

If a light beam hits a particle, the light is diffracted at the particle's surface. The propagation of light waves, after being diffracted on the particle's surface, is similar as described in the double slit example above (see Figure 2.1). The diffracted light waves interfere behind the particle, and thus project a characteristic image on the surface of a detector behind the particle. If the size of the particles changes, also the diffraction angle changes, and thus the interference of the waves behind the particles is different. This can be recognized by the detector and particles of different sizes can be discriminated.

Calculating a particle size from the scattering image is challenging, as it is not possible to directly use the information gained from the scattered light. Usually, the device calculates a result depending on a few parameters and matches it with the scattering image. If the match is good enough, it is presented as a result to the user, if not: some parameters are changed and a new result is calculated and matched again. This will be repeated until a sufficient match can be found. There are commonly two different theories that are used for calculations: Fraunhofer theory and Mie theory. Whilst Fraunhofer is easy

to apply, it tends to overestimate larger particles. If both, large and small particles, are present in a sample, almost only large particles are displayed in the result. Mie theory, on the other hand, works well for small and large particles, but it is necessary to know the refraction indices of the particle substance, the solvent and the absorption of the particles. Since those variables are difficult to determine in some cases (for example for mixtures of a solvent with stabilizers) and since they sometimes have big effects on the result, Mie theory can be very difficult to configure properly.

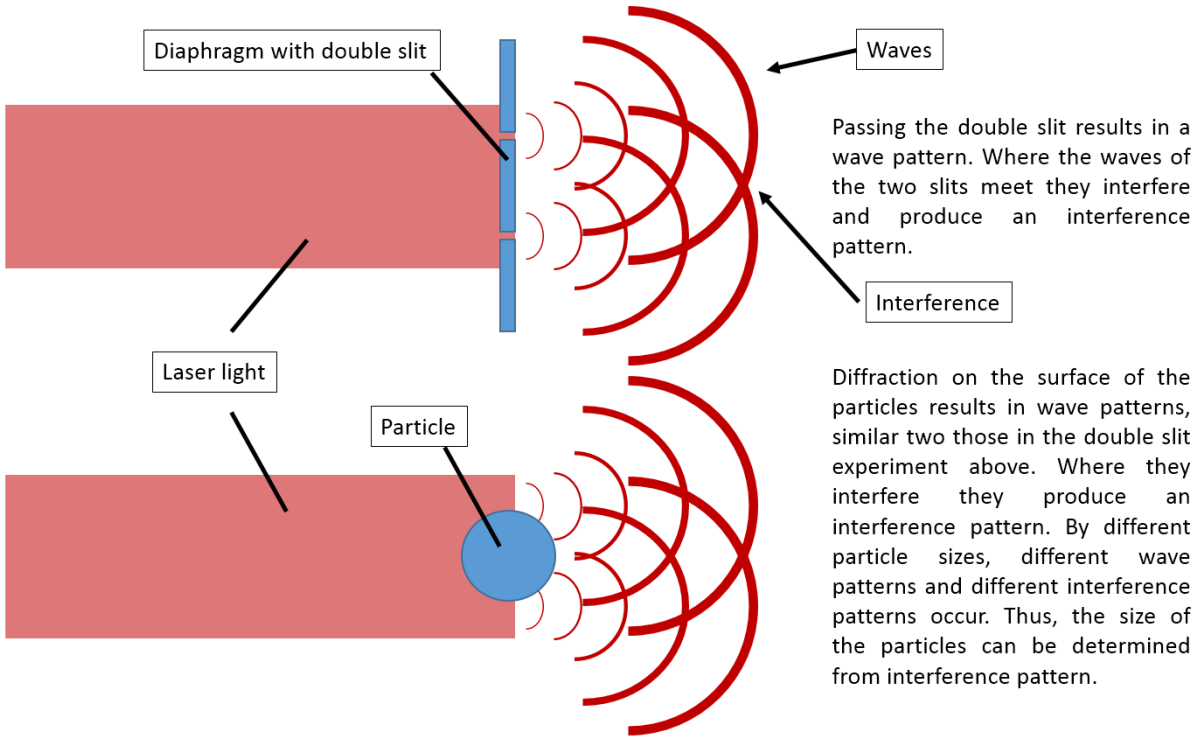

Figure 2.1 Laser diffraction and the double slit experiment.

However, Dynamic Light Scattering and Laser diffraction should not be confused with each other. While in DLS the motion of a whole particle sample is analyzed, in laser diffraction the scattering image of a multiple single particles is taken into account. Laser diffraction thus is more sensitive to the particle concentration. Also, measuring particles of non-spherical shape is more problematic, and more parameters of the used substance have to be known in LD. Furthermore, the size range in which DLS can be used is smaller than for LD, but the method of size calculation has been adjusted for LD, depending on the size range of the particles.

Zeta potential Measurement with Laser-Doppler Velocimetry

Particles in dispersion are covered with small husks of their solvent. The thickness of this husk depends mainly on the interactions between the particles' surface material and the solvent. For example, a particle with negative charges has a negative electric field around it. The field itself decreases quadratically as a function of distance from the particle. Directly where the particle ends, the so-called Helmholtz layer (also Stern layer) starts with the inner Helmholtz plane. At the inner Helmholtz plane, anions are specifically adsorbed directly onto the surface of the negatively charged particle, due to entropic reasons. After a layer of water molecules, the outer Helmholtz plane follows where cations are adsorbed non-specifically, due to the attraction of the negative electric field. After the layer of cations, a diffuse layer of cations and anions follows. The closer to the particle, the more it consists of cations, as the electric field is stronger. Seen from a distant point of view and assuming that the particle does not move, it is of neutral charge. If the particle starts to move, friction is applied to it and to all the ions in its area of influence. In the outer region, the friction will be stronger than the electric field of the particle, and ions will be sheared off the particle. The area, right where the shearing ends, is called the shearing plane, and the electric potential of the electric field of the particle at this point is defined as the zeta potential for the measurement with the device (Malvern Zetasizer Nano ZS) used in this thesis.[127]

During a zeta potential measurement, the particles are being moved by an electric field applied to the sample. This effect is called electrophoresis; The Henry equation (Equation 2.2) explains how electrophoretic mobility U_E is related to the zeta potential z.[127]

$$U_E = \frac{2 * \varepsilon * z * f(kA)}{3 * \eta}$$

Equation 2.2: The Henry Equation shows the dependencies between the electrophoretic mobility U_E, the dynamic viscosity of the medium (η), the dielectric constant (ε), the zeta potential z and Henry's function f(kA). Values of f(kA) are commonly either 1.5 for particles down to approximately 200 nm in aqueous medium or 1 for small particles in low-salt (organic) medium.

The movement of the particles is measured by Laser Doppler Velocimetry: A laser beam is pointed at the moving particles. Upon contact of the laser beam and the moving particles, the frequency of the laser beam changes proportionally to the velocity of the moving particles. Scattered light of the frequency-changed laser beam goes to the detector, together with a reference beam that did not pass the sample and is thus unchanged.[128] The comparison of waves from both beams can be used to calculate the velocity of the particles, and thus by Henry's equation also their zeta potential. By the

orientation of the shift in the wave pattern, it can be determined whether the zeta potential is positive or negative.

High Pressure Liquid Chromatography (HPLC)

High Pressure Liquid Chromatography (HPLC) is one of the most common chromatographic methods in laboratory use. A liquid phase (mobile phase) is pressed through a column filled with a solid phase (stationary phase). Molecules within the mobile phase, interacting with the stationary phase, stay on the column for a longer period of time. Thus, substances can be separated by their different attraction forces to the solid phase. HPLC devices usually have a pump that pumps the mobile phase through a column containing the stationary phase. There is an injection loop for loading a small amount of sample (usually between 5 µl and 20 µl) into the running mobile phase. The mobile phase carries the sample through the column, where it is separated into its components by attraction forces to the stationary phase. After passing the column, the sample is carried by the mobile phase through a detector.

Cation and anion exchanging columns exist as solid phases, but most common are reverse phase (separation through hydrophobic interactions) columns. These columns usually have alkyl groups tightly packed on dextran beads with different chain lengths, depending on their purpose. For separating small molecules or peptides, often C18 alkyl group-columns are used, as it is the case in this thesis. For bigger substances, such as proteins, often C4 columns are the subject of choice. Detection of a substance depends on the characteristics of that substance. There are different kinds of detectors, like for example flame ionization or UV/Vis detectors that can determine different properties of a component. As UV detectors, like they were used in this thesis, detect non-selectively, they have to be adjusted to a wavelength where the desired component exhibits absorption. A control run with only the desired substance is necessary to discriminate the substance's peak from others in the chromatogram. A quantification of the substance can be done by an integration of the peak and a comparison with a respective standard curve.

Mass Spectrometry

Mass spectrometry is a method to analyze each compound in a mixture. The mass spectrometer ionizes the species and then separates and detects them by a mass to charge ratio (usually denoted by "m/z ratio"). In an ideal case, every component in a mixture has its unique mass to charge ratio and can thus be identified properly. However, mass spectrometers have a very high resolution and can determine differences of single Dalton weight in molecules. Therefore, every compound comes with distribution of different weights according to its isotopes. Also, ionization products sticking to compounds, fractured compounds and non-fully ionized compounds make the mass spectrum less clear.

The mass spectrometer always consists of three main units: The ion source/accelerator, the analyzer and the detector. The ion source ionizes the compounds, which results in an individualization of all molecules due to the high charge. The accelerator then accelerates them within an electric field. The ions then move through the analyzer, where they are separated by their mass to charge ratio, and finally they hit the detector. The detector only determines the intensity (amount) of a component hitting it. Combining that information with the parameters of the analyzer at the same time point, results in an intensity peak at a certain mass to charge ratio in the spectrum.

For the analysis of a compound, often a liquid chromatography like HPLC is directly coupled to a mass spectrometer, such that a compound mixture is separated before it is ionized and accelerated. This helps identifying substances that have numerous peaks in a mass spectrum and come from a mixture of substances.

Membrane emulsification

Membrane emulsification is a method to prepare emulsions with the help of a filter membrane. Two phases, aqueous and organic/oily, are separated by a glass membrane with a certain pore size. A gas pressure is applied to the dispersed phase, and thus presses it through the membrane. The other phase (continuous phase) is stirred and rips off droplets of the dispersed phase coming through the membrane (see Figure 2.2). If the dispersed phase is hydrophilic, then the membrane should be lipophilic to avoid droplets from mixing on the membrane surface after they have been pressed through the membrane. Also, higher level emulsions, like for example oil in water in oil, are possible, if the dispersed phase is already an emulsion and the pore size of the membrane is suitable. The size of the produced emulsion droplets depends on the pore size of the membrane and can be explained by Equation 2.3. The parameter 'a' is a constant, usually depending on the kind of the membrane and other experimental conditions. In most cases, 'a' lies within a range of 2.5 to 8.[129]

$$Droplet\_Size = a * Pore\_Size$$

Equation 2.3: Linear relationship between pore size and droplet size in membrane emulsification.

The pressure needed to press the dispersed phase through the membrane varies according to several parameters. The Hagen-Poiseuille equation (Equation 2.4) reveals the length of the pore, the diameter and viscosity to be relevant.

$$p_{beginning\ of\ membrane} = \frac{8 * V_{flow} * \eta * L}{\pi * r^4} + p_{end\ of\ membrane}$$

Equation 2.4: Hagen-Poiseuille Equation: V_{flow} being the volume flow through the pore, η being the dynamic viscosity, L the length of the pore, r being the radius of the pore and p being the pressure.

However, the Hagen-Poiseuille equation leaves out, for example, the pressure loss by friction caused by interactions between dispersed phase and membrane. If the membrane and the dispersed phase have a high interface tension, then this parameter has to be considered and pressure can be calculated by the Darcy-Weisbach Equation (Equation 2.5).

$$p_{beginning\ of\ membrane} = \lambda * \frac{L}{d} * \frac{\rho}{2} * \left(\frac{V_{flow}}{A}\right)^2 + p_{end\ of\ membrane}$$

Equation 2.5: Darcy-Weisbach equation: λ being the Darcy friction factor formulae giving the actual friction value depending on the materials involved, L being the length and d being the diameter. ρ denotes the density of the fluid, V_{flow} the volume flow through the pore, A the area cross-section and p the pressure.

The surface of the membrane inside the pores is exposed to the fluid. Considering that volume scales by sixth power and area only by forth power in the equation, it can be assumed that choosing membranes with larger or smaller pores, and thus the Darcy friction factor, will result in a quadratic change in necessary pressure to overcome the membrane.

A further problem to these considerations is, that both equations assume the pore to be a single pipe; however, in most cases, as well as in the membranes used for this thesis, pores are branched and have obstacles, such that laminar flows are not necessarily given. Usually, required pressures are much higher than what can be calculated by Equation 2.4 and Equation 2.5. Furthermore, in all cases polymer solutions of much higher viscosities than plain water were pressed through membranes. A determination of necessary pressures was therefore conducted by experience rather than by calculation. By starting a membrane emulsification, fluids do not directly move through the membrane, as there is a liquid limit. A certain initial pressure that overcomes the limit has to be reached, in order to start the flow of dispersed phase through the membrane. The manual of the device used in this thesis (External Pressure Type Micro Kit, SPG Technology Co, Ltd., Miyazaki, Japan) suggested a membrane pre-wetting, with continuous phase and stabilizers to lower that limit.

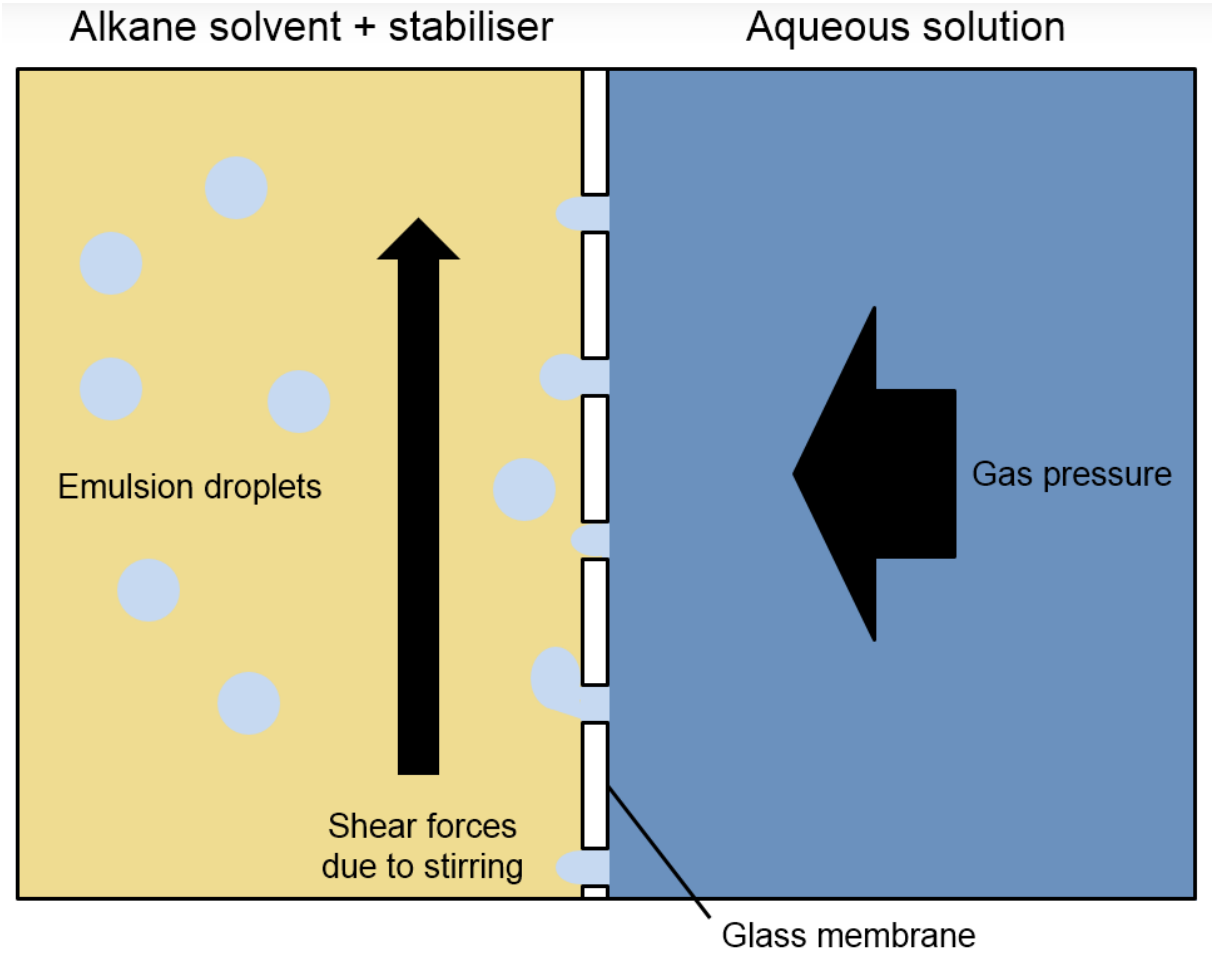

Figure 2.2: Scheme explaining the process of membrane emulsification. A pressure is applied to the dispersed phase (blue). Smaller amounts of the aqueous solution pass the membrane into the stirred alkane, usually pentane (yellow), with stabilizers. The stirring force pulls smaller droplets (light blue) off the membrane for emulsion formation.

An enormous advantage of the membrane emulsification is, that the energy is only applied in form of pressure on one of the liquid phases. Since liquid phases are not compressible, none of this pressure is applied to an API dissolved in the liquid phase. Forces are only applied to the API in form of shear forces when passing the membrane.

Ultrasound sonication

Sonication is the use of sound to apply energy to a system. In most cases, ultrasound is used, as sound of lower frequencies is not potent enough for most applications. Ultrasound sonication can be used to mix substances, redisperse particles, clean surfaces, prepare emulsions and many more things. In pharmaceutical nanotechnology, it plays a major role for the redispersion of aggregated particles and the preparation of emulsions. The high-frequency sound waves generate cavities from dissolved gas,

which form and implode. Upon implosion, shear forces are generated, that can lead to an emulsification or redispersion of particles. The presence of stabilizers then keeps the developed emulsion or redispersed particles stable. For particle dispersions, usually ultrasound baths are used that typically have frequencies around 40-400 kHz. The lower the frequency, the stronger is the effect of cavitation, thus the higher frequent mode is important for ultrasound baths, if for example compounds are supposed to be cleaned gently. Ultrasound probes have single frequencies of operation – usually between 20 and 40 kHz. The probe used in this thesis oscillated at 20 kHz. The strong energy of an ultrasound probe also produces a lot of heat energy, such that a constant cooling (for example sonication on ice) is beneficial. This applies especially, if sensitive biologicals are involved.[130, 131]

Lyophilization

Lyophilization, also called freeze drying, is a method to extract a volatile component (usually a solvent) from a sample, leaving only the non-volatile components as dry powder. In most cases, it is used to remove water from samples. For that purpose, the sample is frozen first, and then a negative pressure is applied to sublimate the volatile substance into its gaseous state (see purple arrows at Figure 2.3). This results in a removal of the water, which has the advantage that the liquid phase is not passed and water sublimates directly from the solid state. Lyophilization can also be done with organic solvents, but as freezing points of organic solvents are lower than water, all processes have to be executed at lower temperatures as done with acetonitrile in this thesis.

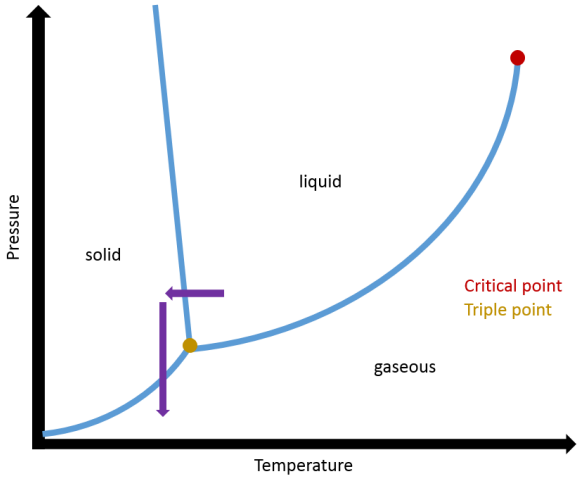

Figure 2.3: Phase diagram of water with arrows indicating lyophilization. First, temperature is decreased to freeze the sample (horizontal arrow), then pressure is reduced to sublimate the volatile component (vertical arrow).

Scanning Electron Microscopy

As nanoparticles are very small in size, visible light with wavelengths longer than the size of the nanoparticles does not qualify for imaging. Nanoparticles with sizes of around 130 nm, as described in this thesis, can be imaged with electron microscopy, because the wavelength of electrons is much shorter (approximately 10^{-3} nm).[132] For electron microscopy, an electron source (usually a tungsten or lanthanum hexaboride filament) is placed above a sample. Upon charging the filament, electrons are emitted towards the sample. The electron ray is accelerated and modified by several lenses that change its focus and magnification. Upon hitting the sample, electrons interact with the outer electron shells, and secondary electrons are emitted. These are caught by a detector and they are interpreted as an intensity signal. The electron beam scans over the whole image line by line, such that the electron ray is always focused on a single spot, as in contrast to light microscopy, where every part of the image is mapped at the same time. Differences in the intensity of reflection/absorption of electrons on the sample create different intensities, brighter or less bright, on the image. A very strong electron ray can change the sample, especially in case of biological and less solid chemical samples. Particles made of polysaccharides often exhibit a glowing pattern that can disturb the imaging process, because they are charged by the electron ray. Since most biological samples do not emit a lot of secondary electrons, they are usually sputter coated with a layer of metal, usually gold or platinum, of few nanometers thickness. These metals emit enough secondary electrons to make the shape, to which they were sputtered, visible, and they can dissipate the electron ray.

Thermogravimetric analysis

Thermogravitmetric analysis (TGA) is conducted to measure changes in weight during heating. This usually happens when there is evaporation, sublimation, degradation or loss or gain of mass, by for example reduction or oxidation. A common application is to determine amounts of crystal water remaining in samples. In case of polymers as used in this thesis, the degradation of the polymer has to be determined beforehand, to at which point a weight loss is not due to evaporating water. In case of this thesis, TGA was used to determine the dry weights of particles' samples for the calculation of loading efficiencies.

Confocal Laser Scanning Microscopy (CLSM)

CLSM is a technology featuring an optical microscope taking pictures enhanced by fluorescence. In principle, CLSM microscopes work like normal fluorescence microscopes. A laser is pointed at a fluorescing sample and activates it. The light emitted from the sample goes through a filter that only allows fluorescing light to pass, not the exciting laser light. In this way, fluorescence of a sample can

be visualized. The difference to an ordinary fluorescence microscope is, that the laser of a CLSM can be focused very precisely, such that fluorescence information can be gathered not only from broad points in X and Y axis but also from within the sample (in Z axis). Thus, the excited volume is very small and different sections within one sample can be excited separately. This allows, for example, to show if certain fluorescing substances are within a larger object or just on its surface. A problem, nevertheless, is that the exciting and the emitting lights have to travel through the whole sample. That can lead to weaker excitations and bleaching outside the focal plane, and to absorption of emitted light by the sample.

2.2.2 PLGA particle preparation and characterization

Nanoparticles were chosen as drug delivery system, as small particles could be able to bypass biological barriers easier than larger particles in the micrometer range. Furthermore, a hydrophilic system would not be suitable, as it would dissolve before it could pass the barrier. Therefore, hydrophobic PLGA nanoparticles were chosen, which are well-characterized in literature for the encapsulation of various therapeutic substances (see section 1.2.1). A commonly used preparation method was employed and adjusted for our purposes.

PLGA particle preparation -- Double Emulsion Solvent Diffusion Centrifugation – method

PLGA nanoparticles were prepared by a modified double emulsion solvent diffusion centrifugation method. For one batch, 50 mg of PLGA were dissolved in 1.5 mL of ethyl acetate and mixed with 0.5 mL of an aqueous solution. The composition of the aqueous solution differed depending on the batch. It contained either the drug (500 µg of desmopressin) and a stabilizer (6.25 mg) or only the drug, or nothing (see Table 2.1). For the coating approach, blank PLGA nanoparticles (inner emulsion was MQ water only) were prepared as described above. After the volume had been adjusted to 20 mL, 500 µg of desmopressin was added. The solution was kept at room temperature (RT) for 15 min before the centrifugation step (as for all other samples). The mixture of both was then sonicated for one minute with approximately 800 J to produce the primary emulsion. After the primary emulsion had formed, another 2.5 mL of aqueous PVA solution (25 mg/mL) were added, and the whole was sonicated again for one minute with approximately 800 Joule to form the secondary emulsion. Afterwards, approximately 15.5 mL of MilliQ (MQ) water were added to precipitate the particles from the emulsion. The volume was adjusted to exactly 20.0 mL. For removing the ethyl acetate, samples were filled into Eppendorf tubes in quantities of 1 mL and centrifuged for 25 min at 24 kRCF and 16 °C. After centrifugation, the supernatant was discarded and the remaining pellet was rinsed with one mL of MQ water. After rinsing the pellet, all water was poured out, but some water remained in the tube sticking

to the plastic walls. The tubes were kept for several hours, in which the remaining water formed a droplet and dispersed the pellet. From this point on, the particles could be used for analysis.

A coating approach (CT), where the particles were coated with desmopressin instead of an incorporation, was used for comparison. For the coating approach, blank PLGA nanoparticles (inner emulsion was MQ water only) were prepared as described above. After the volume had been adjusted to 20 mL, 500 µg of desmopressin was added. The solution was kept at room temperature (RT) for 15 min before the centrifugation step (as for all other samples).

Table 2.1 Different configurations of the primary emulsions

Tag	**Substances**	**Description**
BK	None (only MilliQ water)	blank particles
CT	None (only MilliQ water)	particles for desmopressin coating
PL	Desmopressin (500 µg)	no stabilizer in the prim. emulsion
PVA	PVA (12.5 mg/mL), desmopressin (500 µg)	PVA as stabilizer
PEG	PEG 400 kDa (12.5 mg/mL), desmopressin (500 µg)	PEG as stabilizer
TW21	Tween 21 (12.5 mg/mL), desmopressin (500 µg)	Tween 21 as stabilizer
F68	Pluronic F-68 (12.5 mg/mL), desmopressin (500 µg)	Pluronic F-68 as stabilizer
F127	Pluronic F-127 (12.5 mg/mL), desmopressin (500 µg)	Pluronic F-127 as stabilizer

PLGA particle dissolution

Eppendorf tubes with PLGA particles were prepared as described above. To dissolve the particles, 400 µl of acetone were added to PLGA particles, dispersed in the rinsing water droplet from their preparation. The particles were kept in acetone for at least two hours. After that time, 1600 µl of ethanol were added to the solution. The ethanol precipitated the PLGA with desmopressin staying in solution. The tubes were then centrifuged (24 kRCF, 40 min, 4 °C) to condense the precipitated PLGA into a pellet. The supernatant, containing no PLGA but the desmopressin, was transferred to a new tube where it was left to evaporate overnight under a hood. After ethanol and acetone evaporation, only desmopressin was left in the tube. One milliliter of MilliQ water was then added to the tube to dissolve the desmopressin for analysis.

Dry weight analysis for loading efficiency

Eppendorf tubes of one milliliter washed particle dispersion were frozen at - 80 °C and then freeze dried for two days in a Christ Alpha 2-4 LSC (Martin Christ Gefriertrocknungsanlagen GmbH, Osterode am Harz, Germany). The freeze-dried particles of one tube were then put into a device for thermogravimetric analysis (Perkin Elmer TGA 4000, Waltham, Massachusetts, USA) to remove any

remaining water by heat. The weight at 160 °C, which is shortly before PLGA degradation temperature (*i.e.* approx. 180 °C), was determined as dry weight of the particles.

Desmopressin quantification by HPLC

A Dionex Summit HPLC System with a P680 gradient pump and a Dionex Ultimate 3000 UV/Vis detector was used to quantify amounts of desmopressin from dissolved particles. The column was an endcapped reversed phase LiChrospher® LiChroCart® 125-4 RP-18e (5µm) column with a LiChrospher® RP-18e (5µm) guard column, both Merck KGAA (Darmstadt, Germany). The mobile phase consisted of 50 mmol KH_2PO_4 buffer (pH 7.2), mixed with acetonitrile in a 80:20 (v/v%) ratio in an isocratic elution mode. The column was kept at 30 °C and the injection volume was 50 µL. Usually, the desmopressin peak could be seen in the chromatogram at around 6 min, and quantification was done by peak integration.

The encapsulation efficiency and the loading efficiency of desmopressin were defined and calculated as:

$$Encapsulation\_efficiency\ [\%] = \frac{Amount\_retrieved\_from\_particles\ [\mu g]}{Total\_amount\_used\_during\_preparation\ [\mu g]} * 100\%$$

Equation 2.6: Calculation of encapsulation efficiency.

and:

$$Loading\_efficiency\ \left[\frac{\mu g}{mg}\right] = \frac{Amount\_of\_peptide\_retrieved\_from\_particles\ [\mu g]}{Total\_mass\_of\_the\_formulation\ [mg]}$$

Equation 2.7: Calculation of loading efficiency. The loading efficiency was used for the comparison between the different stabilizers. It is calculated by the division of the amount of peptide retrieved from the particles by the amounts of polymer, peptide and remaining stabilizers summed together (i.e. total mass of the formulation).

Size and zeta potential measurements

Size and zeta potential of particles were measured with a Zetasizer Nano ZS or ZSP (Malvern Instruments GmbH, Herrenberg, Germany). Particle pellets were redispersed in MilliQ water. pH values of the particle suspensions were measured, and then 1:10 dilutions (with MilliQ water) were measured for size (173 ° backward scatter mode) and zeta potential (13 ° forward scatter mode).

Desmopressin integrity analysis

The integrity of the desmopressin after encapsulation and dissolution of the particles was checked with a liquid chromatography coupled electrospray ionization mass spectrometer (LC-ESI-MS). An Accela UHPLC system (Thermo Fisher Scientific, Waltham, MA, USA) with a built-in degassing system and a quaternary mixing pump was used. It was coupled to a Thermo Scientific TSQ Quantum Access Max mass spectrometer. Detection was performed by a full scan acquired from m/z 15 to 1100 after Electrospray-Ionization in positive ion mode.

Particle imaging

SEM images of particles were made with a Zeiss Evo HD 15 Electron Microscope (Carl Zeiss AG, Jena, Germany) and coated with approx. 10 nm gold with a Quorum Q150R ES sputter coater (Quorum Technologies Ltd., East Grinstead, UK) or with a Hitachi S-510 (Hitachi, Chiyoda, Japan) with an integrated DISS 5 image converter (point electronic, Halle (Saale), Germany). Samples were coated with gold in an Edwards S150 sputter coater (Edwards, Crawley, UK).

Confocal microscopy was conducted with a Zeiss Axiovert 100M (Carl Zeiss AG, Jena, Germany). For excitation, an argon laser from Coherent Inc. (Santa Clara, CA, USA) with 488 nm wavelength was used. Emission was detected with a BP filter of 505-530 nm wavelength.

PLGA-particle coating with human lactoferrin peptide (hLF) for barrier permeation enhancement

The hLF-peptide was dissolved in a KH_2PO_4 buffer and incubated at 37 °C for 2 hours to form disulfide bonds. Blank PLGA nanoparticles were prepared as described above. One mL of particle dispersion was placed in an Eppendorf tube (n = 3) and centrifuged (24 kRCF, 20 min, 16 °C). The supernatant was discarded and particles were washed with pure MQ water. The redispersed particles were then incubated with KH_2PO_4 buffer and hLF-peptide for 2 hours. After incubation, the sample was centrifuged again (24 kRCF, 20 min, 16 °C). The supernatant was removed, but not discarded and stored for analysis. The pellet was washed with MQ water and the redispersed particles were taken up in 2 mL KH_2PO_4 buffer and left at room temperature for 7 days. Samples were analyzed on day 0 (i.e. day of preparation), 1, 2, 3, 4 and 7.

For analysis, 100 µL of sample were taken and mixed with 900 µL of MQ water. The sample was analysed for pH and zeta potential. Another 200 µL were taken and put in an Eppendorf tube. The Eppendorf tube was centrifuged (24 kRCF, 20 min, 16 °C), particles and supernatant were separated and both measured with a QuantiPro™ BCA Assay Kit (Sigma Aldrich, Taufkirchen, Germany). The pellet was washed once with MQ water and then redispersed in 200 µL MQ water. BCA solution was prepared

according to the manual and 150 µL were mixed with the samples (either 150 µL of supernatant or particle dispersion) in a 96-well plate. The plate was incubated for 2 hours at 37 °C and then analyzed with the TECAN® Reader Infinite 200 PRO (Tecan Group Ltd., Männedorf, Switzerland) at a wavelength of 562 nm. All retrieved values were zeroed to comparing solutions. Therefore, plain particle dispersion without hLF-peptide (for particle dispersion), pure buffer (for supernatants) and pure water (for standards) were measured as well.

2.2.3 Hydrophilic particle preparation

As nanoparticles cannot be sufficiently delivered into the deep lung via inhalation, the PLGA particles had to be encapsulated into microparticles; however, for a local application in the lungs, or if the drug passed the lung barrier on its own, PLGA nanoparticles would be an unnecessary step, as the drug could be directly loaded into microparticles. If, on the other hand, a drug would not work well with the microparticulate carrier or needed a functionalized delivery vehicle, a combination of the two systems could be necessary. Thus, a new, versatile method was developed that allowed encapsulation of functionalized hydrophobic nanoparticles, as well as direct encapsulation of hydrophilic drugs for the delivery to the deep lung. Furthermore, it was a goal to be able to adjust the size of the particles as well as the hydrophilic polymer that was to be used. In most cases, dextran was used as hydrophilic polymer because it is used as a blood plasma expander [51] and thus has a good solubility in water, it is compatible with the human body.

Preparing emulsions by membrane emulsification

An “External Pressure Type Micro Kit” fabricated by SPG Technology (Miyazaki, Japan) was used for membrane emulsification. If not stated otherwise, hydrophobic glass membranes with a pore size of 0.5 µm diameter were used for emulsification. The dispersed phase was 2 mL of a 10 wt% dextran (150 kDa) (Sigma Aldrich) in aqueous solution. The continuous phase was pentane mixed with 0.25 vol% Span 80 and Tween 85 each (Sigma Aldrich). It was used in quantities of 80 mL pentane in a 100 mL beaker (50x70 mm) with a magnetic stirring rod (40x8 mm) at 400 RPM. The applied pressure to the dispersed phase was nitrogen at 2 bar. Runs were conducted until gas bubbles were floating up from the membrane, indicating that all aqueous solution had passed the membrane.

Table 2.2 Overview of membrane emulsification experiments. (Each experiment: n = 3)

Experiment #	Inner phase	Outer phase
# 1	10 wt% dextran	Pentane + 0.25 vol% Span80 + 0.25 vol% Tween85
# 2	10 wt% dextran + 0.1 wt% Pluronic F-127	Pentane + 0.25 vol% Span80 + 0.25 vol% Tween85
# 3	10 wt% dextran + 1.25 wt% Pluronic F-127	Pentane + 0.25 vol% Span80 + 0.25 vol% Tween85
# 4	10 wt% dextran + 5 wt% Pluronic F-127	Pentane + 0.25 vol% Span80 + 0.25 vol% Tween85
# 5	10 wt% dextran	Liquid paraffin + 0.25 vol% Span80 + 0.25 vol% Tween85
# 6	2.5 wt% chitosan (Novamatrix Protasan) (see description below)	Pentane + 0.25 vol% Span80 + 0.25 vol% Tween85

In Experiment # *6* a 2.5 wt% chitosan solution was used as inner phase. To produce more homogenous small emulsion droplets, multiple membrane cycles were used. First, the emulsification was carried out in the same way as for all other experiments. After that, it was left to sediment for at least 15 minutes. The sedimented droplets on the bottom of the beaker were collected with a pipette. The collected droplets were then used for the next cycle of membrane emulsification. Thus, they were put into the membrane emulsification device and pressed through the membrane into the continuous phase again to further homogenize the emulsion. For all cycles after the first, a pressure of about 5 bar was necessary. This procedure was repeated three times.

Preparing emulsions by high shear homogenizer method

For preparing emulsions with the high shear homogenizer, an Ultra Turrax® with a T25 base unit was used with an 18G rotor-stick (IKA®-Werke GmbH & Co. KG, Staufen, Germany). 80 mL of continuous phase (the same that was used for the membrane emulsification method) was directly mixed with 2 mL of dispersed phase (water with dissolved hydrophilic polymer) and emulsified in a 100 mL glass bottle. Homogenization was conducted at 16,000 RPM for 10 seconds.

Table 2.3 High shear homogenizer experiments overview. (Each experiment: n = 3)

Experiment #	Inner phase	Outer phase
# 7	10 wt% dextran	Pentane + 0.25 vol% Span80 + 0.25 vol% Tween85
# 8	2.5 wt% chitosan (Novamatrix Protasan)	Pentane + 0.25 vol% Span80 + 0.25 vol% Tween85
# 9	1 wt% alginate	Pentane + 0.25 vol% Span80 + 0.25 vol% Tween85
# 10	1 wt% glucomannan	Pentane + 0.25 vol% Span80 + 0.25 vol% Tween85
# 11	2.5 wt% gelatin	Pentane + 0.25 vol% Span80 + 0.25 vol% Tween85
# 12	1 wt% lignin NaOH was added until Lignin dissolved	Liquid paraffin + 0.25 vol% Span80 + 0.25 vol% Tween85

Precipitation and particle formation

For particle preparation, the polymer in the emulsion droplets was precipitated. Therefore, 5 mL of the emulsion (prepared either by membrane emulsification of by high shear homogenizer method) were taken up into a 10 mL plastic syringe. The syringe was equipped with a 0.6 mm diameter needle and mounted into a syringe pump (kd Scientific Legato 210, Holliston, MA, USA). The mounted syringe/needle was placed in 40 mL of ethyl acetate residing in a 100 mL beaker being stirred at 400 RPM with a magnetic stirring rod (40x8 mm). The syringe pump then injected the emulsion into the stirring ethyl acetate at a speed of 1 mL/min. Upon mixing, both, the outer phase of the emulsion (usually pentane with stabilizers) and the water of the inner phase, mixed with the ethyl acetate. The hydrophilic polymer (usually dextran) precipitates and forms particles as displayed in Figure 2.4.

Washing and solvent exchange

The precipitated particles were washed by taking the dispersion up into a syringe and pressing it through a syringe filter equipped with 100 nm pore size PTFE membrane. The solvent mixtures easily passed the membrane, whilst particles were retained. To wash off remaining solvents and stabilizers from the particles, 10 mL of pure ethyl acetate were pushed through the syringe filter. Afterwards, particles were redispersed by adding fresh ethyl acetate that was sucked up through the syringe filter from the other side, carrying the particles back into the syringe (similar as seen in Figure 2.5).

Afterwards, a solvent exchange from ethyl acetate to acetonitrile was carried out for lyophilisation. Therefore, 5 mL of acetonitrile were pushed through the syringe to remove the ethyl acetate remaining in the syringe filter, then 10 mL of acetonitrile were sucked through the syringe filter, carrying the particles into the syringe as displayed in Figure 2.5.

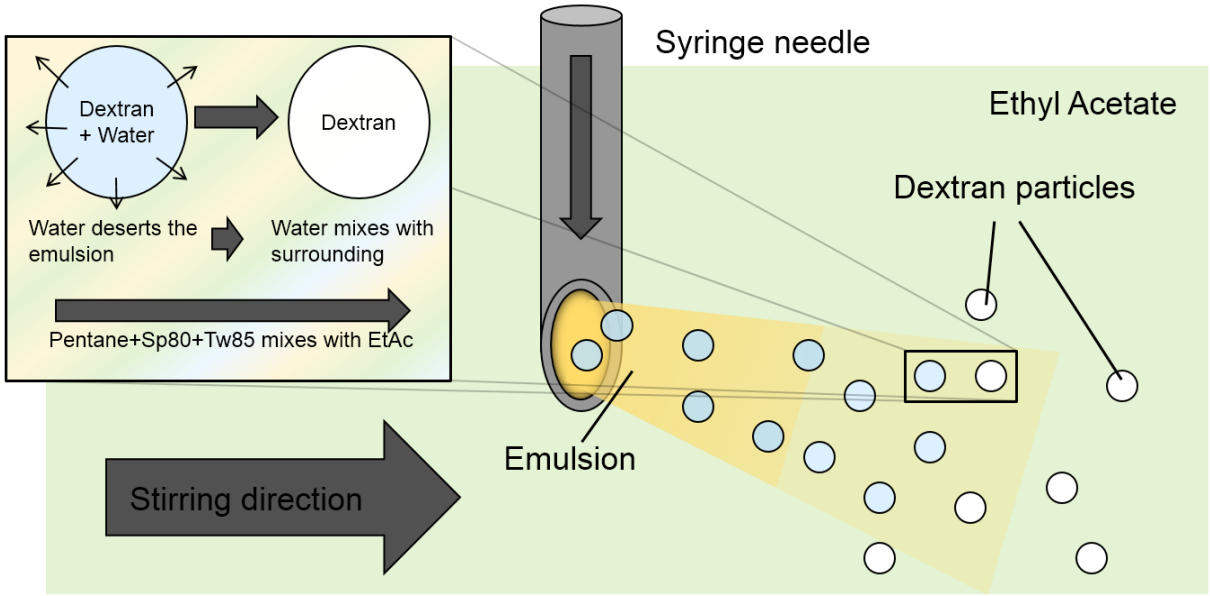

Figure 2.4 Schematic explanation of the precipitation process. Ethyl acetate is displayed in green, water in blue, pentane in yellow and pure dextran in white.

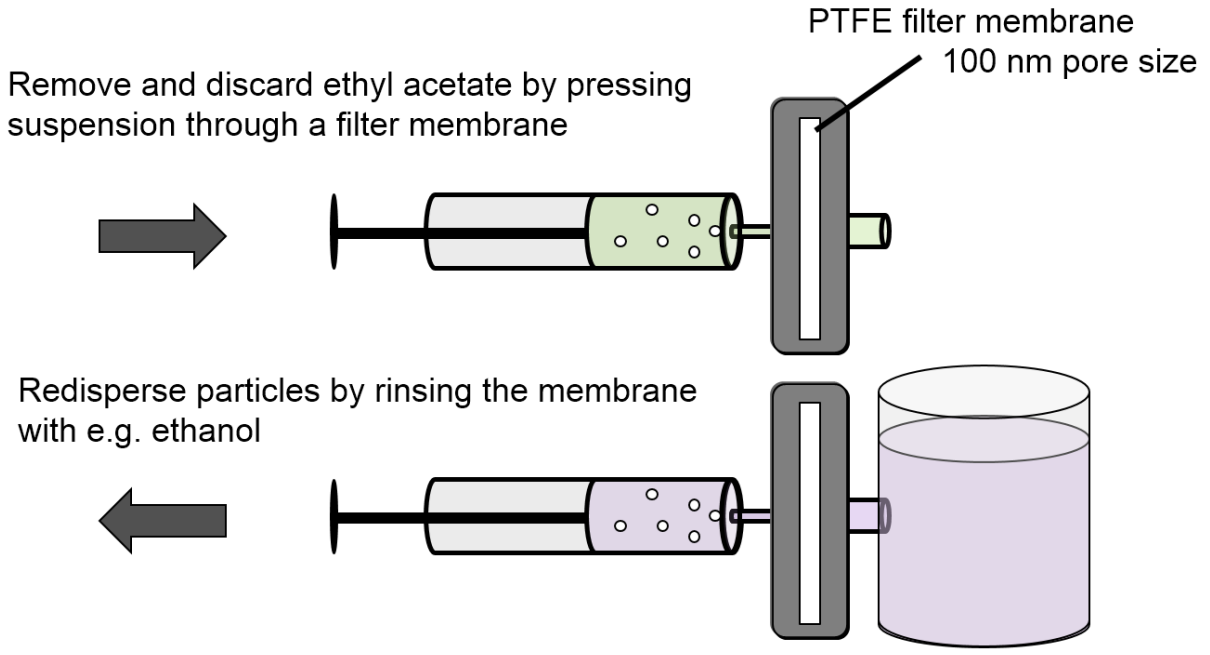

Figure 2.5: Schematic explanation of the solvent change by syringe and syringe filter. Ethyl acetate is displayed in green, another solvent, like for example ethanol or acetonitrile, is displayed in purple. Particles are displayed as white dots.

Size measurements

Sizes of microparticles were measured before washing in ethyl acetate with a Horiba LA-950 (Retsch GmbH, Haan, Germany). Calculation of the results was done with Mie-Theory using refractive indices of 1.530 for the solid phase and 1.371 for the liquid phase ethyl acetate.

Lyophilisation and drying

For lyophilisation, particles were washed and solvent was exchanged from ethyl acetate to acetonitrile, as described above. The dispersion was then put into glass vials with small holes in their lids. The acetonitrile was frozen by immersion of the lower half of the glass vials into liquid nitrogen for roughly 30 seconds. The glass vials were then placed in the pre-frozen freeze drier (Christ Alpha 2-4 LSC, Martin Christ Gefriertrocknungsanlagen GmbH, Osterode am Harz, Germany) at -80 °C condenser (and about -35 °C shelf) and a negative pressure of 0.2 mbar was applied. In every run, a maximum of 6 vials were placed in the freeze drier and left for 48 hours to sublimate acetonitrile. After retrieving the glass vials from the freeze drier, the holes in the lids were closed with tape to avoid additional air humidity entering the vials.

Direct encapsulation of desmopressin into dextran microparticles

For preparing the microparticles, 300 mg of Dextran were mixed with 1 mg desmopressin acetate in 1 mL of MQ water. Additionally, 500 µg of Pluronic F-68 were added. The mixture was then emulsified by membrane emulsification into pentane with 2.5% Span85 as stabilizer. Sediment substance was removed and the pentane of the remaining emulsion was removed by evaporation, until the emulsion was entirely in Span85. Then 25 mL of ethyl acetate with 10 mg/mL PEG were added to precipitate the emulsion droplets. The dispersion was stirred for 5 minutes and then centrifuged at 5000 RPM for 10 minutes in 50 mL tube vials. The supernatant was discarded and 20 mL of fresh ethyl acetate were added to wash the particles. After particle redispersion, it was centrifuged as above and the supernatant was removed. The wet particles were left to dry overnight under a hood. Analysis was conducted by HPLC: 5 mg of particles powder were dissolved in 1 mL of MQ water and analyzed as described in section 2.2.2.

Long-term stability

For checking long-term stability, the particles were stored at room temperature in sealed vials containing air atmosphere. After at least 11 months, SEM images of the particles were taken again for comparison.

2.2.4 Combination of PLGA and hydrophilic particles

Nanoparticles, as described in section 2.2.2, do not face impaction or sedimentation when applied to the lung, as those are only relevant above 1-2 µm. Below 1 µm, most particles reach the deep lungs but are exhaled again, with particles around 250 nm size having the worst deposition rates. At around 200 nm size and smaller, deposition improves due to diffusion effects.[96] However, separating single 100–150 nm sized particles for a pulmonary application can be challenging, such that a combined approach was chosen for this thesis.

The hydrophilic particles described in section 2.2.3 have the potential to deliver a payload to the deep lung, if prepared with the right aerodynamic properties, but they would most likely immediately dissolve, so that a controlled release over time or an enhanced barrier penetration would be impossible. A combined approach of both systems could be a solution to these problems. The drug could be encapsulated into functionalized PLGA nanoparticles and then packed into hydrophilic microparticles that reach the deep lung and release the nanoparticles there. The microparticles would dissolve quickly after transporting the nanoparticles to the deep lungs. The released nanoparticles could then mediate the transport through the lung barrier.

Preparation of PLGA nanoparticles for encapsulation into dextran microparticles

PLGA nanoparticles were prepared from PLGA, covalently coupled with fluorescein-amine (FA-PLGA). The particles were prepared in the same way as described in section 2.2.2, with the difference that no primary emulsion was used. I.e. FA-PLGA dissolved in ethyl acetate was directly mixed with aqueous PVA solution and sonicated (see Figure 2.6). After preparation, the particle suspension was adjusted to 20 mL volume, and 1 mL of it was centrifuged in an Eppendorf tube (24 kRCF, 25 min, 4 °C). The supernatant was discarded, and the pellet was rinsed with MQ water and then redispersed in 1 mL MQ water.

Preparation of dextran microparticles loaded with FA-PLGA nanoparticles

The preparation of dextran microparticles followed the description in section 2.2.3 experiment # *1*, with the difference that the stabilizers used in the outer phase were 1.25% of Span 85 and Brij O2 each, instead of the described 0.25% of Span 80 and Tween 85, and the glass membrane had a pore size of 2 µm instead of 0.5 µm. For the emulsification, 2 mL of 10% dextran (20 kDa) solution were prepared and 0.5 mg of FA-PLGA nanoparticles were added. Then the membrane emulsification was carried out with the PLGA nanoparticles in the dispersed phase. After the emulsification, the emulsion was left to evaporate roughly half of its volume to increase the droplet concentration. Precipitation was carried

out by hand instead of a syringe pump, all other parameters (volumes etc.) remained the same. Following that, 20 mL of the precipitated suspension were pressed through a 100 nm pore diameter PTFE filter membrane retaining the particles. The membrane was rinsed with 10 mL of ethanol, and thus the particles were brought back into ethanol. A few drops of this sample were dropped on a glass slide for CLSM analysis. A cover glass was directly put on top to prevent the evaporation of ethanol and drying of the sample, as the small 20 kDa dextran particles would instantly dissolve in air humidity, due to their hygroscopic nature.

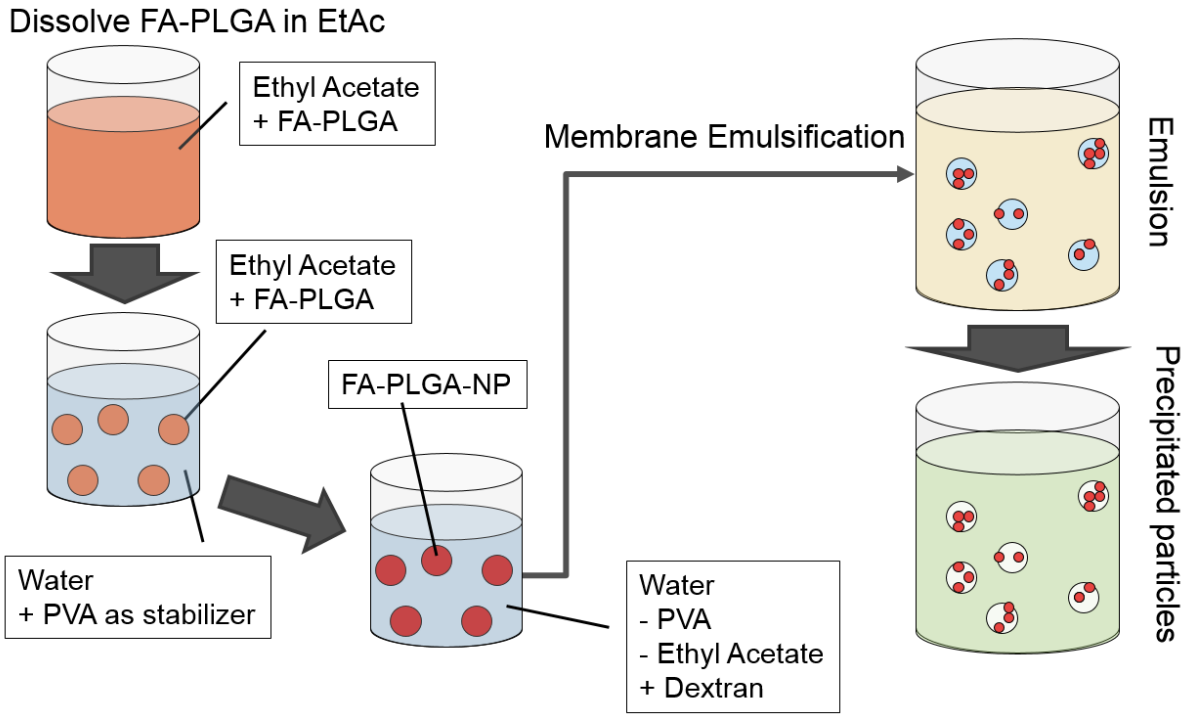

Figure 2.6: Preparation of FA-PLGA-NP loaded dextran microparticles for CLSM examination.

3 Results and Discussion

3.1 PLGA nanoparticles

This part will deal with the results of the preparation of hydrophobic PLGA nanoparticles, as well as with the encapsulation of desmopressin, its integrity after encapsulation, and the coating of the PLGA nanoparticles with hLF-peptide. Parts of the data shown have already been published by Primavessy et al.[38]

3.1.1 Characterization of PLGA nanoparticles

The PLGA nanoparticles, prepared as described in section 2.2.2, had sizes of 106-130 nanometers with small deviations (< 2 nm) in their triplicates. The PDI values were all well below 0.05; therefore, a monomodal distribution of particles can be assumed.[133] Zeta potentials were measured with values between -35 and -44 mV, which indicates, together with low PDIs, a stable dispersion. The pH values of all preparations were similar and lied between 5.5 and 6 (see Table 3.1).

Table 3.1: Sizes, PDI values, zeta potentials and pH values of the prepared particles. (Mean values, each experiment: n = 3)

	Size [nm]		PDI		Zeta potential [mV]		pH Value	
	Mean	Dev	Mean	Dev	Mean	Dev	Mean	Dev
BK	131.37	1.07	0.02	0.01	-44.36	2.81	5.65	0.06
CT	130.40	1.42	0.05	0.01	-39.03	3.82	5.56	0.05
PL	126.17	1.70	0.05	0.02	-38.64	2.26	5.82	0.54
PVA	125.64	1.77	0.02	0.01	-35.92	3.51	5.91	0.15
PEG	128.33	1.29	0.01	0.01	-40.70	1.67	5.91	0.03
TW21	106.32	1.66	0.08	0.03	-43.73	2.06	5.56	0.03
F68	119.14	0.94	0.05	0.01	-40.59	1.92	5.77	0.11
F127	118.19	1.52	0.06	0.02	-40.97	1.08	5.58	0.27

Depending on the stabilizer used, differences in particle size occurred, but made no substantial differences for the outcomes of the encapsulation experiments (see section 3.1.3). However, differences in size were unexpected in some cases:

As the Pluronics (F68/F127) and the Tween (TW21) are amphiphilic molecules, their function as stabilizers in the primary emulsion could have an impact on the particle size during the preparation as well (see Figure 3.1). PVA and PEG are both polymeric molecules, not consisting of different blocks. While PVA mainly stabilizes due to its partly deacetylation, PEG may only be able to act as spacer between molecules, as no amphiphilic parts are present in the structure. A small yet significant decrease ($p < 0.05$ in comparison to BK) of size can be observed. The most interesting result considering

that is the size of the PL particles. In their primary emulsion, asides from water, only desmopressin was present. Nevertheless, there is a significant drop in size ($p < 0.05$), compared to the blank particles (BK), where there was nothing but water in the primary emulsion. The particles of the coating approach (CT), which were prepared in the same way as the blank particles (BK) and later coated with desmopressin, had no significant size difference ($p > 0.1$) to the blank particles. As desmopressin is to be expected to sit on the surface of coated (CT) as well as on plainly encapsulated particles (PL), a measuring artifact by change of hydrodynamic diameter, due to desmopressin on the surface, can be ruled out. This leads to the assumption, that the emulsion of ethyl acetate in water is likely to be influenced even by non-amphiphilic non-polymer molecules – in this case desmopressin.

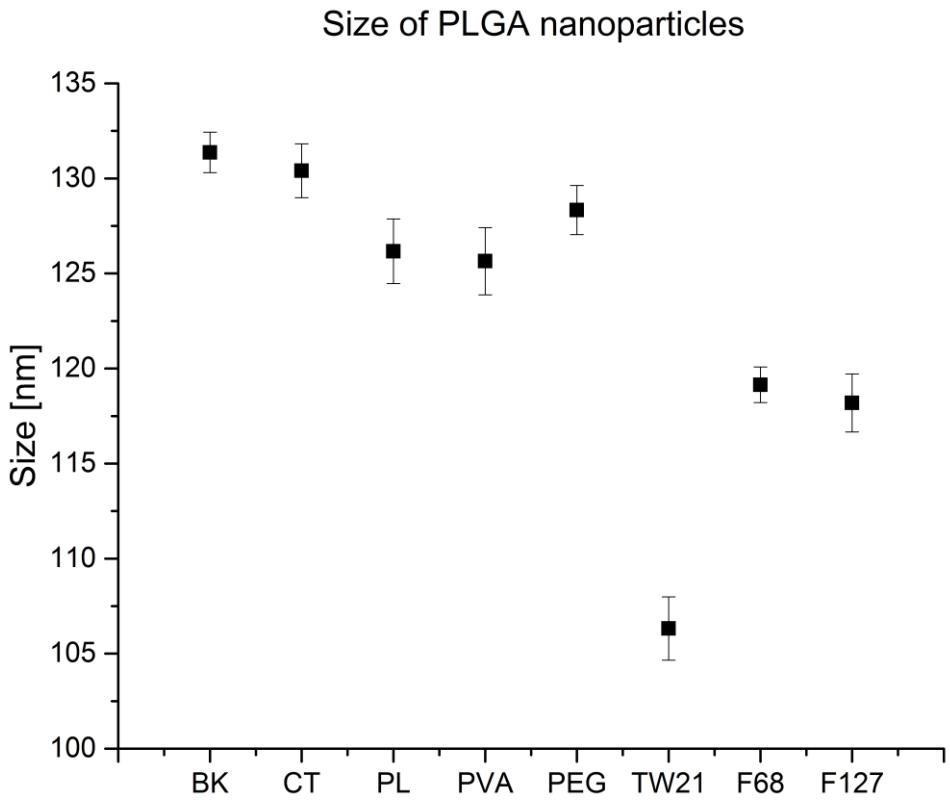

Figure 3.1: Sizes of PLGA nanparticles prepared with different stabilizers in the inner/primary emulsion. Stabilizer in the secondary emulsion was PVA.

The three amphiphilic stabilizers create much smaller particles than the others. Especially Tween 21 particles are small. Comparing those three stabilizers, what stands out is, that the two Pluronics are quite hydrophilic with HLB values of 29 (F-68) and 22 (F-127), while Tween 21 has a HLB value of 13.3.

Probably, the value of Tween 21 (13.3) is closer to the optimum HLB value of ethyl acetate, and therefore the emulsion droplets and the particles become smaller.

3.1.2 Particle dry weights

To calculate the loading efficiency, as drug to polymer ratio, the amount of polymer in 1 mL of particle dispersion was determined, as described in section 2.2.2 (Dry weight analysis).

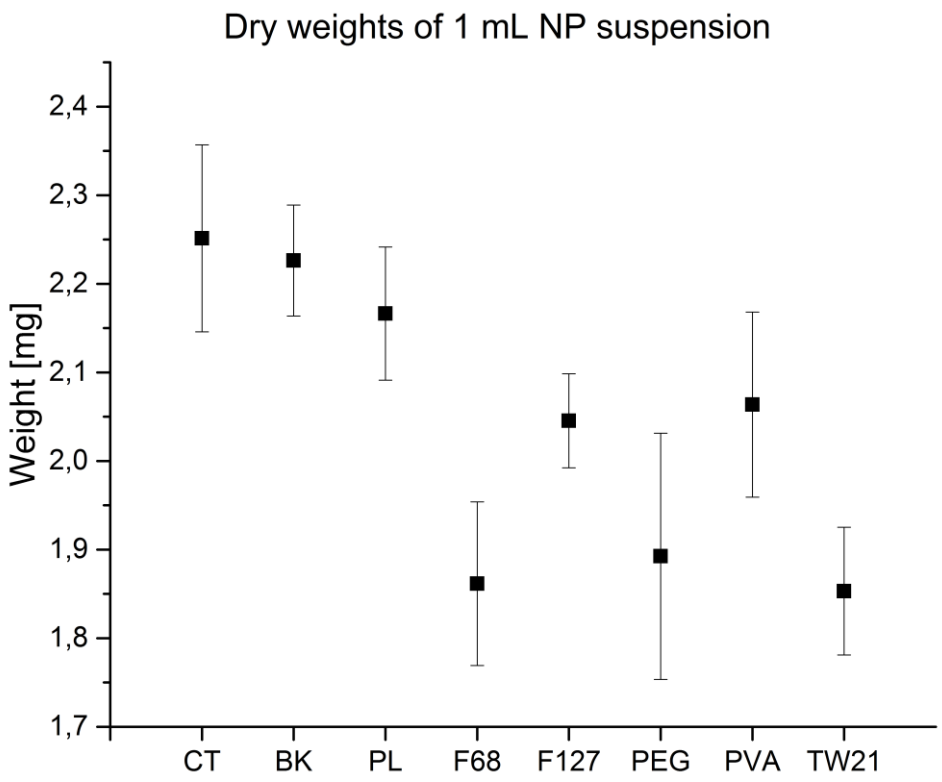

Figure 3.2: Dry weights of nanoparticle dispersions, measured after freeze drying and thermogravimetric analysis. (n = 3)

The amount of PLGA particles that should occur in 1 mL dispersion in case of no loss, would be 2.5 mg. The found values indicate, that the applied method provides the particles in dimensions close to its input. While no strong variation from the blank (BK) can be seen for coating (CT) and plain encapsulation (PL) samples, all other samples exhibit a smaller amount of dry weight. In first place, this is contrary to expectations, as the stabilizer that was additionally put into the samples, in contrast to CT, BK and PL, should also have its weight. However, this could indicate, that washing the samples

removed the stabilizer and the PVA of the secondary emulsion quite well. A reason for the lower weight could be, that the nanoparticle pellets were not as dense after centrifugation with additional stabilizers as without, and thus more particles were lost in the washing procedure. A stronger adsorption to surfaces, and thus a loss during production process, could also be a reason.

3.1.3 Encapsulation of desmopressin into PLGA nanoparticles

For the encapsulation, desmopressin acetate was chosen. It is a hydrophilic, robust and synthetic peptide of nine amino acids length. Encapsulating the hydrophilic compound into a hydrophobic polymer posed a challenge and provided the opportunity to test the effects of different stabilizers on encapsulation. Encapsulation efficiency and loading efficiency were calculated. While encapsulation efficiency is especially important from an economical point of view, as it shows how much of the expensive drug actually goes to the produced formulation, the loading efficiency is more of therapeutic importance, as it relates the mass of the excipient to the mass of the drug, and thus provides information on dosage dimensions (see Equation 2.6 and Equation 2.7 in section 2.2.2).

The exact values of loading and encapsulation efficiencies, determined with HPLC, can be seen in Table 3.2. The highest loading efficiency was obtained with Pluronic F-68 as stabilizer (1.16 ±0.07 µg/mg), with a small difference to Pluronic F-127 (1.06 ±0.11 µg/mg). For the PEG (0.95 ±0.04 µg/mg) and the TW21 (0.90 ±0.05 µg/mg) approach, a higher loading efficiency than the coating approach could be determined, while for PVA (0.77 ±0.17 µg/mg) the result was not conclusive, due to a high standard deviation. The value of the PL (0.88 ±0.09 µg/mg) approach was close to the CT (0.74 ±0.01 µg/mg) approach that did not allow a clear statement; therefore, a statistical analysis by applying a two sample t-test with different variances was performed. The result of the test was that PEG, TW21, F68 and F127 significantly differ from the CT approach ($p < 0.05$), while for PVA and PL this could not be found. Especially interesting is the fact that F68 is also significantly higher than PL, which underlines that there is no significant difference between PL and CT, and thus using no stabilizer results in coating the outer surface of the particles.

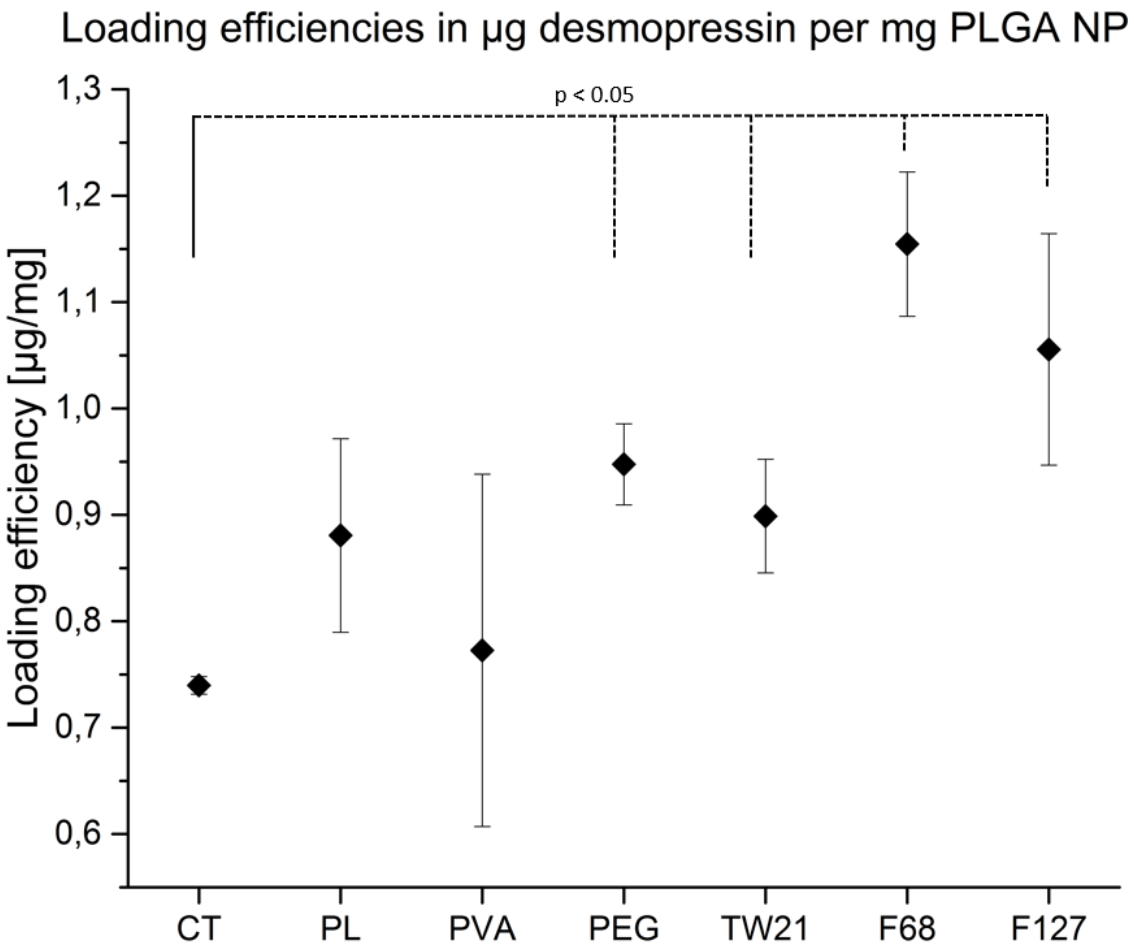

Figure 3.3: Loading efficiencies of desmopressin in PLGA nanoparticles in dimensions of µg per mg. The dry weights, measured with thermogravimetric analysis displayed in Figure 3.2, were used for calculation. T-tests revealed that the samples PEG, TW21, F68 and F127 each are different from the CT approach with p < 0.05. (N = 3)

Table 3.2 Encapsulation and loading efficiencies of desmopressin into PLGA nanoparticles

	CT	PL	PVA	PEG	TW21	F68	F127
Encapsulation efficiency [%]	6.66 ±0.02	7.63 ±0.20	6.38 ±0.34	7.17 ±0.07	6.66 ±0.10	8.60 ±0.13	8.64 ±0.22
Loading efficiency [µg/mg]	0.74 ±0.01	0.88 ±0.09	0.77 ±0.17	0.95 ±0.04	0.90 ±0.05	1.16 ±0.07	1.06 ±0.11

3.1.4 Desmopressin integrity after encapsulation

Desmopressin as a peptide is more prone to degradation than most other substances. To ensure that desmopressin is still intact, it was analyzed with mass spectrometry after the dissolution of the particles and the complete release of desmopressin.

The dissolved desmopressin was first separated by liquid chromatography in the LC-MS device, and then a total ion chromatogram was measured in positive scanning mode. Desmopressin has two charges, such that with a molecular weight of 1068.4269 the main peak of the ion would be at an m/z ratio of 535.5.[134]

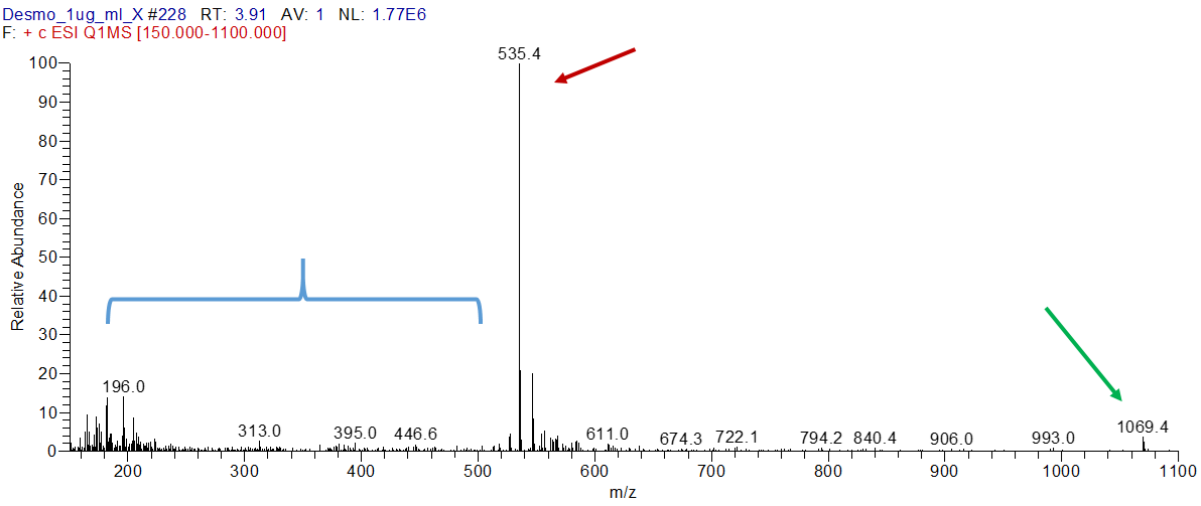

Figure 3.4: Total ion chromatogram of desmopressin determined with mass spectrometry. The peak at 535.4 (red arrow) is the double positively charged desmopressin. The peak at 1069.4 (green arrow) is desmopressin with only a single group charged. The area indicated by the blue bracket is where fragments of desmopressin should be visible if there were any.

Figure 3.4 shows the total ion chromatogram of a 1 µg/mL desmopressin standard (not dissolved particles). The peak at 535.4 m/z (red arrow) shows the intact desmopressin, fractured desmopressin could not be found as explained below:

A fractured piece of desmopressin could have two charges, and thus be lower in m/z ratio than the whole molecule (and the second fractured part would not appear, as it had no charge). Or there would be two parts with one charge each, then one would be larger than the ion at 535.4 m/z and one would be smaller (or both would be 535.4, which is highly unlikely). The fact, that there is no significant peak below 535.4 m/z (blue bracket area in Figure 3.4), shows that desmopressin has not been fractured. The peak at 1069.4 (green arrow) is exactly the molecular weight of desmopressin plus one proton that is responsible for the charge; furthermore, the double charged desmopressin has an m/z ratio of 535.2, if the two ionization protons are taken into account ((1068.4 + 2)/2 = 535.2). This demonstrates that the disulfide bond between the two cysteine residues is still intact, as otherwise the m/z ratio should be 1070.4 or 636.2, because of the protonation of the two sulfur groups.

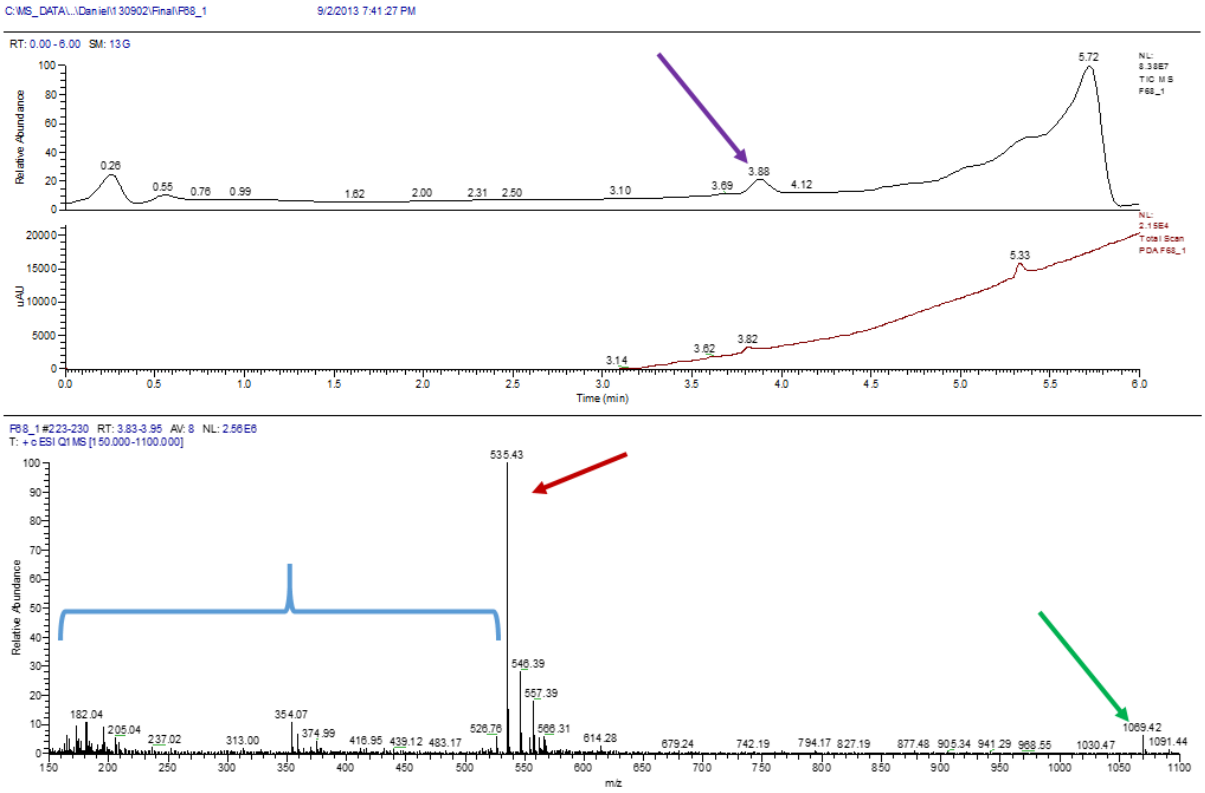

Figure 3.5: The upper part of the image shows the liquid chromatogram, with the retention peak of desmopressin at 3.88 minutes (purple arrow), where the total ion chromatogram (lower half of the image) was measured. Analogous to the standard in Figure 3.4, the red arrow points at the double charged desmopressin peak, the green arrow at the single charged desmopressin peak, and the blue bracket indicates the area where fragments of desmopressin should be visible, if there were any.

Figure 3.5 shows the LC chromatogram (upper) as well as the total ion chromatogram of the mass spectrometer (lower) of the F68 sample. In the chromatogram, the retention of desmopressin occurred after roughly 3.9 minutes (see purple arrow). All other peaks are either due to the sample injection, or due to baseline drift; thus, they are not relevant for the analysis. The mass spectrum has therefore been taken from a retention time of 3.83 – 3.95 minutes. As can be seen in the lower graph, the peaks map perfectly to the peaks of the standard in Figure 3.4. Therefore, it can be concluded, that desmopressin is not affected by encapsulation or particle dissolution in any way. These findings were analogous to the results of all other experiments (CT, PL, PVA, F127 and TW21). The total ion chromatogram of the PEG approach looks different, compared to the other samples, as PEG itself produces very typical peaks in the mass spectrometer. If these PEG-typical peaks are ruled out, the chromatogram looks analogous to all others.

3.1.5 Coating of PLGA nanoparticles with hLF-Peptide

A functionalization of the PLGA nanoparticles is an important next step towards the application. The human lactoferrin peptide is derived from the lactotransferrin protein, which is known for anti-microbial and anti-fungal activity.[135, 136] It was already known, that the peptide is a penetration enhancer that can be used to mediate penetration into cells.[105] A coating of PLGA particles with hLF-peptide could result in an increased uptake of particles into the cells or through the thin squamous epithelium of the deep lungs, and in this way it could result in a better bioavailability of a drug transported in functionalized particles.

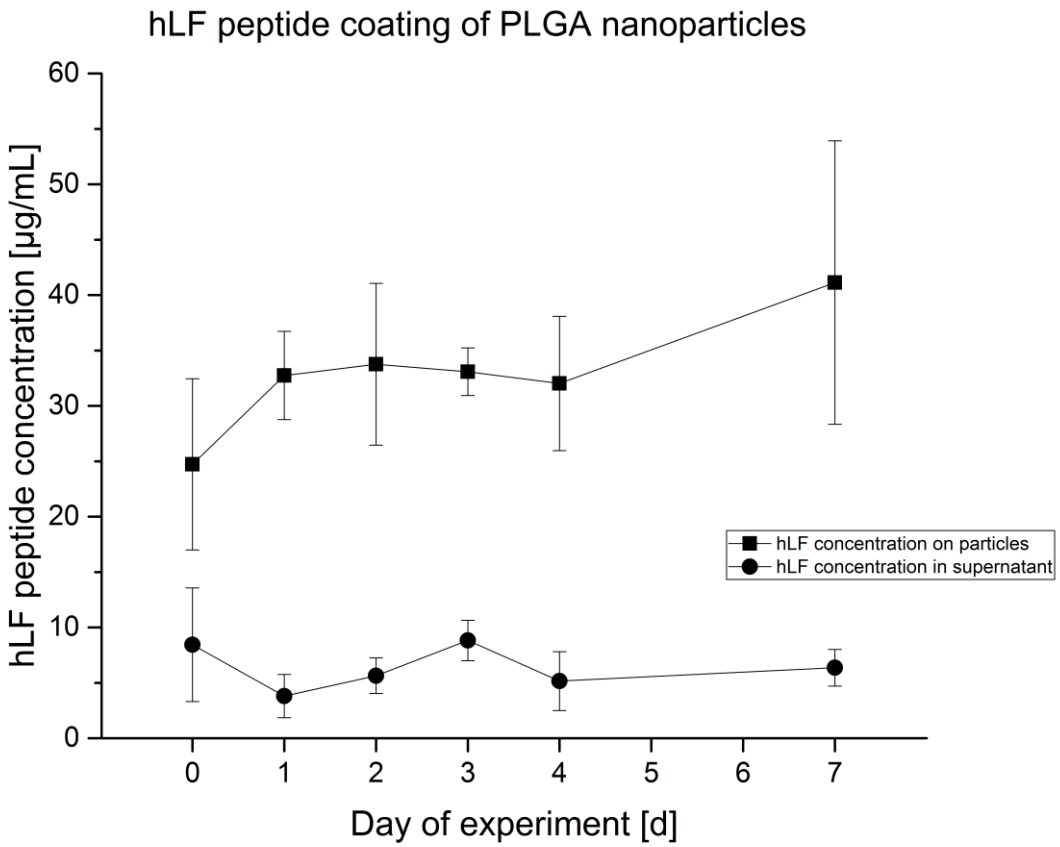

Figure 3.6: Concentration of hLF-peptide on PLGA nanoparticles and in the supernatant posterior to coating. Over seven days, the concentration of the hLF-peptide on the particle stays constant, as no release to the medium (MQ water) could be seen. The data point of day 0 was taken right after the coating experiment. (n = 3)

Figure 3.6 shows the surface coating experiment of hLF-Peptide on PLGA nanoparticles (described in section 2.2.2). As can be seen, the concentrations of hLF-Peptide in the supernatant (round) and on the particles (squares) do not change over time. As each data point has been prepared as a single sample and not as one sample from which amounts were taken every day, there was no change in

concentration in the samples. The concentration in the vial that was left for one day, is the same as in the vial that was left for seven days – in case of both: particles and supernatant. This indicates, that the hLF-Peptide can be stably adsorbed to the surface of PLGA particles, and thus a functionalization is possible.

3.2 Hydrophilic microparticles

This section explains the results of the preparation of hydrophilic microparticles. Aside from the characterization of the prepared particles, the method is explored in more depth and the encapsulation of desmopressin directly into the microparticles is discussed.

Particle preparation – An overview

The preparation of particles follows a simple process, which is quite similar to the preparation of PLGA nanoparticles. The core difference is, that the phases are switched. While in case of PLGA nanoparticles, an emulsion of ethyl acetate in water is produced and by volume expansion of water the partially soluble solvent ethyl acetate dissolves in water leaving the PLGA to precipitate, a method with switched phases is more complex. Ethyl acetate in water emulsions are easy to stabilize with PVA or water soluble stabilizers; however, water in ethyl acetate emulsions are different, as PVA has a very low solubility in ethyl acetate. Therefore, a step in between, where a stable emulsion was formed prior to precipitation, had to be introduced. This disadvantage of an extra step, on the other hand, leaves the opportunity to process the emulsion before the precipitation step, without worrying about volume changes. During the precipitation step (see Figure 2.4), both liquids of the emulsion mix with the precipitation solvent; only the compound dissolved in the inner phase of the emulsion will be precipitated by the precipitation solvent. The choice of the three solvents that interact with each other, is crucial for the method. While the two solvents of the emulsion must not mix with each other, they both have to mix in the precipitation solvent at the same time. In most experiments conducted, pentane was used as outer phase of the emulsion; however, hexane and heptane both worked as well. Pentane was used because it evaporated quickly, and thus provided a possibility to condense emulsions easily during the development phase. At a later point, liquid paraffin was introduced, because of the better biocompatibility. Also, the emulsions in paraffin tended to be more stable than those in pentane, which could be due to the higher viscosity of paraffin. Besides, ethyl acetate, acetone and ethanol were tested as precipitation solvents; however, in both cases no homogenous particles could be prepared, but flocks that sedimented quickly. Also, ethanol was too polar for some of the stabilizers used for the emulsion. It is probable, that the partial miscibility of water and ethyl acetate

is the necessary characteristic for a proper particle formation; however, other partially miscible solvents have not been tested, as most of them are not as biocompatible as ethyl acetate.

The preparation of the emulsion had two primary aspects: the choice of a suitable stabilizer, as well as a way to apply energy to form the emulsion. One of the most common ways to produce emulsions is a high shear homogenizer (e.g. UltraTurrax®) that blends the mixture in an emulsion. This method is easy and quick, but was only used for proof-of-principle experiments. Many modern pharmaceutical formulations have peptides or proteins as therapeutically active ingredients, which are very sensitive to the application of energy. Forming an emulsion without directly applying energy to the compounds, was desired. Membrane emulsification provides a scalable method that allows to apply energy, while ensuring that this energy is not applied to the active ingredient. However, the size of the emulsion droplets correlates with the pore diameter of the membrane used, and thus causes a higher friction between solvent and membrane. Since polymer solutions had to be turned into emulsions, the viscosity of the polymer in solution added a large factor to the friction between solvent and membrane. For dextran, as an extremely water soluble polymer, small pores posed not much of a problem, in comparison to gelatin or even glucomannan, which were unable to pass the membrane in some cases. Applying higher gas pressures would rather result in a separation of polymer and water on the membrane surface. Therefore, membrane emulsification experiments were only conducted with dextran and chitosan.

The choice of the correct stabilizer was difficult. For the first experiments, Brij O2 (2.5%) was used; however, despite being a very lipophilic stabilizer (HLB: 5), the dissolution in alkanes did not always work well. For this reason, the more lipophilic component Span 85 (HLB: 1.8) was chosen. Preparing the emulsion worked well, but for the precipitation, and especially for further washing steps with ethanol, the stabilizer was too hydrophobic, and thus it did not mix with the washing solvent and stayed in the sample. The stabilizers were then changed to a concentration of 0.25% of Tween 85 and Span 80 each, following an example in the manual of the membrane emulsification device. Tween 85 with an HLB of 11 could not dissolve in the alkane; however, upon adding Span 80 (HLB 4.3), both stabilizers dissolved well. Also, the mixture of these two stabilizers (HLB 7.65) dissolved in ethyl acetate and could be washed with more polar solvents like ethanol. Since droplet size mainly depends on the pore size of the membrane, as described in the “membrane emulsification” part of section 2.2.1, experiments with different HLB values or stabilizers were not of higher priority.

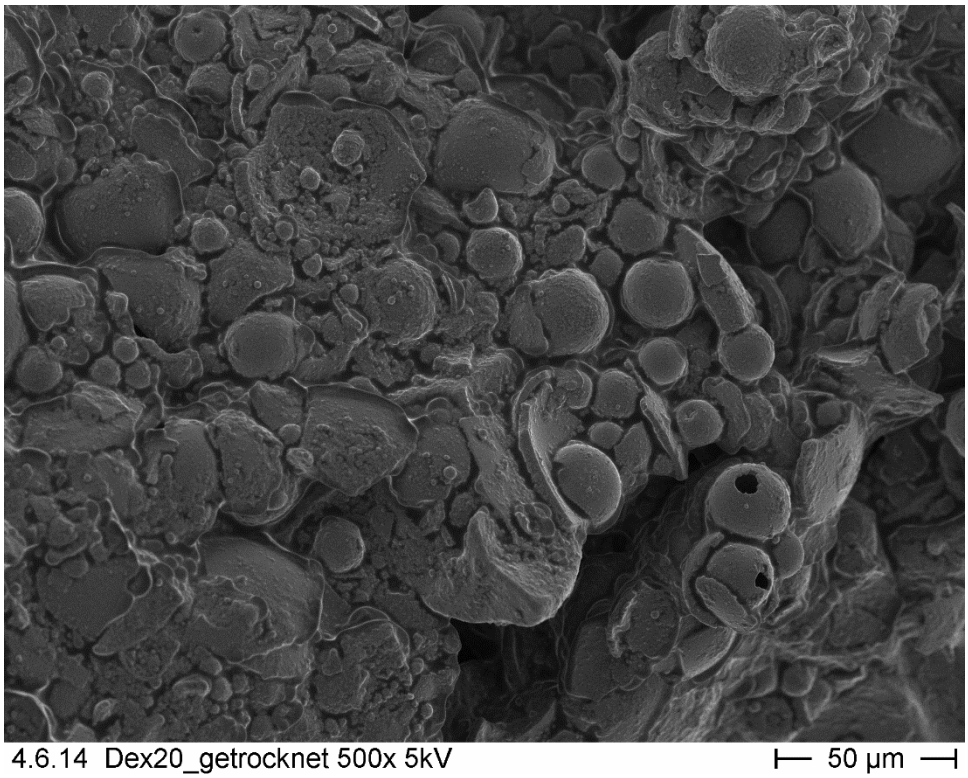

Figure 3.7: The image shows dried dextran particles. Many dextran particles are fractured or broken down to debris.

Among the organic solvents, ethanol is probably one of the most biocompatible; however, particles cannot be administered in pure ethanol, neither on pulmonary route nor on any other, such that the ethanol had to be removed as well. The first approach taken for this problem was the evaporation of ethanol. Since the raising concentration of particles during the evaporation caused aggregation of the particles, as a step to prevent aggregation the sample was placed in an ultrasound bath. The continuous ultrasound did not only prevent the particles from aggregation, it also fractured many of them, resulting in particle debris (see Figure 3.7). As a result of this, freeze drying was chosen as a possible approach to overcome that problem. Once frozen, the particles would not move anymore, and the solvent could be removed. Since ethanol has a very low freezing point (-114.5 °C), this was impracticable in our laboratory. Therefore, after the washing step with ethanol, the solvent was changed to acetonitrile, which has a freezing point around -45 °C. Except for the experiments with Pluronic F-127, there was no other reason to use acetonitrile than this, and for any pharmaceutically relevant application in production acetonitrile should be left out, as it is more toxic than ethanol.

3.2.1 Preparation of uniform sized particles

Particles are prepared by precipitation from an emulsion droplet; therefore, it is assumed that the particle size correlates with the size of the emulsion droplets. Emulsions prepared by membrane

emulsification usually have a wider size distribution, but multiple membrane cycles can homogenize the droplet size distribution very well, as shown by [137] for oil in water emulsions.

In the experiment to prepare uniform sized particles (Experiment # *6*, see section 2.2.3), in the first cycle an aqueous chitosan solution was pressed through a glass membrane. The result of the first cycle was larger droplets that sedimented quickly. After sedimentation, the droplets were taken into a second cycle, in which they passed the membrane again. This was repeated 2 more times. (see Figure 3.8)

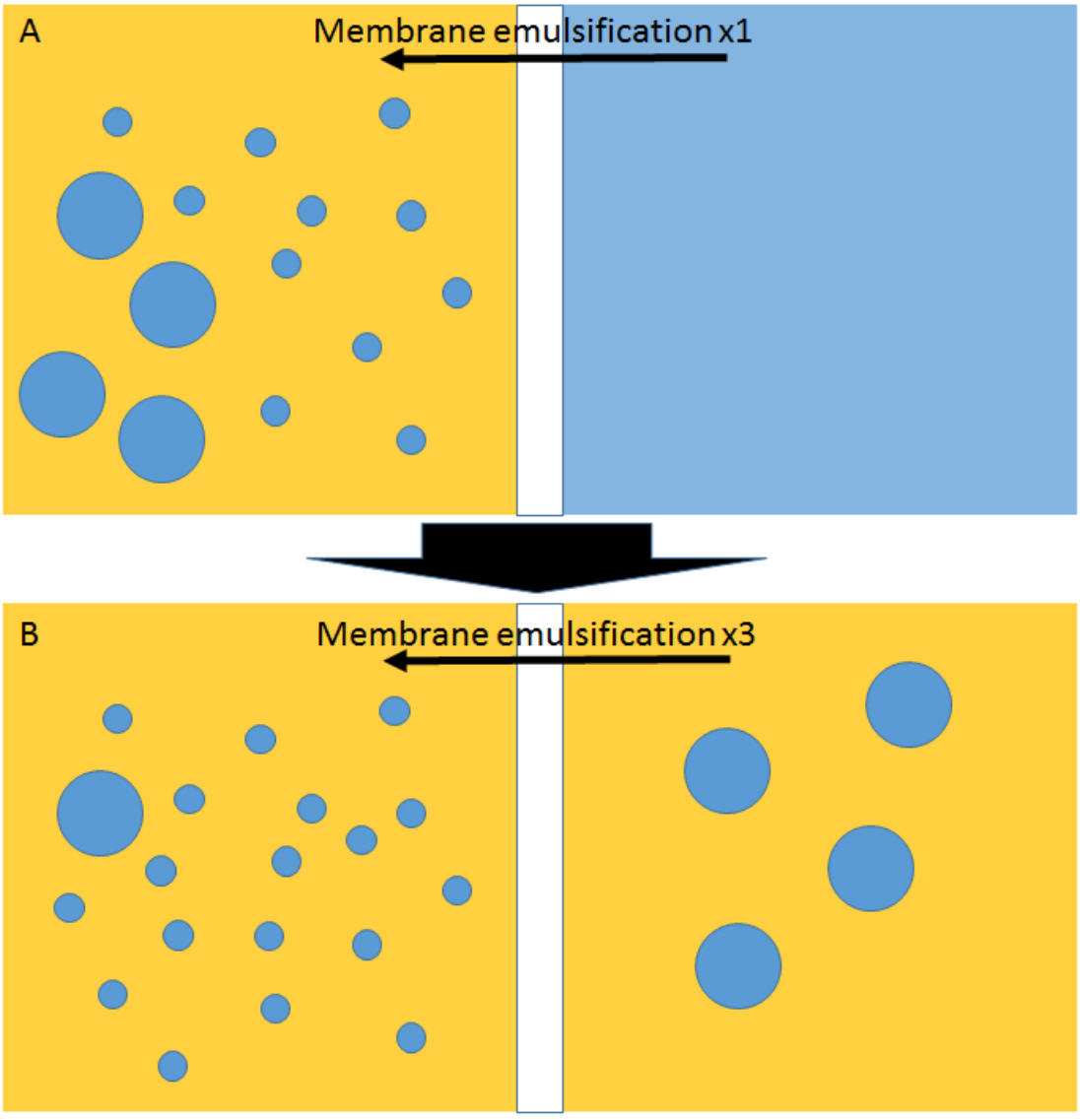

Figure 3.8: Homogenization of the emulsion droplets. The emulsion is prepared (A), after sedimentation the larger droplets are collected and emulsified again (B). The latter step is executed three times.

As a result of further membrane cycles, the emulsion turned more opaque with each step. An SEM image of the precipitated particles suggests, that there is a distribution of smaller particles and one of larger particles (see Figure 3.9). To determine the actual size distribution, the dispersion was analyzed with a Retsch Horiba LA-950. The result graph (Figure 3.10) plots particle diameters versus the volume % of the particle's corresponding diameter. The peaks shown are rather broad and unexpected, when comparing to what can be seen in Figure 3.9. However, the result yields some interesting numbers. The cutoff in the image (purple line) was chosen at 1 µm, indicating that 31.35% of the total volume are of 1 µm size or lower. As volume scales by third power, ten times larger particles have 1000 times more volume. Considering this fact, it becomes clear that there must be more small particles than large particles. To visualize this, particle sizes of 361 particles in three different images were measured by hand. The result in Figure 3.11 shows that most particles are below 1 µm, peaking in sizes between 0.6 and 0.69 µm.

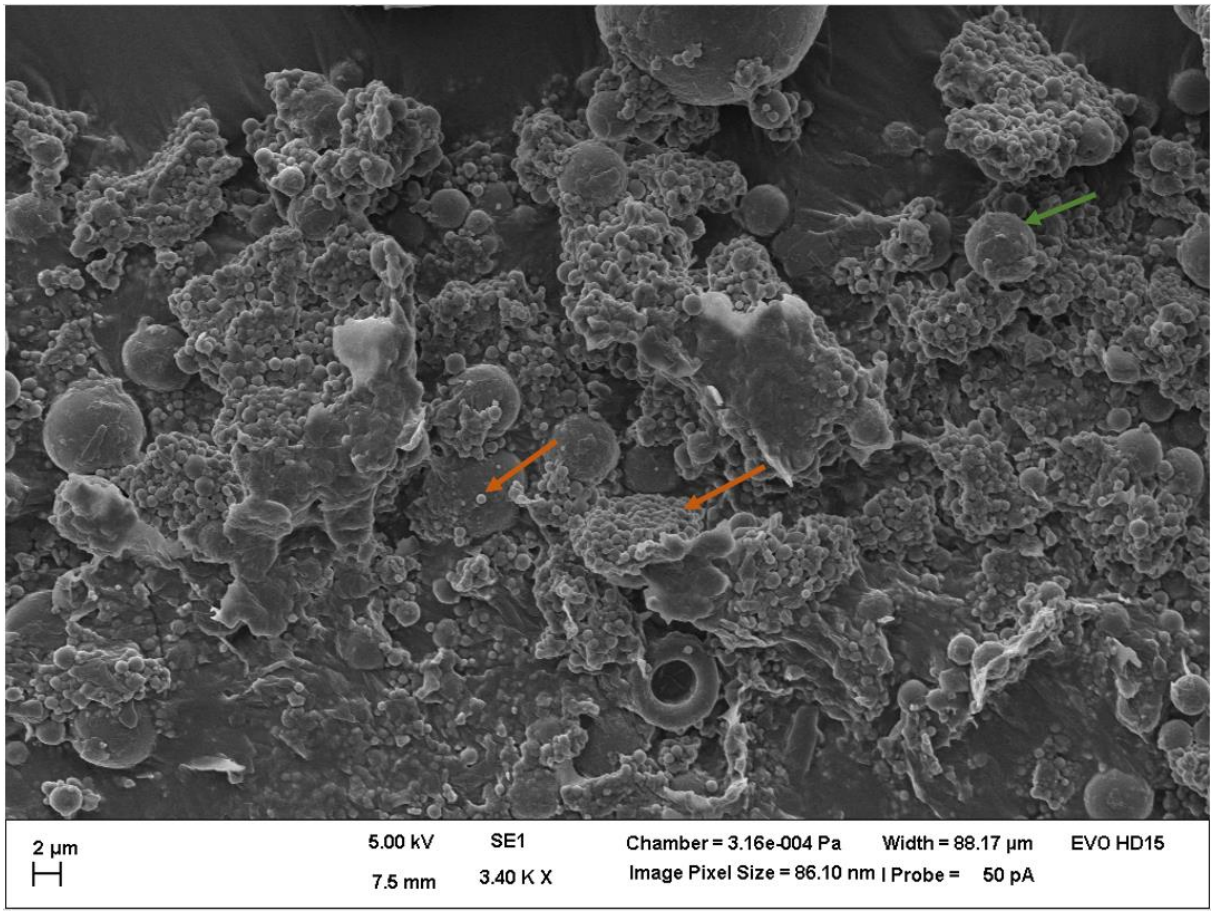

Figure 3.9: Chitosan particles prepared with membrane emulsification, multiple membrane cycles and precipitation. Among many small particles (orange arrows) few larger particles (green arrow) can be seen.

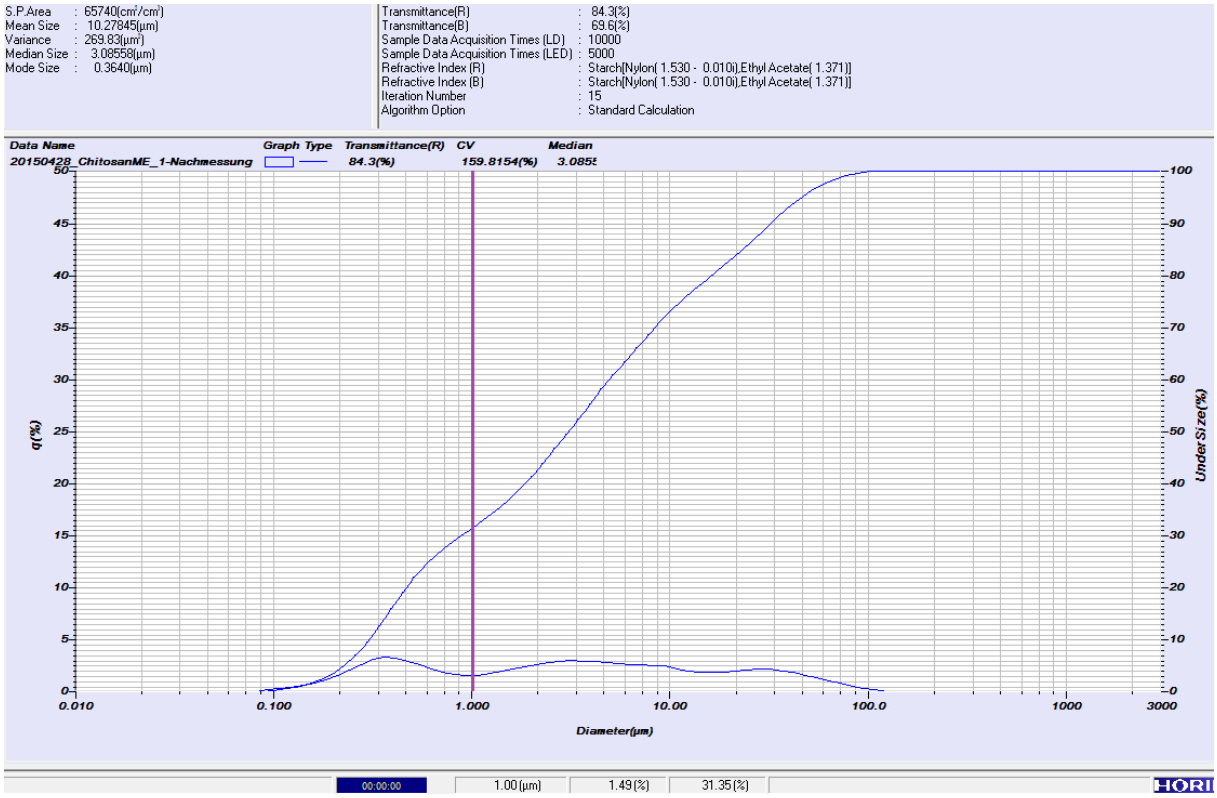

Figure 3.10: Particle size distribution by volume, measured with a Retsch Horiba LA-950. The X-axis shows the size of the particles, while the left Y-axis (referring to the lower blue line) shows the figures of volume-% in particles of the corresponding size. The right Y-axis refers to upper blue line and shows the cumulative volume-% of particles. The purple line at 1.0 µm shows the cutoff, at which the three values written below the graph are indicated: 1 µm particles make 1.49% of the total volume, while 31.35% of the total volume are of 1 µm size or lower. Refractive indices for calculation were used from starch and nylon, as they were closest to the values. The sample was measured in ethyl acetate.

These results indicate, that it is possible to produce large amounts of Chitosan nanoparticles with the presented method. The multiple membrane cycles created a large fraction of smaller particles. Maybe, more membrane cycles would even pronounce this effect. Also, the size is quite surprising, as 0.6 – 0.7 µm is only 1.2 to 1.4 times the size of the pore size of the membrane used (0.5 µm). The peak in the volume distribution result in Figure 3.10 has its maximum between 0.3 and 0.4 µm, in contrast to 0.6 µm in Figure 3.11. As the refractive index of Chitosan is only estimated with similar components, the laser diffraction method probably underestimates the actual size of the particles. A loss of smaller particles during washing is rather unlikely, as the PTFE filter membrane that was used had a pore size of 0.1 µm which would hold back particles of sizes around 0.3 – 0.4 µm without a larger loss. Nevertheless, this concludes to the suggestions to use a membrane with slightly larger pore size for future experiments, as the particle distribution should then move rather in the direction of 1 µm sized particles.

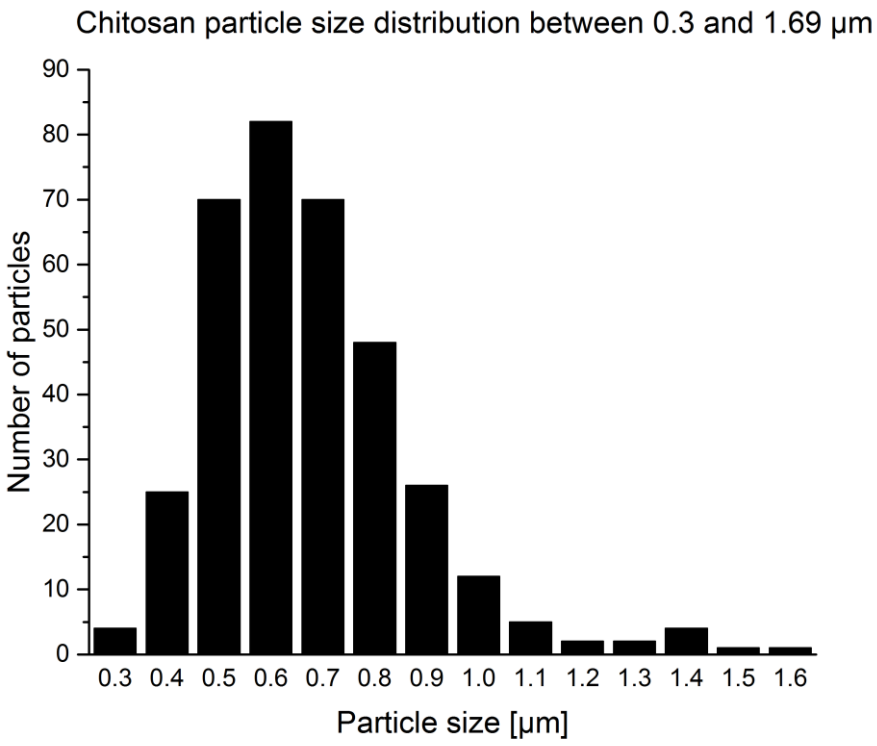

Figure 3.11: Particles size distribution by numbers. For measuring all values, 361 particles in three different images were counted and measured. Only particles of the size between 0.3 µm and 1.69 µm were considered, as larger particles occurred only very sparsely. The size distribution peaks between 0.6 and 0.69 µm.

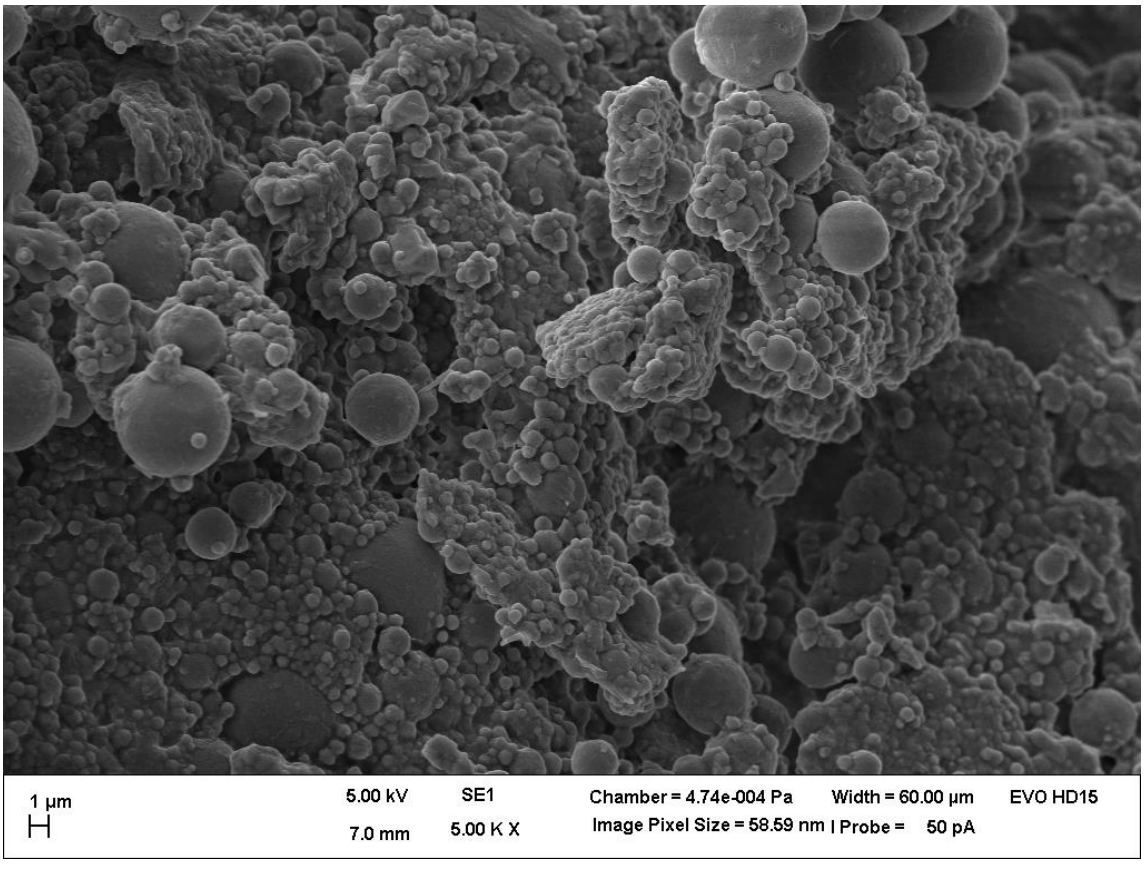

Figure 3.12: Long-term stability image of ME Chitosan particles. The image was taken about 11 months after the image of Figure 3.9.

Figure 3.12 shows the same sample as in Figure 3.9, but about 11 months later. Upon a close look, no differences between the particles can be seen. Considering the fact, that the particles were stored at room temperature and sealed under air atmosphere, the particles seem to be stable. This counts not only for the big, but also for the small particles, where the surface is larger in comparison to their volume.

3.2.2 The use of Pluronic F-127 as porosity agent

In the first place, Pluronic F-127 was used in the aqueous phase of the emulsion to have a stabilizer that helps to decrease the friction during the emulsification process inside the pores of the membrane. The significant reason for higher friction, however, was rather an obstruction of the membrane pores by the polymer than the friction, as the Pluronic did not solve this problem. But it was found in preliminary experiments, that particles that contained Pluronic F-127 had unexpected structures (see Figure 3.13). Both particles shown in Figure 3.13 seem to have similar inverse structures. The only difference between them is the solvent that was used for purification. Water-ethanol mixtures dissolve Pluronic F-127 well; however, pure ethanol does not dissolve, but probably soften and swell it. The dextran particle on the left image (A) was washed with ethanol only; a porous structure cannot be seen, but the popping out parts are probably Pluronic F-127. The dextran particle on the right (B) was washed with acetonitrile which dissolves Pluronic F-127 well. From this it was concluded that Pluronic F-127 can be washed out from Pluronic/Dextran particles, in order to obtain porous dextran particles.

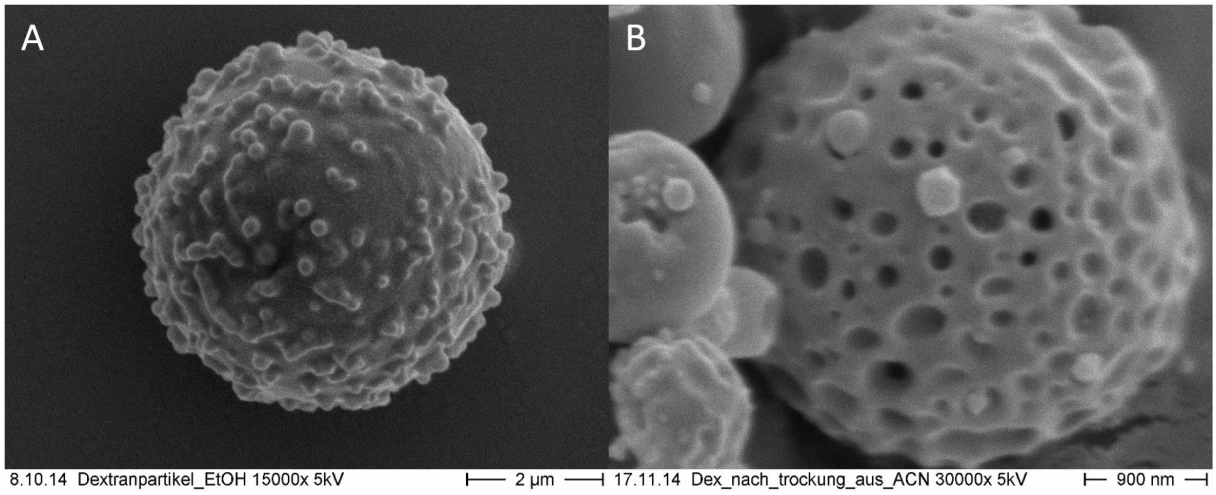

Figure 3.13: Dextran particles prepared with Pluronic F-127. While the particle on the left side (A) has been washed with ethanol, a substance that softens, but not fully dissolves Pluronic F-127, the particle on the right side (B) was washed with acetonitrile which dissolves Pluronic F-127 easily.

To confirm this, a set of experiments was conducted with different concentrations of Pluronic F-127. The experiments are described as Experiments # *1*, # *2*, # 3 and # 4 in section 2.2.3). While experiment # *1* was a negative control, in experiments # *2*, # 3 and # 4 Pluronic F-127 was added in concentrations of 0.1, 1.25 and 5 wt% respectively.

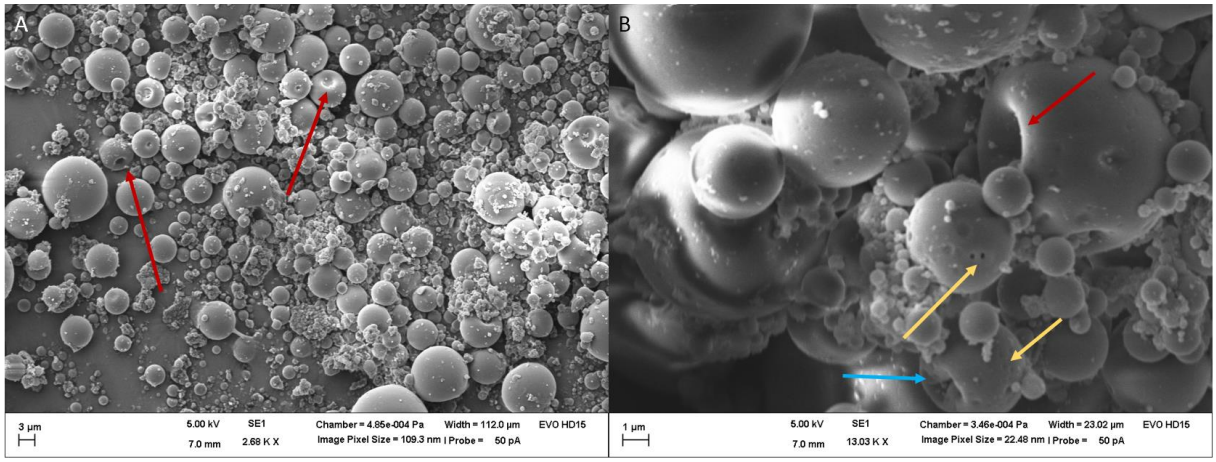

Figure 3.14: Dextran particles prepared without Pluronic F-127 (A) and with 0.1 wt% Pluronic F-127 (B). Red arrows mark preparation-typical dents (deformations) of particles. Yellow arrows mark porous like structures and blue arrows mark unusual deformations.

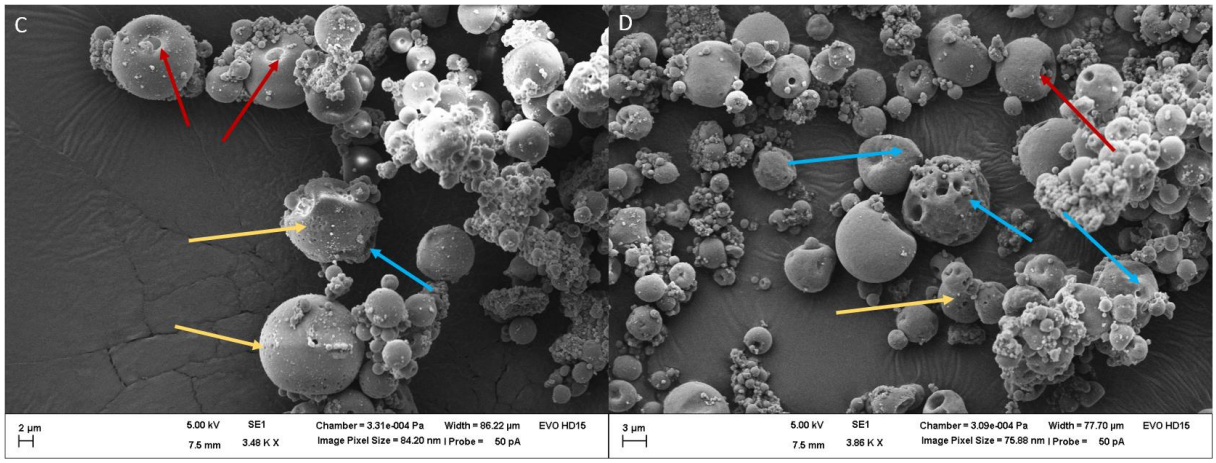

Figure 3.15: Dextran particles prepared with 1.25 wt% Pluronic F-127 (C) and with 5 wt% Pluronic F-127 (D). Red arrows mark preparation-typical dents (deformations) of particles. Yellow arrows mark porous like structures and blue arrows mark unusual deformations.

The image of particles prepared without Pluronic F-127 (Figure 3.14, Image A) shows particles that are of round shape. Some of them have dents (red arrows). These dents are typical for dextran particles prepared with this method, they can be observed in all samples. Looking at image B, where 0.1% Pluronic F-127 was used, we additionally recognize slightly deformed particles (blue arrows) and

porous structures (yellow arrows). The image of particles with 1.25% Pluronic F-127 (Figure 3.15, Image C) shows much stronger deformations than on image B; however, there are also more porous structures that can be seen. Comparing that with Image D, we even have more deformations there, but not more porous structures. It appears, that the images with Pluronic F-127 have porous structures in comparison to the one without, but the degree if porosity does not seem to change much. On the other hand, the degree of deformation seems to increase with an increasing amount of Pluronic F-127. At first glance this does not propagate the results of Figure 3.13; however, during the experiments it could be observed that aqueous Pluronic F-127 solution and the aqueous dextran solution tend to separate into two different phases. While the experiments of Figure 3.13 were prepared as single experiments in relatively short time, the experiments of Figure 3.14 and Figure 3.15 were prepared simultaneously, generating longer periods where the emulsified sample batches idled for further processing. Therefore, there is a high possibility that a phase separation took place in the droplets of the emulsion. This would not only explain why there are only few porous structures, but also why there are increasing amounts of deformations with raising concentrations of Pluronic F-127. Then, during the washing step with acetonitrile, whole parts of the dextran/Pluronic particles were dissolved and washed away. Looking at Figure 3.13 B again and considering the size of the holes that are between 50 and 150 nm, it becomes clear that holes of this size could not develop if dextran solution and Pluronic solution were well-mixed.

Unfortunately, the experiments conducted cannot prove the hypothesis derived from Figure 3.13, so that an additional experiment was necessary to confirm the assumptions. Since time seemed to be a factor, the emulsion was not prepared with membrane emulsification but with a high shear homogenizer. In the process, 2 mL of a 10 wt% dextran and 2.5 wt% PLuronic F-127 solution were emulsified in 18 mL of pentane with stabilizers as before. The particles after precipitation were washed with ethyl acetate and then transported and kept in acetonitrile to dissolve the Pluronic F-127. For imaging, the particles were dried on an SEM wafer and then imaged.

The particles of the conducted experiment have a clearly porous structure, as it had been expected according to the assumptions (see Figure 3.16). Indeed, it is possible to prepare porous particles by mixing dextran and Pluronic F-127, and probably the degree of porosity can be adjusted by the ratio of dextran and Pluronic F-127, but this also shows that there are two different aqueous phases (dextran and Pluronic F-127) and that both tend to separate by time. A better stabilization of the water in water emulsion would be beneficial for future work.

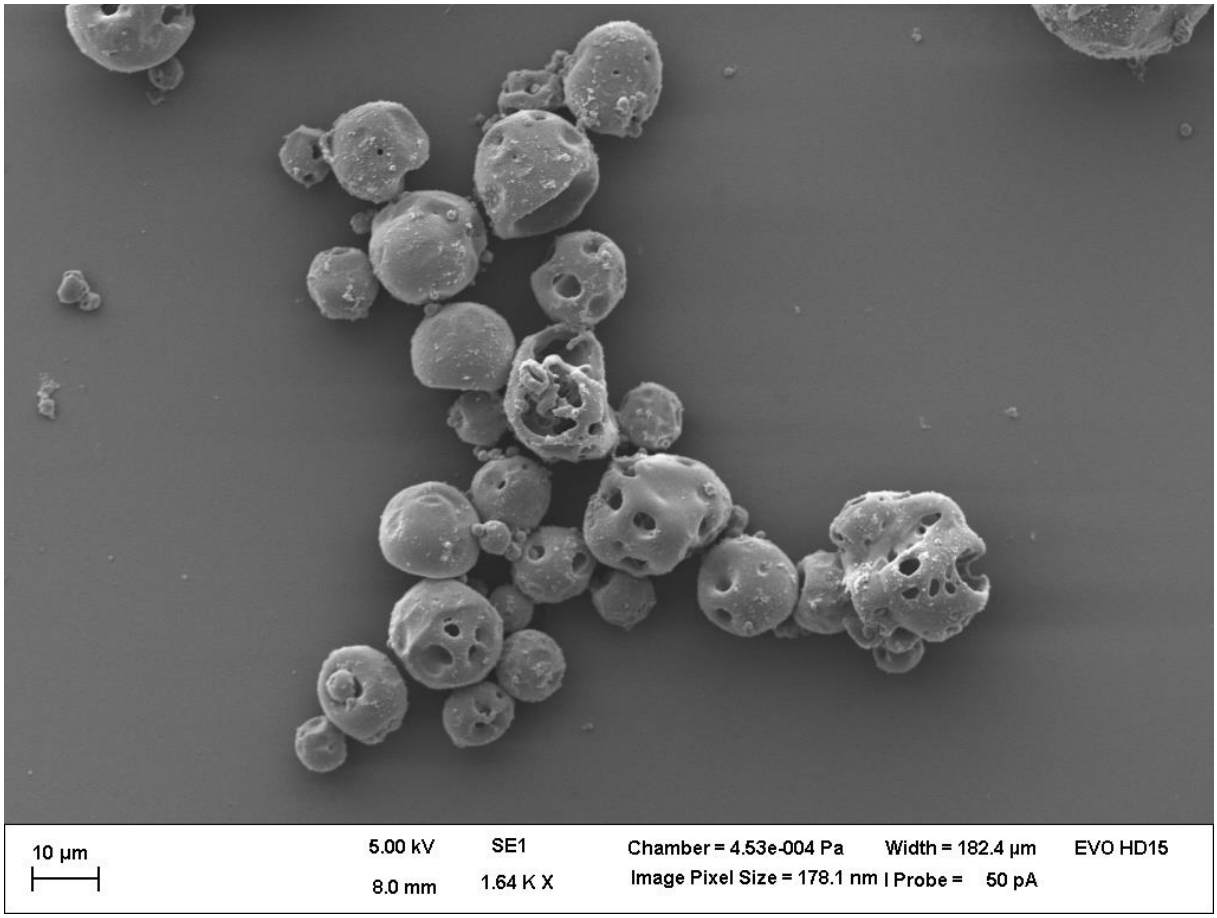

Figure 3.16: SEM-image of particles prepared with Pluronic F-127 as porosity agent. The emulsion was prepared with a high shear homogenizer to achieve a precipitation before phase separation of dextran and pluronic. The porous structure can be seen on many particles.

3.2.3 Preparing particles with different polymers

To further demonstrate the flexibility of the presented preparation method, particles were prepared from various biocompatible and biodegradable polymers. Since most of the polymers had a higher viscosity in solution than dextran and chitosan, the emulsions were not prepared by membrane emulsification but with a high shear homogenizer (section 2.2.3, Table 2.3, Experiments # 7 till # 12). These experiments were not adjusted for homogeneous particle distributions, but they demonstrate the feasibility of the method for many different polymers very well.

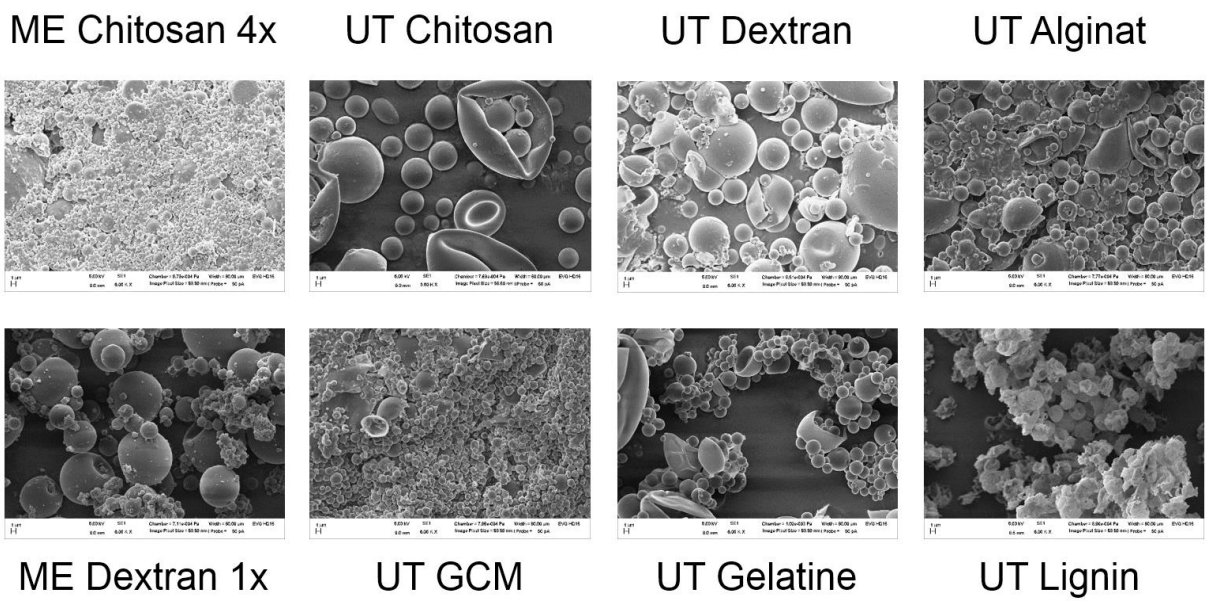

Figure 3.17: Comparison of particles of different polymers, prepared with either "membrane emulsification precipitation" (ME) or with "high shear homogenizer emulsification precipitation" (UT). The two membrane emulsification images have four and one membrane cycle for chitosan and dextran respectively. All images show particles with the same magnification. Scale bar = 1 µm, (GCM = glucomannan). The ME Chitosan image has previously been discussed in section 3.2.1.

The comparison image (Figure 3.17) shows particles prepared from different biocompatible, biodegradable and thus pharmaceutically relevant polymers. The only exception to this is lignin which has currently no pharmaceutical relevance, but it is suggested that the prerequisites for that are given.[138] All images in the figures are taken with the same magnification, such that a comparison of the different particles is possible. While particles of UT Chitosan, UT Dextran and ME Dextran are similar in size, particles of UT Gelatine, UT Alginat and UT Lignin are a bit smaller. The particles of UT GCM and ME Chitosan are much smaller in comparison to the others.

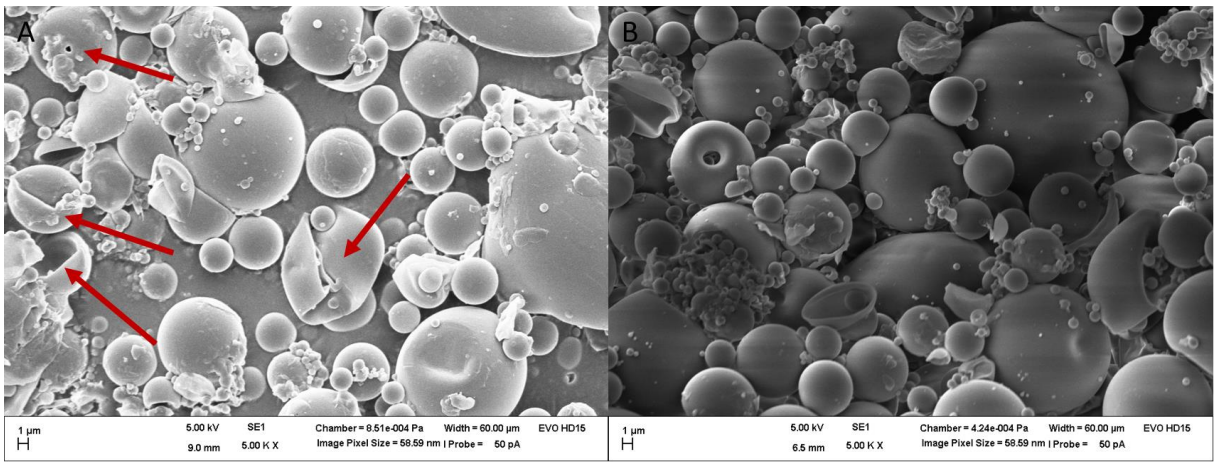

Figure 3.18: The image (A) shows dextran particles prepared with the high shear homogenizer precipitation method. Image (B) is the long-term stability image of the same particles about 11 months later. (Experiment # 7, Table 2.3)

Dextran particles prepared with the high shear homogenizer method (Figure 3.18) (A) show a relatively wide size distribution. While there are a lot of very small particles well below 1 µm in size, there are also many larger particles. As many of the larger particles are collapsed or just shells (red arrows), it is suggested that many, or possibly all, larger particles are hollow to some extent. It also occurs that some of the larger particles merge into each other and into the larger particles.

The long-term stability image (B) shows stable particles; however, the surface of those particles seems a little bit smoother than in (A). Probably, the surface of the dextran particles dissolved slightly, due to the hydrophilicity of the polymer in air humidity.

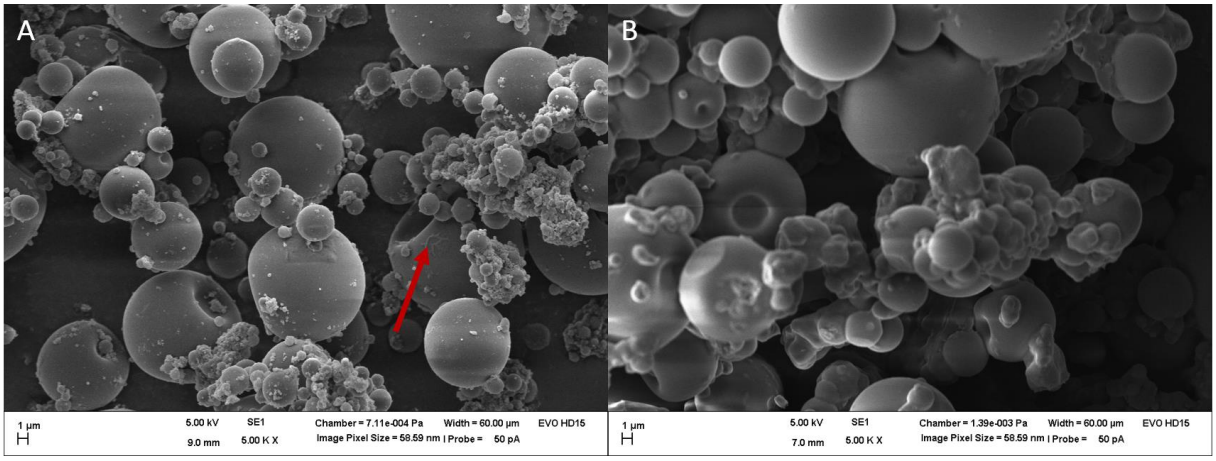

Figure 3.19: Dextran particles prepared with membrane emulsification precipitation method (A). Long-term stability image (B) taken after about 11 months. (Experiment # 1 Table 2.2)

In Figure 3.19 (A), dextran particles prepared with membrane emulsification are shown. The size distribution is very wide, similar to the Figure 3.18. Also, the smaller particles are sticking to each other. Hollow particles cannot be seen on this image, but the large dent (red arrow) indicates that some of them are hollow as well. On other membrane emulsification/dextran images in this thesis, hollow dextran particles have been shown (e.g. Figure 3.7), such that we can assume that there is no difference in this case to the particles prepared with the high shear homogenizer. What appears to be different, is the amount of small particles which merge into each other. While in Figure 3.18 the smaller particles are still well distinguishable, here, they often seem to have merged into a single mass without form.

The long-term stability image (B) shows, just as in Figure 3.18, stable particles with a slightly smoother surface. Also, smaller particles seem to be more melted into each other than on image (A).

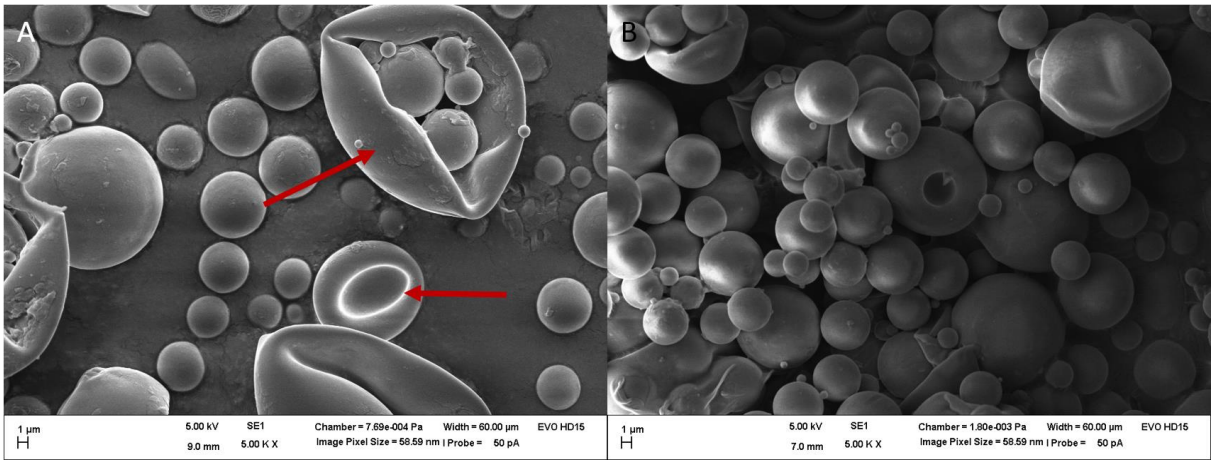

Figure 3.20: Chitosan particles prepared with high shear homogenizer precipitation method (A). Long-term stability image (B) taken after about 11 months. (Experiment # 8, Table 2.3)

The chitosan particles in Figure 3.20 (A) seem to have a more narrow size distribution, compared to the dextran particles. Especially, there are only few very small particles in comparison to the batches of dextran particles. Also, all larger particles seem to have collapsed, because they are hollow (red arrows). Some of the particles merge with the background; however, barely any particles can be seen that merge with each other, which is also a difference to the dextran particles.

The long-term stability image shows no differences to image (A), therefore it can be concluded, that the storage did not affect the chitosan particles. This is also consistent with the finding of Figure 3.12.

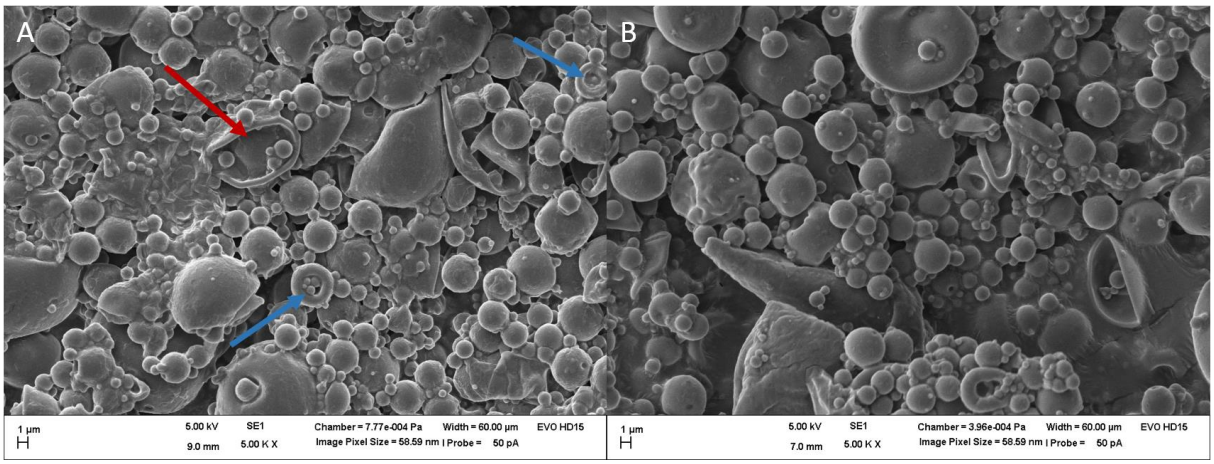

Figure 3.21: Alginate particles prepared with the high shear homogenizer precipitation method (A). Long-term stability image (B) taken after about 11 months. (Experiment # 9, Table 2.3)

The alginate particles shown in Figure 3.21 (A) have a relatively wide size distribution. While large particles seem to be hollow and collapsed (red arrows), also some of the smaller particles seem to

have hollow characteristics (blue arrows). What stands out is the fact that many particles seem to have merged with others or with non-particulate mass in the background. Most alginate particles in literature are crosslinked with divalent ions such as Ca^{2+} or Mg^{2+}. Obviously, this is not a prerequisite for preparing particles from alginate, but maybe using a crosslinker could reduce the amount of merging particles. The long-term stability image (B) shows no differences to image (A).

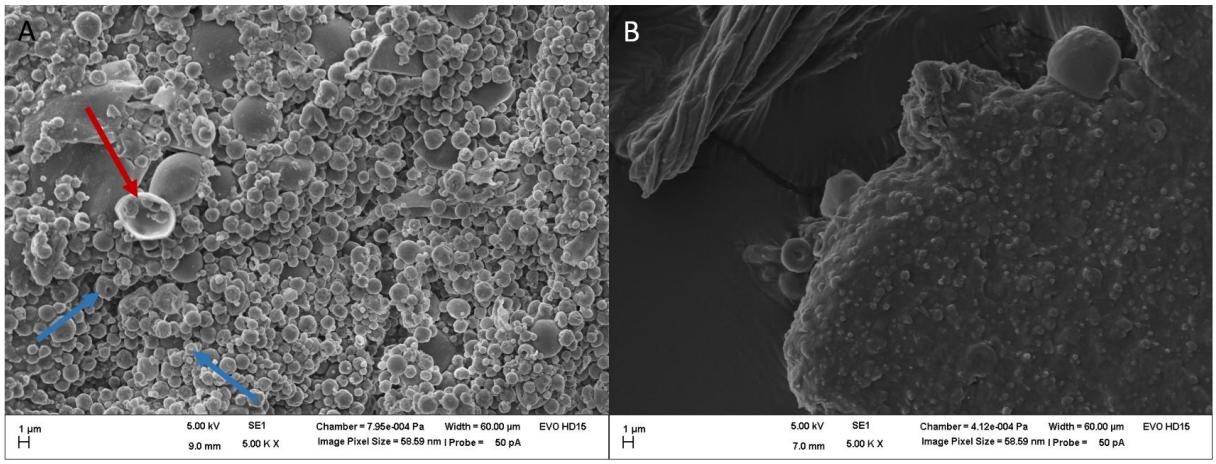

Figure 3.22: Particles prepared from glucomannan with the high shear homogenizer precipitation method (A). Long-term stability image (B) taken after about 11 months. (Experiment # 10 Table 2.3)

The particles in Figure 3.22 (A) have a very homogeneous size distribution and are relatively small compared to the dextran, chitosan (High shear homogenizer approach) and alginate particles. While the few larger particles seem to be hollow (red arrows), there are some smaller particles with dents (blue arrows) which could indicate that at least some of the smaller particles are hollow as well. Merging particles can be seen, but they are relatively rare, compared to the amount of all particles. A reason for the great number of small particles could be, that prepared samples of the glucomannan approaches only yielded a tiny amount that could be analyzed. It is highly likely, that there once were many larger particles that got lost during preparation, as the final sample contained almost no mass. Possibly, the sticky nature of the polymer resulted in adsorption to surfaces during the process. The smaller particles that did not sediment, would not touch the surfaces of their storage vials, and thus would not attach to it.

On the long-term stability image Figure 3.22 (B), only a very small number of particles can be seen at the border to the bulk material. The reason could either be, that the particles are unstable and degraded over time, or as mentioned above, that there was only a tiny amount of the sample and in the measured preparation no particles could be found.

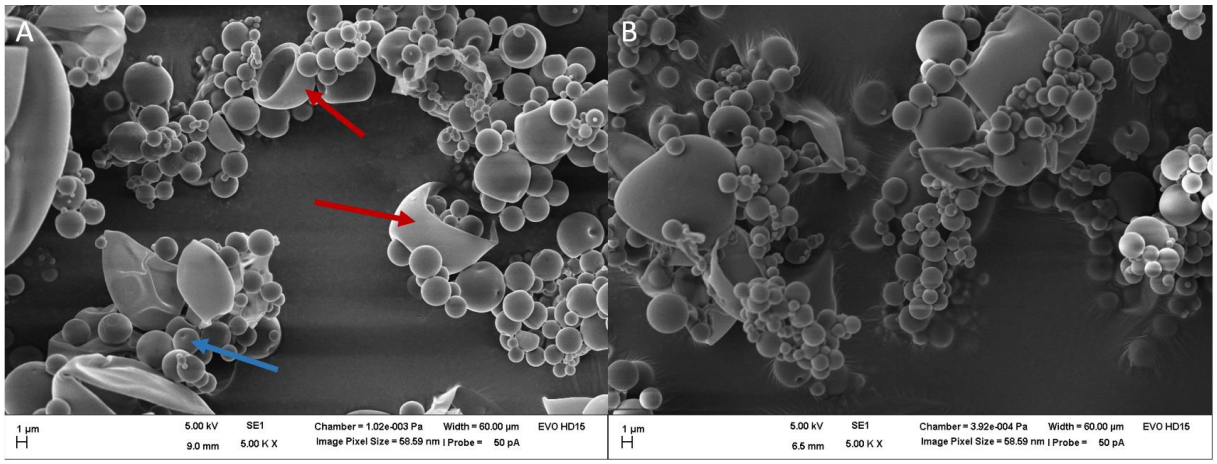

Figure 3.23: Gelatin particles prepared with high shear homogenizer precipitation method (A). Long-term stability image (B) taken after about 11 months. (Experiment # 11, Table 2.3)

The gelatin particles in Figure 3.23 (A) look very different, as the surface of the particles appears much smoother compared to the polysugar particles shown before; however, they exhibit the same characteristics: larger particles are hollow and collapsed. The thin nature of the particles walls is well visible because of the high contrast. Also, some smaller particles show dents which could indicate that they are hollow as well. The size distribution is wide, as in case of most other high shear homogenizer experiments.

The long-term stability particles in Image (B) do not look different from those in (A), which is surprising, as gelatin as a protein is prone to degradation of many microorganisms. The sample was kept sealed, yet not sterile. The dry conditions seem to be sufficient to prevent microbial settling.

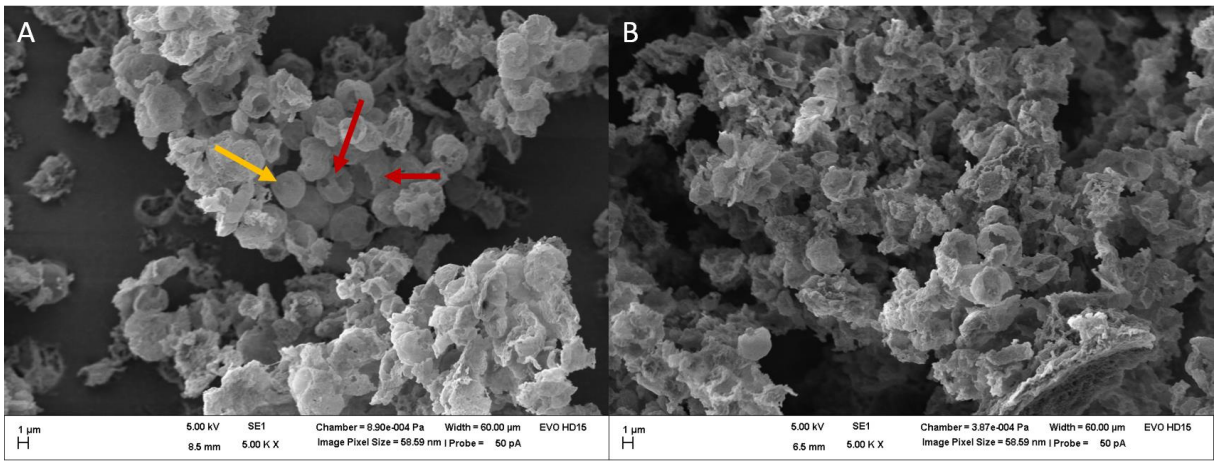

Figure 3.24: Lignin particles prepared with high shear homogenizer precipitation method (A). Long-term stability image (B) taken after about 11 months. (Experiment # 12, Table 2.3)

The lignin particles in Figure 3.24 (A) look very different from all others. This has multiple reasons: the main one is probably that NaOH was used in Experiment # 12 to dissolve the lignin in water. Since the NaOH could not be removed in the process, it is still a part of the particles shown on the image. Crystallization of smaller fragments of NaOH could be the reason for some sharper edges of the particulate structures or for the etched surfaces. In general, it is easy to find particle-like structures but hard to find actual particles; however, some are there (yellow arrow). Also, some of the remaining particles seem to have hollow structures (red arrows), but in this case it is unclear if it is for the same reason as in all other experiments, or if it is due to the nature of the lignin or the NaOH. Furthermore, it should be considered that the particles were prepared in paraffin instead of pentane. This did not make a difference during preparation, but could have had an influence on the result. The long-term stability image (B) shows no differences to image (A).

3.2.4 Encapsulation of desmopressin into dextran microparticles

As desmopressin is a hydrophilic substance, it can be encapsulated into dextran directly. The prepared particles, as described in section 2.2.3, were dissolved in water (5 mg of particles in 1 mL of MQ water) and then analyzed with HPLC. As some amounts get lost during the membrane emulsification due to its dead volume, only relative values of encapsulated desmopressin are considerable: Assuming that 1 mg of desmopressin was distributed in 300 mg dextran plus 0.5 mg Pluronic F-68, a maximum concentration of 3.32 µg desmopressin in 1 mg particulate substance is possible. From three produced batches, that all were measured three times in HPLC, an average amount of 2.46 ± 0.33 µg desmopressin per 1 mg could be detected. This means, that the concentration of desmopressin in the particles is 74% of the maximum possible amount defined by the experimental setting. It shows, that desmopressin and dextran are well miscible and that desmopressin does not much tend to mix with ethyl acetate.

On the other hand, the difference between the three batches is quite high, as it can be seen in Figure 3.25. This can also be seen, when considering that the standard deviation of the mean value is more than 10%. Since all three samples were prepared in a row, and thus batch 1 was at rest while batches 2 and 3 were prepared, and likewise batch 2 was at rest while batch 3 was prepared. The linear raise of encapsulated desmopressin by batch number could be an indication of release of desmopressin over time. However, since this would be a release into pentane, the argument is not very solid. There might as well be an accumulation at the droplet interphase and a washing off during precipitation and afterwards.

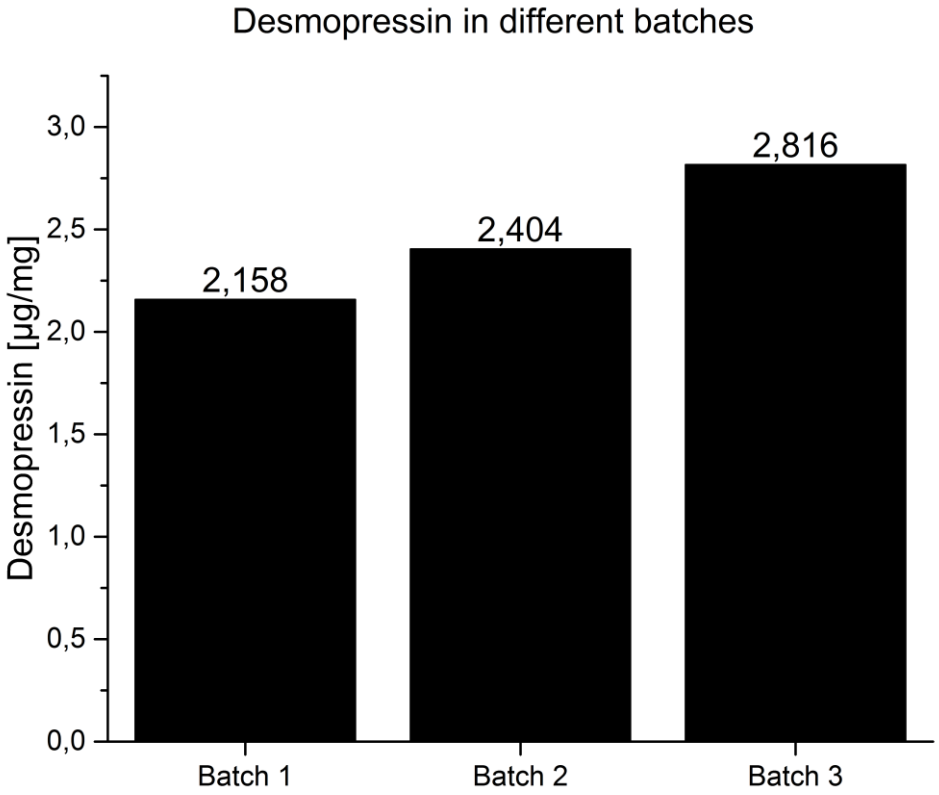

Figure 3.25: Amounts of desmopressin per milligram particle powder. The dextran particles were prepared with membrane emulsification.

3.3 Encapsulating PLGA nanoparticles into dextran microparticles

The logical conclusion to the findings of a nanoparticle system that can be functionalized in section 3.1 and a water-soluble microparticulate system in section 3.2, would be a combination of both. To see, whether it is possible to encapsulate PLGA nanoparticles into the dextran microparticles and to have an optical readout, fluoresceinamin-PLGA (covalently linked) was used to prepare nanoparticles. The nanoparticles were prepared analogously to normal PLGA nanoparticles. After centrifugation and washing of the pellet, these fluorescent nanoparticles were then mixed with the dextran solution and processed to become dextran particles, by membrane emulsification. Since the PLGA particles had sizes too large for 0.5 µm pore membrane, the dextran particles were prepared by using a membrane with a pore size of 2 µm. The dextran particles were not dried, but their solvent was changed to ethanol to avoid the further dissolution of PLGA nanoparticles (in ethyl acetate) or the dissolution of dextran particle under humid air atmosphere. The confocal images were taken directly in ethanol, as described in section 2.2.4.

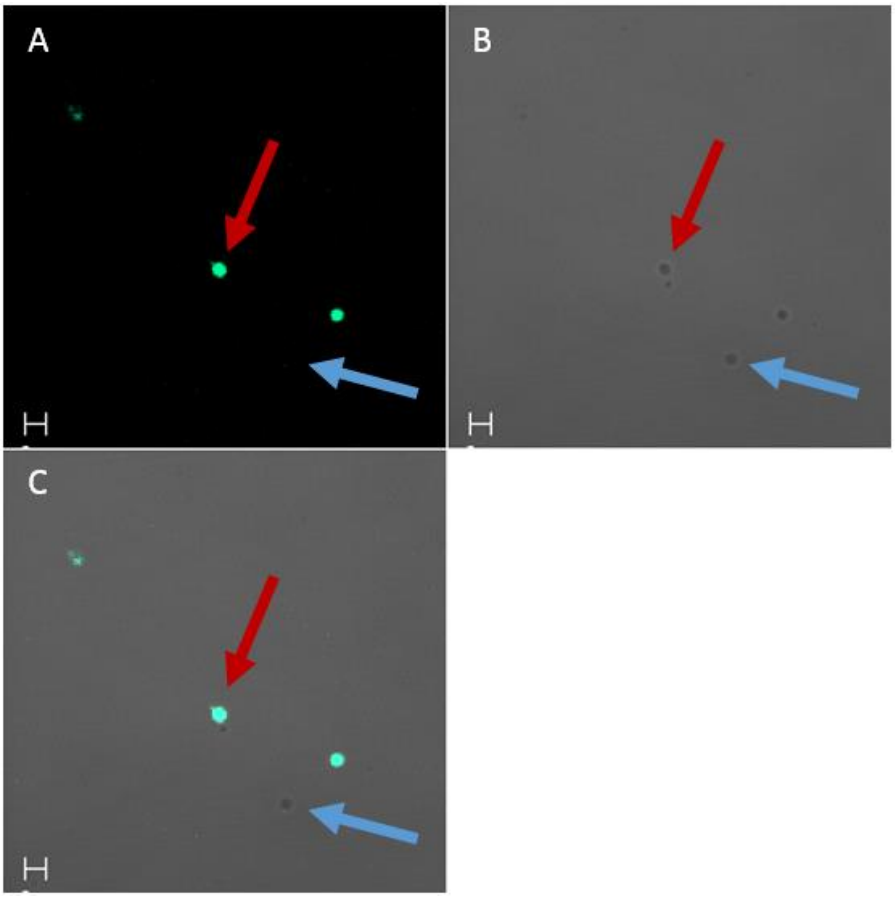

Figure 3.26: Image of dextran particles prepared with FA-PLGA nanoparticles. FA-PLGA nanoparticles are fluorescing in green color. The upper left image (A) is a fluorescence image, the upper right (B) a non-fluorescence light image, the lower left (C) an overlay of the two upper images. The scale bars are 2 µm. The red arrow shows a dextran particle that has been loaded with nanoparticles, while the blue one shows a particle that remained unloaded.

The resulting particles were investigated with confocal microscopy, as it can be seen in Figure 3.26. The fluorescing spots in image A can be identified as particles in image B (red arrows). Therefore, it can be concluded that FA-PLGA nanoparticles are incorporated into dextran microspheres. However, there are also particles that can be identified as such in images B and C, but no fluorescence can be observed in image A and C (blue arrows). Therefore, it can be concluded that not all particles are loaded with the nanoparticles and some plain dextran particles remain.

Aside from particles of 1-2 µm size, also larger particles could be found. An example of one of these particles can be seen in Figure 3.27. Many of these particles also contained FA-PLGA nanoparticles.

The image shows a large dextran particle of roughly 50 µm size. There is a clearly visible core of the particle (purple arrow) that fluorescents brightly. Around it, there is a light absorbing and thus black appearing shell with few fluorescent spots (yellow arrow). On the surface of this layer, there is another, very thin layer of fluorescent material. The inner core is probably mainly a bulk of FA-PLGA nanoparticles. The shell around the core is supposedly dextran that precipitated during the

manufacturing process. There are still some FA-PLGA nanoparticles present; however, much less than in the core.

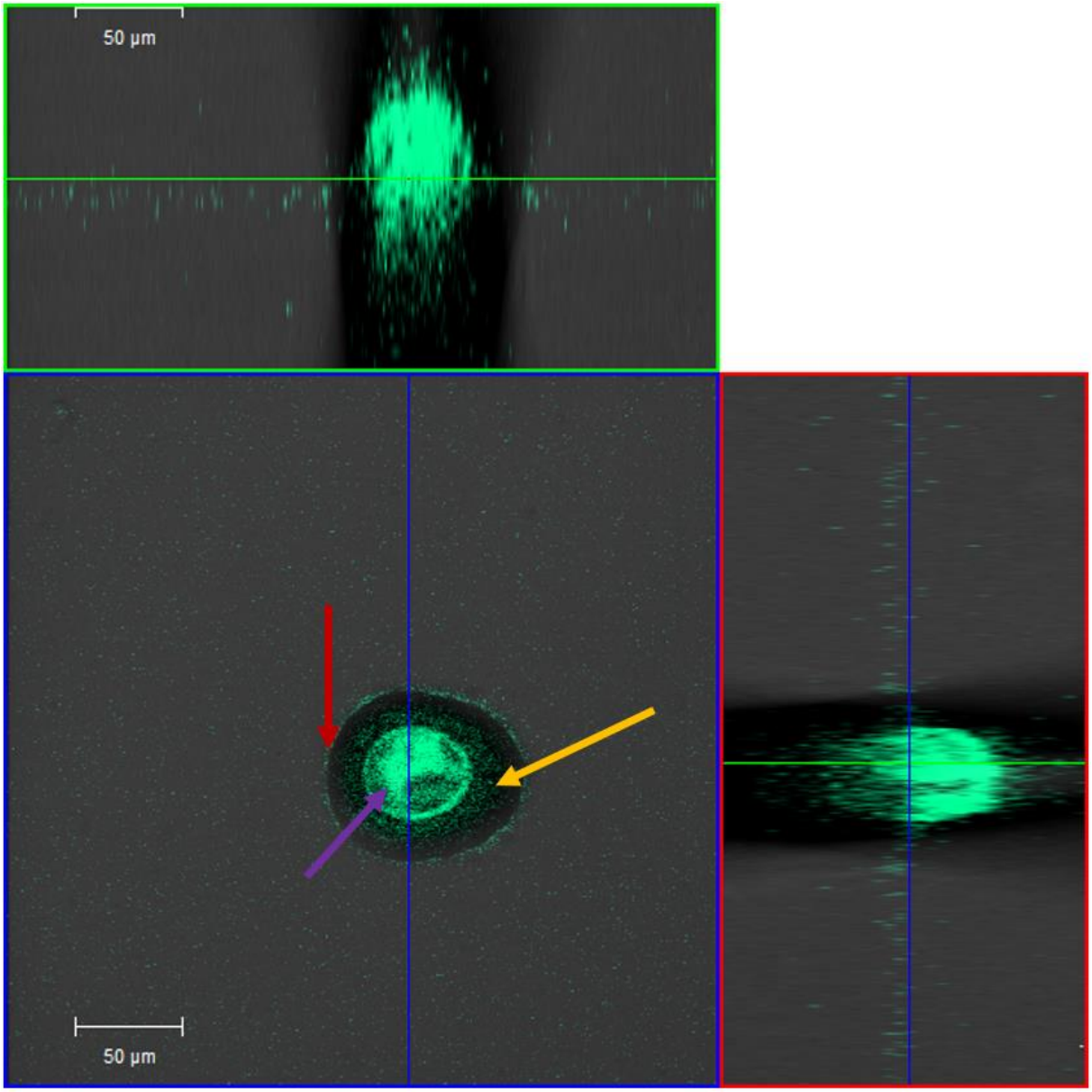

Figure 3.27: Confocal image of a large dextran particle filled with fluorescent PLGA nanoparticles (green fluorescing).

While the core contains most fluorescent particles, the shell has an outer and an inner layer, where there are more fluorescent spots in the inner than in the outer layer. The ethanol, in which the particles are dispersed during imaging, does not dissolve any material involved and keeps air humidity from the sample, such that no dissolutions can occur during the measuring. A release of FA-PLGA nanoparticles is unlikely, as dextran is bulk material and should immobilize large objects such as the nanoparticles, also there is no strong affection between FA-PLGA and ethanol. An explanation of the precipitation

process will be given in section 3.4. It is likely, that FA-PLGA nanoparticles moved to the core during the precipitation process. In the inner layer of the shell, the dextran is probably less dense, and therefore more nanoparticles can be found in this area. The fluorescent layer on the surface of the particle consists most likely of free FA-PLGA nanoparticles from other dextran particles that were destroyed during the washing process on the filter membrane.

On the other hand, looking at the core rises the interesting question, why there is a core structure at all. In SEM images before, many larger particles were hollow on the inside and had holes to the surface. This can be excluded for this particle: If the particle would be hollow, then ethyl acetate would have entered the particle during the precipitation process and dissolved the FA-PLGA nanoparticles inside. The dissolved FA-PLGA polymer would probably have been washed out, and the little remaining polymer would be stuck to the inner surface rather than existing as bulk in the middle of the particle. On the other hand, we have to consider that FA-PLGA is hydrophobic, compared to the dextran shell. A self-assembly of hydrophobic particles in the center of hydrophilic particles is possible. A detailed attempted explanation for this phenomenon is provided in the next section.

3.4 Explanation for the core shell structure of hydrophilic particles

On most SEM images it can be seen, that many particles, regardless of the polymer used, have dents, and many particles, especially the larger ones, are hollow. A possible explanation of this effect needs to focus on the moment of precipitation. When the emulsion (Figure 3.28 (A)) is injected into the ethyl acetate, the alkane outer phase of the emulsion mixes with ethyl acetate (B), and thus the concentration of ethyl acetate around the droplet raises. Since ethyl acetate and water are only partially soluble solvents, it is to assume, that upon the first contact of ethyl acetate molecules with the water droplet, there is no mixing between both phases. As the alkane further mixes into the ethyl acetate, the concentration of ethyl acetate around the water droplet raises. At some point, the concentration of ethyl acetate around the water droplet is high enough to allow the mixing of water into ethyl acetate, so the droplet begins to precipitate (C).

At this point, water diffuses out into the ethyl acetate, as well as ethyl acetate moves on into the water. The concentration of ethyl acetate in the water results in a precipitation of polymer in the aqueous phase. Since the polymer and the ethyl acetate do not mix at all, it is to assume that the outer rim of the particle holds back the incoming ethyl acetate on its surface; however, water constantly diffuses out from that surface into the ethyl acetate. If that assumption is correct, then the surface of the particle and its interior could exhibit different patterns, as the outer rim is precipitated by the invasion of ethyl acetate, while the inner part is rather dried out by loss of water. Figure 3.29 shows the breaking

edge of a dextran particle. The red arrows indicate the surface of the particle, where a very dense pattern can be seen. The blue arrow points to the inner part of the particle that has a clearly different pattern than the surface. Air humidity, and therefore surface dissolution as a reason for different patterns of the particle, can be ruled out, since the air humidity would have affected the breaking edge as well. The bubbles could be remains of water or of gas that were entrapped during the precipitation process and formed their bubble shape during the lyophilisation, because of the strong negative pressure. During SE microscopy, focussing the scanning beam on a part of the surface that has bubbles underneath, can result in inflation of the bubbles. This may be a reaction of possible gas expanding inside.

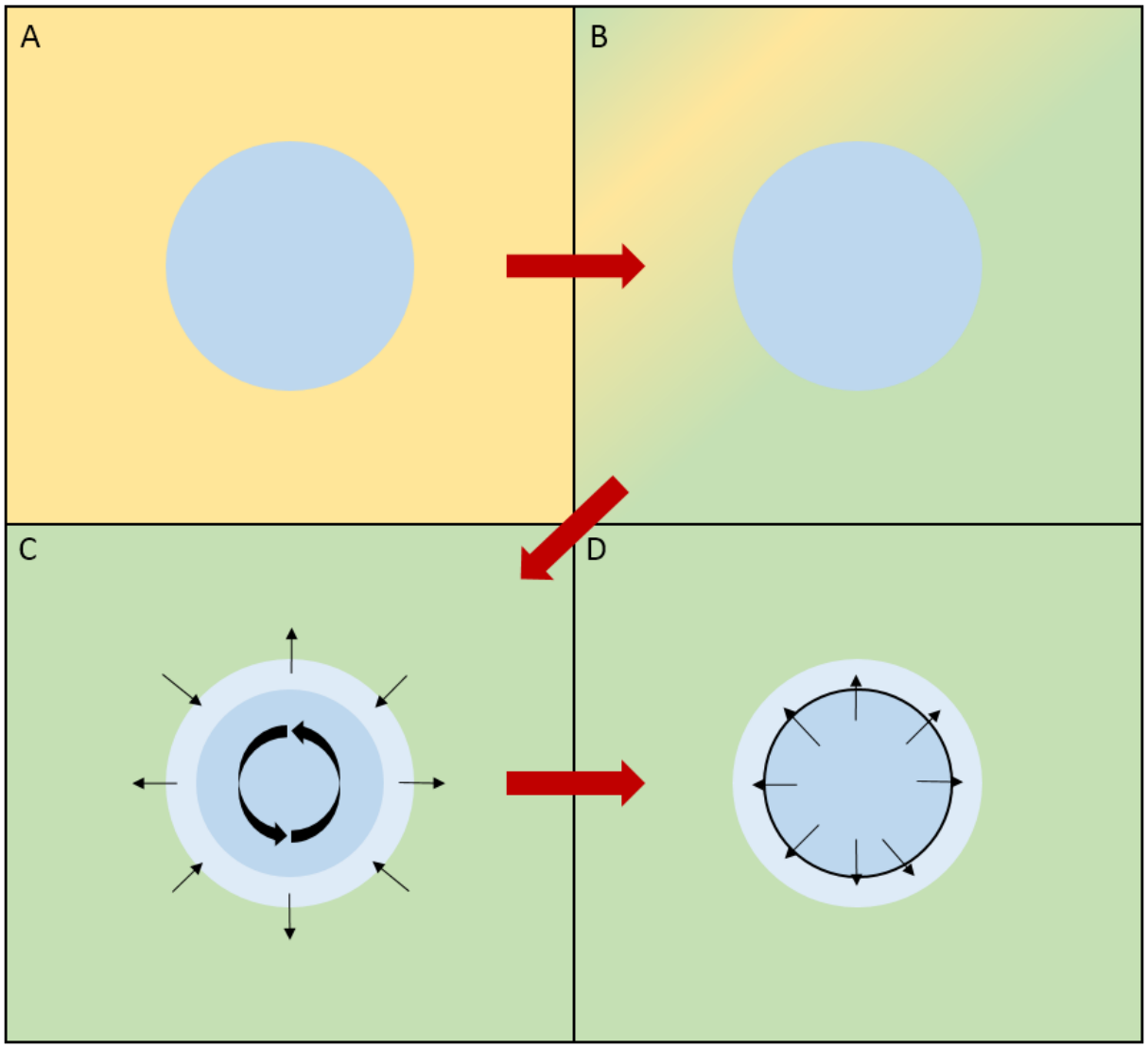

Figure 3.28: General steps of the precipitation process. Aqueous emulsion droplet surrounded by alkane (A), alkane mixing with ethyl acetate after injection (B), start of the precipitation process at the outer rim of the droplet once enough ethyl acetate is present (C), diffusion of water from the inner part of the droplet to the outer 'dried' part (D).

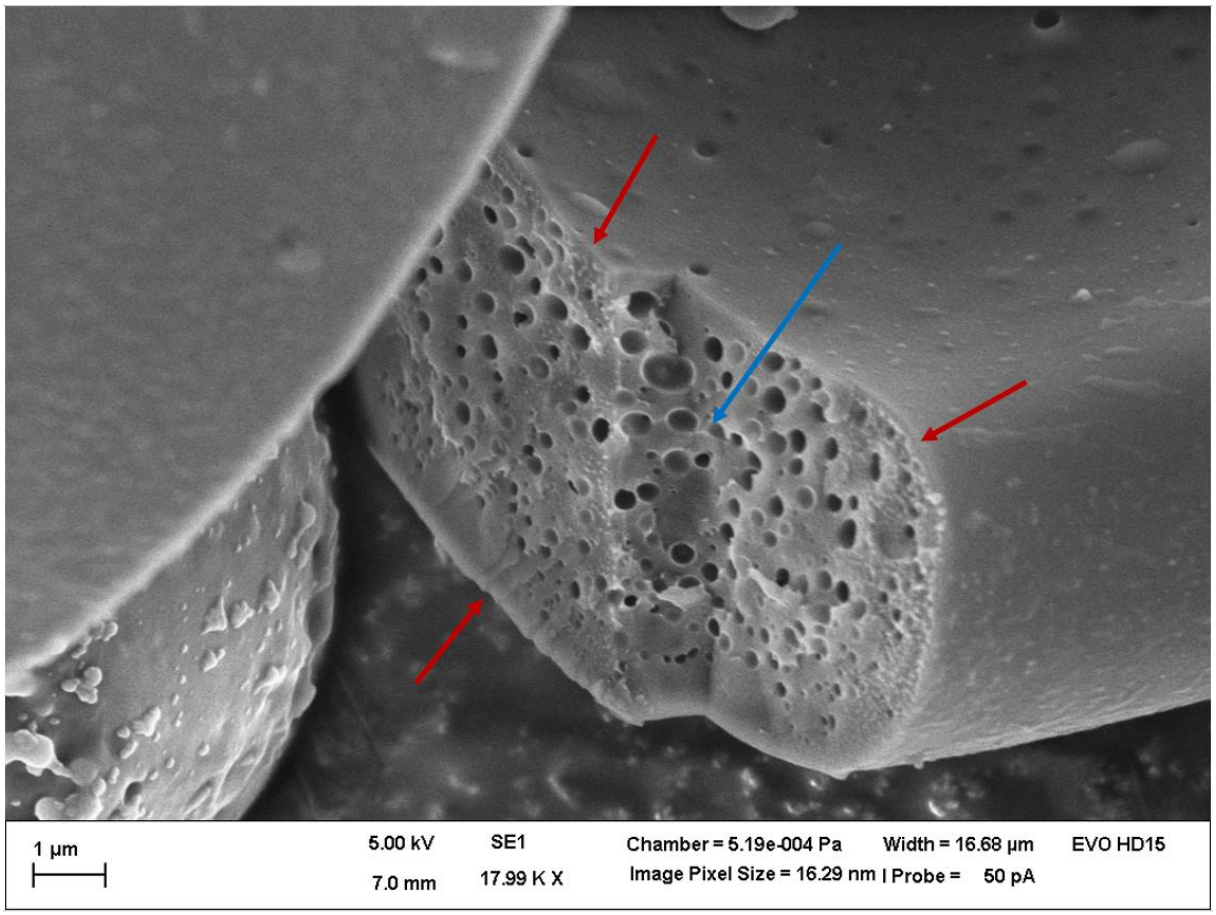

Figure 3.29: Breaking edge of a dextran particle. Outer rim of the particle exhibiting a denser pattern (red arrows) than the inner part with bubble holes (blue arrow).

It is likely to assume, that the deserting water in the outer part of the particle results in a flux of the water from the inside to the outside, especially since many of the hydrophilic polymers are quite hygroscopic. This flux from the inside to the outside (Figure 3.28 (D)) might even drag some of the polymer from the inner of the particle along to the outer part. An indication for that is the dense structure at the surface shown in Figure 3.29, as the polymer would concentrate here. This would also lead to a negative pressure in the center of the particle (Figure 3.30 (E)). Since it can be assumed, that the particles are still not very hard in this state, the formation of a dent is a probable result of negative pressure compensation. If, like assumed before, the water flux from the inside to the outside drags most of the polymer along, a break of the particle surface in the moment of dent formation seems possible. The result would be ethyl acetate flowing into the particle and pursuing its precipitation process from two sides (F). The extent to which these things occur, seems to vary for different polymers. While dextran particles exhibit holes and dents quite often, chitosan particles, especially the smaller ones, do not seem to have any. Larger chitosan particles also rather appear collapsed than with holes.

The velocity of the water flux from the inside to the outside could vary with the hydrophilicity of the material; however, this would have to be investigated in further experiments.

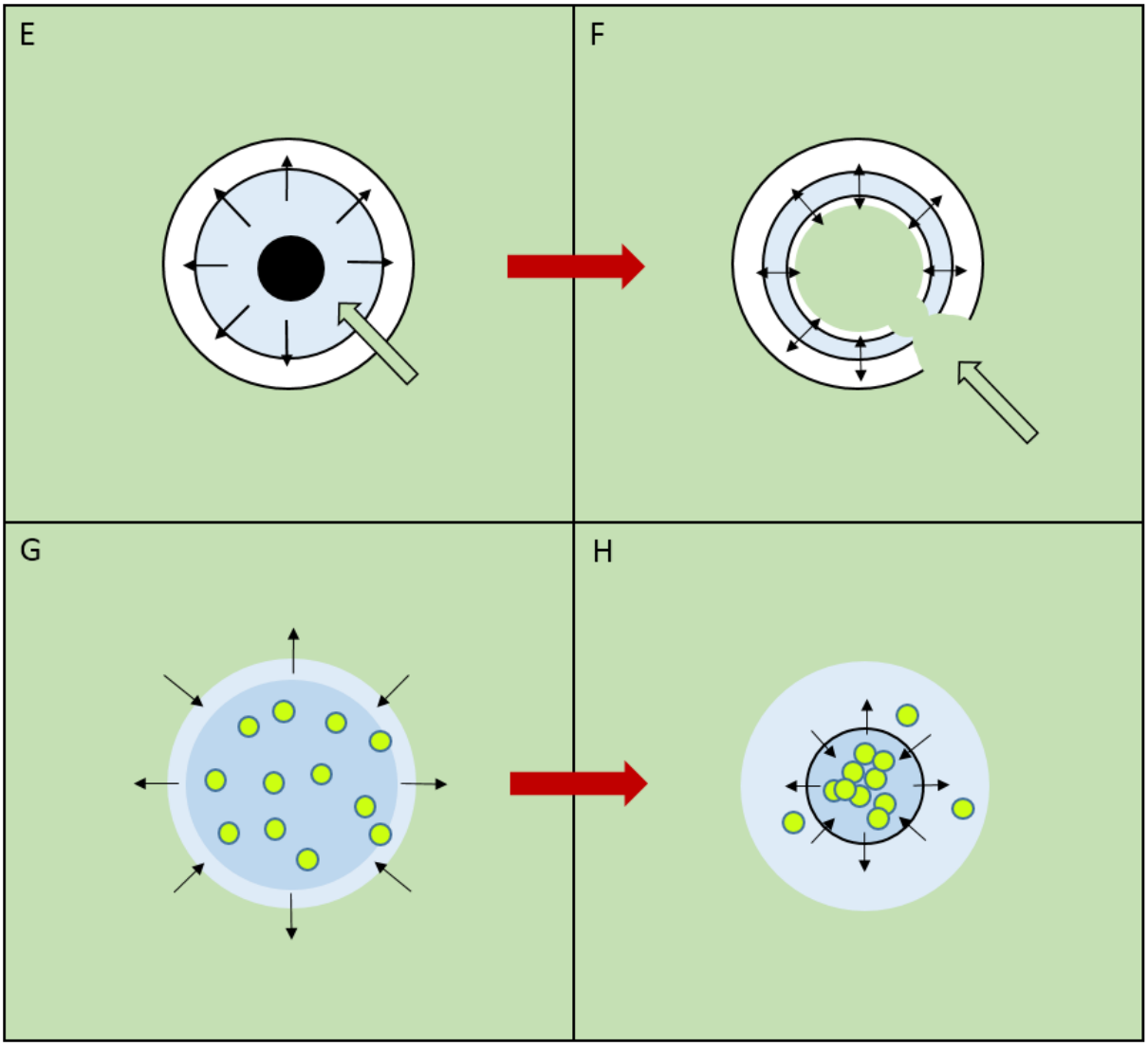

Figure 3.30: Steps of the precipitation process, that presumably result in the formation of dents and hollow structures (E,F) or core shell structures in case of loaded PLGA nanoparticles (G,H).

The core shell structure of the FA-PLGA nanoparticle loaded dextran microparticles could result from this matter as well. Considering, that the hydrophilic dextran assembles in the shell of the particle (Figure 3.30 (G)) and water further flows from the inside to the outside, a movement of rather hydrophobic PLGA particles to the inside and founding a mainly hydrophobic domain seems rational. This would also counter the emerging negative pressure in the center of the particle.

4 Conclusion

4.1 Hydrophobic nanoparticles

The results of the preparation of PLGA nanoparticles in section 3.1 showed, that particles could be loaded with a peptide drug, and that the surface of the particles could be functionalized with hLF-peptide. This has not yet been shown for the chosen set (PLGA, desmopressin and hLF-peptide), but the preparation of PLGA nanoparticles in general, and the incorporation of a peptide into PLGA, is a common method in the field of pharmaceutical technology [18, 32], and it was thus a good starting point.

The results of the particle preparation suggested, that the particle size could be reduced with the right choice of stabilizer in the inner emulsion (Tween 21 strongly reduced particle size); for a better loading efficiency, the most hydrophilic stabilizer Pluronic F-68 showed the best result. Pluronic F-127, being less hydrophilic than Pluronic F-68, had the second best result. This indicates, that there could be a connection between loading efficiency and hydrophilicity of the stabilizer for the encapsulation of desmopressin; however, the data produced in this thesis are not sufficient to serve as full evidence.

The loading efficiency approach with Pluronic F-68 is significantly higher ($p < 0.05$) than the coating approach (CT), and also significantly higher than the approach without stabilizers (PL). A significant difference between CT and PL could not be found. This suggests, that the drug can only be incorporated into the particle if a stabilizer is present. The theory of the double emulsion technique says that the primary emulsion results in small bubbles inside the nanoparticles, in which the drug can be contained. If there is no significant difference between the PL and the CT approach, and thus the double emulsion approach encapsulates as much as a surface coating, it is questionable whether the double emulsion actually produces the proposed structure of bubbles inside nanoparticles.

Tween 21 is by far the most hydrophobic stabilizer and produced by far the smallest particles (HLB 13.3 versus 28 and 22 for the Pluronics). This indicates, that there could be a connection between the size of the particles and the hydrophobicity of the stabilizer, but also the different molecular weights of the stabilizers might have an impact.

As Pluronic F-68 resulted in the best loading efficiency and Tween 21 in the smallest particles, a combination of both seemed to be a reasonable choice to optimize the system; however, if the HLB values of the stabilizers are responsible for the changes in loading efficiency and size, what is suggested by the data, this approach would not work. Upon mixing stabilizers, HLB values would turn average and none of the two effects would occur. In this case, we would only have the choice between smaller particles and higher loading efficiency.

Regarding the results from a plainly therapeutic point of view, we could reach a concentration of 1.16 µg desmopressin per mg PLGA, which matches the ratio of common medicinal products on the market. Oral formulations usually have doses of 100 or 200 µg per tablet, while the average weight of a tablet is around 200 mg. (Desmopressin Teva®; TEVA Pharmaceutical Industries Ltd.; Petach Tikwa, Israel). Therefore, we can conclude that our particles should meet the therapeutic window in an application, and can compete with this formulation with respect to drug loading.

Considering the efficiency of the whole process, there is a major drawback due to comparably low encapsulation efficiencies. Even though the encapsulation efficiency rises by about 30% due to the use of Pluronic F-68, less than 10% of total desmopressin are actually encapsulated into the particles. The rest of the peptide is removed with the supernatant. From a commercial point of view, the encapsulation would probably not be reasonable.

The system would work better for hydrophobic drugs that mix well with the organic phase, and thus PLGA;[139] however, for targeting reasons and protection of the drug, the encapsulation into a carrier system is necessary. If then the microparticulate carrier system of higher order is hydrophilic, the nanoparticulate system to be filled into the hydrophilic microparticles has to be hydrophobic.

In the case of a hydrophilic drug, it can directly be encapsulated into the hydrophilic carrier system (as described in section 3.2.4). For topical applications without a strongly degrading environment, such as the skin, the direct encapsulation into the hydrophilic particles is suitable and means a simplification. For applications where targeting, protection or continuous release is relevant, additional measures like a hydrophobic nanoparticulate carrier system have to be taken.

4.2 Hydrophilic microparticles

The method for preparing microparticles out of hydrophilic polymers, was created as a modification of the Emulsion Solvent Diffusion method, which was used to prepare hydrophobic nanoparticles. As a water in ethyl acetate emulsion is difficult to prepare - there is a lack of suitable stabilizers - an additional step of an emulsion in an alkane was introduced. This led to a method, with which particles of various different polymers (dextran, chitosan, alginate, lignin, glucomannan and gelatin) could be prepared. The particle size could be adjusted by the droplet size of the emulsion. Thus, the essential problem of the method is to prepare homogeneous emulsions of a certain droplet size. The mixture of two non-miscible solvents that mix with each other when introduced into a third solvent, is a new technique that has not yet been used to prepare particles in the field of pharmaceutical sciences. The question of toxicity is essential to pharmaceutical applications; therefore, the use of more biocompatible materials is desirable. If components can be replaced or do not depend on their

chemical properties: The polymers can be replaced as long as they stay soluble in water and insoluble in pentane and ethyl acetate. In that way, the system is very flexible with regard to the encapsulation of APIs with different properties.

In case of the solvents, an exchange of ethyl acetate and pentane would be desirable. While for pentane the much less problematic liquid paraffin has already shown its potential in this thesis, a good replacement for ethyl acetate is still missing. Unfortunately, ethanol did not work out, which might be the case because it is fully miscible with water and not partially miscible like ethyl acetate. The need for full miscibility with pentane/paraffin and dissolution of the polymer further complicates the exchange.

The encapsulation of hydrophilic components into the particles is easy, as they just have to be mixed with the polymer before the emulsion step, whereas hydrophobic components cannot be encapsulated directly; however, many of the therapeutic agents used today are not only hydrophilic or hydrophobic. If encapsulating an amphiphilic component, it should be considered that the component could easily arrange itself at the interface between oil and water. This could lead to denaturation in the case of proteins and peptides. This thesis did not address this issue, as the model drug (desmopressin) was very hydrophilic.

The chemical properties of dextran and Pluronic F-127 led to the possibility of preparing an emulsion with two different aqueous phases. The simultaneous precipitation led to the preparation of porous dextran particles, when the Pluronic F-127 was washed out by acetonitrile. This effect and the prepared method allow to change the aerodynamic diameter of the prepared particles. As the aerodynamic diameter is important for a pulmonary delivery, this could further help to adjust a pulmonary formulation in a later step.

4.3 Conclusion on the aim of this thesis

Within this thesis, it was possible to set up a method of preparation that exhibits many of the desired characteristics. Up to the current point, the system includes the following possibilities:

- preparation of hydrophilic microparticles of different polymers
- no use of toxic substances is necessary
- suitable cleaning and drying process for hydrophilic microparticles
- particle stability at room temperature under air conditions for at least 11 months, depending on the formulation
- encapsulation of hydrophilic compounds into hydrophobic nanoparticles
- encapsulation of hydrophobic nanoparticles into hydrophilic microparticles

- encapsulation of hydrophilic compounds into hydrophilic microparticles
- surface modification of hydrophobic nanoparticles for targeting
- preparation of porous dextran microparticles

All used substances are not classified as ‘toxic’; however, at certain concentrations they are toxic to the human body. The lungs are a very sensitive organ and might react to some of these substances, even at low concentrations. Currently, there are no polymers approved for pulmonary drug delivery by EMA or FDA, but it is likely that especially biopolymers such as dextran do not show a severe impact on the lungs, if used. The organic solvents and stabilizers are more problematic. For a final formulation, they have to be minimized. For pentane, this should not be much of a problem, as it is very volatile and will not mix with the hydrophilic particles. Ethyl acetate also would not mix with the particles and should be possibly removed by freeze drying. Also, ethyl acetate is contained in, for example, wine, fruits and some kinds of nail polish. An ingestion and inhalation of smaller amounts is obviously without risk for a healthy person. Acetonitrile is more toxic than ethyl acetate, but not essential for the drying process. It has been used in this thesis, because its freezing point is at -45 °C, and it was therefore suitable for freeze drying from an organic solvent on a laboratory scale. For an industrial application, an exchange to ethanol and subsequent freeze drying would be more suitable and less toxic.

The stabilizers, on the other hand, could be a major problem for pulmonary application, as they cannot be removed by freeze drying. Since they are very hydrophobic, it is not clear whether they dissolve in the alveolar lining fluid or not, but if they do, they have the potential to change its properties and affect the breathing ability.

Some features of the system are only assumed and could not be proven within this thesis:

- particle sizes prepared with multiple membrane cycles are suitable for lung deposition
- particle sizes prepared with multiple membrane cycles are suitable for entering hair follicles

These features require future work to prove or disprove them.

5 Outlook

While the aimed goal, systemic delivery to the lungs, has not been reached yet, the given results are a good basis for making it possible in future work. The prepared particles' sizes were all in range for getting to the deep lung; however, flight studies with, for example, a cascade impactor or a next generation impactor (NGI) would be necessary to see how much of a prepared powder could actually be deposited. This is especially important considering the hollow nature of some particles and the resulting change in aerodynamic behaviour.

The use of Pluronic F-127 as porosity agent and its practicability in the preparation process would have to be examined in more detail. Up to now, it is just an interesting additional feature of the method of preparation and not part of its core properties. For washing out Pluronic F-127, acetonitrile is necessary, whereas it was only used as a substitute for the purpose of freeze drying because of its low freezing point, and could be exchanged easily by other organic solvents for non-laboratory scale applications. Also fully enclosed Pluronic F-127 would not be removed by washing and would then be delivered to the lungs, where it could be problematic for the alveolar lining fluid.

Furthermore, the parameters of toxicity need to be addressed in future experiments. The exact amounts of remaining stabilizers and solvents in the particles are still unknown but necessary for any final application.

Lastly, all hydrophilic polymers used in this thesis are not officially approved for pulmonary application. For any commercial product in the future, this step has to be taken as well. If no polymers are desired, salts or non-polymeric sugars might work as well to prepare particles.

6 Zusammenfassung

Die Dissertation besteht aus drei Elementen: der Einkapselung des Peptidwirkstoffs Desmopressin acetat in PLGA Nanopartikel (3.1), die Entwicklung einer Methode zur Herstellung von Mikropartikeln aus hydrophilen Polymeren (3.2) und der Einkapselung der PLGA Nanopartikel in eben diese hydrophilen Mikropartikel (3.3).

Die PLGA Nanopartikel werden mit einer leicht modifizierten „Double Emulsion Solvent Diffusion"-Methode hergestellt. Die zentrale Änderung zu gängigen Ansätzen ist, dass vor der Emulgierung mit einer Ultraschall Sonde keine Durchmischung der beiden Phasen vorgenommen wurde und das organische Lösungsmittel nach der Herstellung durch Abzentrifugation der Partikel und Verwerfen des Überstands und nicht durch Verdampfen entfernt wurde (2.2.2). Die derart hergestellten Nanopartikel waren im Größenbereich zwischen 106 und 131 nm (hydrodynamischer Durchmesser) mit PDI < 0,1. Zetapotential und pH-Werte wurden ermittelt zwischen -38 und -44 mV und pH 5,5 und 5,9 (3.1.1). Die Beladung der Partikel wurde durch eine Doppelemulsion im ersten Schritt realisiert. Hierbei wurden unterschiedliche Stabilisatoren in der Primäremulsion getestet, um feststellen zu können, ob diese einen Einfluss auf die Einkapselung haben. Verglichen wurden alle Ergebnisse statistisch mit einer Kontrolle, in der lediglich die Oberfläche beschichtet war (keine Doppelemulsion). Es konnte hierbei gezeigt werden, dass es einen signifikanten Unterschied zwischen der Einkapselung unter Zuhilfenahme des Stabilisators Pluronic F-68 und dem Beschichtungsansatz gab. Des Weiteren war auch der Unterschied zwischen Pluronic F-68 und einer Kontrolle ohne Stabilisatoren (Doppelemulsion, aber Einkapselung ohne Stabilisator) signifikant unterschiedlich. Die beiden Kontrollen jedoch zeigten untereinander keinen signifikanten Unterschied in der Beladung, was den Schluss zulässt, dass für eine Einkapselung in die Partikel ein Stabilisator nötig ist. Die Beladungseffizienz war im besten Experiment (Pluronic F-68) hoch genug, um mit kommerziell erhältlichen Formulierungen mitzuhalten, die Einkapselungseffizienz allerdings war mit 6 bis 9% zu niedrig für eine sinnvolle Anwendung (3.1.3). Neben der quantitativen Analyse des Peptids mittels HPLC wurde auch mittels LC-MS geprüft, ob das Peptid durch die Einkapselung Schäden davonträgt, was verneint werden konnte (3.1.4). In einem weiteren Experiment wurden die PLGA Nanopartikel mit hLF-Peptid, einem Penetrationsverstärker, durch Inkubation beschichtet. Nach der Inkubation konnte gezeigt werden, dass das Peptid für mindestens 7 Tage stabil in wässriger Dispersion auf den Partikeln verbleibt. Neben der Beladung war auch eine Funktionalisierung der Partikel möglich (3.1.5).

Im zweiten Teil wurde ein Transportsystem, primär für pulmonale Applikation entwickelt. Hierbei wurde besonderer Wert darauf gelegt, das System so flexibel wie möglich zu halten, um es über diese Dissertation hinaus auch für andere Anwendungen einsetzen zu können. Das erarbeitete System ist eine Abwandlung der „Emulsion Diffusion"-Methoden, anhand derer auch die PLGA Nanopartikel

hergestellt wurden. Da sich die Phasen der Emulsion, die für die PLGA Nanopartikel eingesetzt wurden, aber nicht einfach vertauschen ließen, musste ein Zwischenschritt eingefügt werden, in dem die Emulsion in einem anderen Lösungsmittel als dem Präzipitationsmittel hergestellt wird (3.2). Das daraus entstehende Dreiphasensystem ist in der Lage, Partikel aus unterschiedlichen hydrophilen Polymeren (z.B.: Dextran, Chitosan, Alginat, Gelatine, Glucomannan und Lignin) herzustellen (3.2.3). Die Größen der Partikel, die mit dieser Methode hergestellt werden, lassen sich über die Größe der Emulsionstropfen steuern. Um möglichst homogene Emulsionen herzustellen, wurde eine Membranemulgierung eingesetzt, bei der die zu dispergierende Phase mehrfach eine Membran passierte und damit entsprechend der Porengröße der Membran in kleine Tropfen dispergiert wurde. Hierbei konnten Partikel aus Chitosan im Größenbereich um 500-600 nm hergestellt werden (3.2.1). Zur Vereinfachung und um schneller arbeiten zu können, wurde für einige Experimente die Emulsion mit einem Hochdruckhomogenisator hergestellt, oder es wurde bei der Membranemulgierung auf multiple Membranpassagen verzichtet. Neben der Herstellung wurde auch eine Trocknungsmethode entwickelt. Hierfür wurden die Partikel zunächst mit organischem Lösungsmittel von überschüssigem Stabilisator befreit und dann mit flüssigem Stickstoff in organischem Lösungsmittel eingefroren und daraus gefriergetrocknet (2.2.3). Derart getrocknete Partikel wiesen eine Lagerstabilität (in mit Luft gefüllten abgeschlossenen Gefäßen) von mindestens 11 Monaten auf. Einzig die Dextran Partikel wiesen nach 11 Monaten eine glattere Oberfläche auf, was auf ein Anlösen der Oberfläche in der Luftfeuchtigkeit hindeutet (3.2.3). Auch die direkte Einkapselung von Desmopressin in Dextranpartikel mittels dieser Methoden wurde getestet und führte zu deutlich höheren Einkapselungseffizienzen als bei PLGA Nanopartikeln (3.2.4). In einem weiteren Experiment wurde die Dextranlösung vor der Emulgierung mit Pluronic F-127 gemischt. Diese Mischung führte zu einer Phasentrennung zweier wässriger Phasen. Dieser Effekt konnte genutzt werden, um poröse Partikel herzustellen, indem beide Phasen vor der Emulgierung gut durchmischt wurden und dann gemeinsam emulgiert und präzipitiert wurden. Die daraus entstehenden Partikel bestanden aus zwei festen Phasen, von denen eine durch ein organisches Lösungsmittel ausgewaschen werden konnte. Die resultierenden Partikel hatten Löcher und waren porös (3.2.2).

Im dritten Teil wurden dann erneut PLGA Nanopartikel hergestellt aus einem Fluoresceinamin-gelabelten PLGA. Diese Nanopartikel wurden in Dextranpartikel eingekapselt und mittels Konfokalmikroskopie untersucht. Auf diese Weise konnte gezeigt werden, dass sich PLGA Nanopartikel in Dextranpartikel einkapseln lassen (3.3).

Ein flexibles hydrophiles Trägersystem zum Transport beladener und funktionalisierter hydrophober Nanopartikel konnte erfolgreich hergestellt werden.

7 References

1. Reddy, L.H. and R.S. Murthy, *Lymphatic transport of orally administered drugs.* Indian J Exp Biol, 2002. *40*(10): p. 1097-109.
2. Xie, Y., T.R. Bagby, M.S. Cohen, and M.L. Forrest, *Drug delivery to the lymphatic system: importance in future cancer diagnosis and therapies.* Expert Opin Drug Deliv, 2009. *6*(8): p. 785-92.
3. Shrewsbury, S.B., R.O. Cook, G. Taylor, C. Edwards, and N.M. Ramadan, *Safety and pharmacokinetics of dihydroergotamine mesylate administered via a Novel (Tempo) inhaler.* Headache, 2008. *48*(3): p. 355-67.
4. Bosquillon, C., *Drug Transporters in the Lung-Do They Play a Role in the Biopharmaceutics of Inhaled Drugs?* Journal of Pharmaceutical Sciences, 2010. *99*(5): p. 2240-2255.
5. Demain, A.L. and P. Vaishnav, *Production of recombinant proteins by microbes and higher organisms.* Biotechnol Adv, 2009. *27*(3): p. 297-306.
6. Swartz, J.R., *Advances in Escherichia coli production of therapeutic proteins.* Curr Opin Biotechnol, 2001. *12*(2): p. 195-201.
7. Gerngross, T.U., *Advances in the production of human therapeutic proteins in yeasts and filamentous fungi.* Nat Biotechnol, 2004. *22*(11): p. 1409-14.
8. Woehlecke, H. and R. Ehwald, *Characterization of Size-Permeation Limits of Cell-Walls and Porous Separation Materials by High-Performance Size-Exclusion Chromatography.* Journal of Chromatography A, 1995. *708*(2): p. 263-271.
9. Fischer, H., J. Scherz, S. Szabo, M. Mildner, C. Benarafa, A. Torriglia, E. Tschachler, and L. Eckhart, *DNase 2 is the main DNA-degrading enzyme of the stratum corneum.* PLoS One, 2011. *6*(3): p. e17581.
10. Simanski, M., S. Dressel, R. Glaser, and J. Harder, *RNase 7 protects healthy skin from Staphylococcus aureus colonization.* J Invest Dermatol, 2010. *130*(12): p. 2836-8.
11. Langer, R., *New Methods of Drug Delivery.* Science, 1990. *249*(4976): p. 1527-1533.
12. De Jong, W.H. and P.J. Borm, *Drug delivery and nanoparticles:applications and hazards.* Int J Nanomedicine, 2008. *3*(2): p. 133-49.
13. Panyam, J. and V. Labhasetwar, *Biodegradable nanoparticles for drug and gene delivery to cells and tissue.* Advanced Drug Delivery Reviews, 2003. *55*(3): p. 329-347.
14. Soppimath, K.S., T.M. Aminabhavi, A.R. Kulkarni, and W.E. Rudzinski, *Biodegradable polymeric nanoparticles as drug delivery devices.* Journal of Controlled Release, 2001. *70*(1-2): p. 1-20.
15. Dinarvand, R., N. Sepehri, S. Manoochehri, H. Rouhani, and F. Atyabi, *Polylactide-co-glycolide nanoparticles for controlled delivery of anticancer agents.* Int J Nanomedicine, 2011. *6*: p. 877-95.
16. Mirakabad, F.S.T., K. Nejati-Koshki, A. Akbarzadeh, M.R. Yamchi, M. Milani, N. Zarghami, V. Zeighamian, A. Rahimzadeh, S. Alimohammadi, Y. Hanifehpour, and

S.W. Joo, *PLGA-Based Nanoparticles as Cancer Drug Delivery Systems.* Asian Pacific Journal of Cancer Prevention, 2014. *15*(2): p. 517-535.
17. Wu, X.S. and N. Wang, *Synthesis, characterization, biodegradation, and drug delivery application of biodegradable lactic/glycolic acid polymers. Part II: biodegradation.* J Biomater Sci Polym Ed, 2001. *12*(1): p. 21-34.
18. Acharya, S. and S.K. Sahoo, *PLGA nanoparticles containing various anticancer agents and tumour delivery by EPR effect.* Adv Drug Deliv Rev, 2011. *63*(3): p. 170-83.
19. Brady, J.M., D.E. Cutright, R.A. Miller, and G.C. Barristone, *Resorption rate, route, route of elimination, and ultrastructure of the implant site of polylactic acid in the abdominal wall of the rat.* J Biomed Mater Res, 1973. *7*(2): p. 155-66.
20. Farinelli, M.P. and K.E. Richardson, *Oxalate synthesis from [14C1]glycollate and [14C1]glyoxylate in the hepatectomized rat.* Biochim Biophys Acta, 1983. *757*(1): p. 8-14.
21. Lametec_Medizintechnik_Germany. *Templax resorbierbare Akupunktur-Templantate*. 2011 [cited 2016 08/01/2016]; Resomer implants: Templax]. Available from: http://www.lametec.de/corporate/deutsch/produkte/templax.html.
22. Cohen-Sela, E., M. Chorny, N. Koroukhov, H.D. Danenberg, and G. Golomb, *A new double emulsion solvent diffusion technique for encapsulating hydrophilic molecules in PLGA nanoparticles.* J Control Release, 2009. *133*(2): p. 90-5.
23. Murakami, H., M. Kobayashi, H. Takeuchi, and Y. Kawashima, *Preparation of poly(DL-lactide-co-glycolide) nanoparticles by modified spontaneous emulsification solvent diffusion method.* Int J Pharm, 1999. *187*(2): p. 143-52.
24. Mainardes, R.M. and R.C. Evangelista, *PLGA nanoparticles containing praziquantel: effect of formulation variables on size distribution.* Int J Pharm, 2005. *290*(1-2): p. 137-44.
25. Mu, L. and S.S. Feng, *A novel controlled release formulation for the anticancer drug paclitaxel (Taxol): PLGA nanoparticles containing vitamin E TPGS.* J Control Release, 2003. *86*(1): p. 33-48.
26. Bhardwaj, V., D.D. Ankola, S.C. Gupta, M. Schneider, C.M. Lehr, and M.N. Kumar, *PLGA nanoparticles stabilized with cationic surfactant: safety studies and application in oral delivery of paclitaxel to treat chemical-induced breast cancer in rat.* Pharm Res, 2009. *26*(11): p. 2495-503.
27. Nafee, N., S. Taetz, M. Schneider, U.F. Schaefer, and C.M. Lehr, *Chitosan-coated PLGA nanoparticles for DNA/RNA delivery: effect of the formulation parameters on complexation and transfection of antisense oligonucleotides.* Nanomedicine, 2007. *3*(3): p. 173-83.
28. Sahana, D.K., G. Mittal, V. Bhardwaj, and M.N. Ravi Kumar, *Estradiol loaded PLGA nanoparticles for oral administration: effect of polymer molecular weight and copolymer composition on release behavior in vitro and in vivo.* J Control Release, 2007. *119*(1): p. 77-85.
29. Ravi Kumar, M.N., U. Bakowsky, and C.M. Lehr, *Preparation and characterization of cationic PLGA nanospheres as DNA carriers.* Biomaterials, 2004. *25*: p. 6.

30. Rietscher, R., C. Thum, C.M. Lehr, and M. Schneider, *Semi-automated nanoprecipitation-system-an option for operator independent, scalable and size adjustable nanoparticle synthesis.* Pharm Res, 2015. *32*(6): p. 1859-63.
31. Govender, T., S. Stolnik, M.C. Garnett, L. Illum, and S.S. Davis, *PLGA nanoparticles prepared by nanoprecipitation: drug loading and release studies of a water soluble drug.* J Control Release, 1999. *57*(2): p. 171-85.
32. Barichello, J.M., M. Morishita, K. Takayama, and T. Nagai, *Encapsulation of hydrophilic and lipophilic drugs in PLGA nanoparticles by the nanoprecipitation method.* Drug Dev Ind Pharm, 1999. *25*(4): p. 471-6.
33. Bilati, U., E. Allemann, and E. Doelker, *Development of a nanoprecipitation method intended for the entrapment of hydrophilic drugs into nanoparticles.* Eur J Pharm Sci, 2005. *24*(1): p. 67-75.
34. Yang, Y.-Y., T.-S. Chung, and N.P. Ng, *Morphology, drug distribution, and in vitro release profiles of biodegradable polymeric microspheres containing protein fabricated by double-emulsion solvent extraction/evaporation method.* Biomaterials, 2000. *22*(3): p. 231-241.
35. Lamprecht, A., N. Ubrich, M. Hombreiro Perez, C. Lehr, M. Hoffman, and P. Maincent, *Influences of process parameters on nanoparticle preparation performed by a double emulsion pressure homogenization technique.* Int J Pharm, 2000. *196*(2): p. 177-82.
36. Li, Y., Y. Pei, X. Zhang, Z. Gu, Z. Zhou, W. Yuan, J. Zhou, J. Zhu, and X. Gao, *PEGylated PLGA nanoparticles as protein carriers: synthesis, preparation and biodistribution in rats.* J Control Release, 2001. *71*(2): p. 203-11.
37. Blanco, M.D. and M.J. Alonso, *Development and characterization of protein-loaded poly(lactide-co-glycolide) nanospheres.* European Journal of Pharmaceutics and Biopharmaceutics, 1997. *43*(3): p. 287-294.
38. Primavessy, D., N. Gunday Tureli, and M. Schneider, *Influence of different stabilizers on the encapsulation of desmopressin acetate into PLGA nanoparticles.* Eur J Pharm Biopharm, 2016.
39. Kocbek, P., N. Obermajer, M. Cegnar, J. Kos, and J. Kristl, *Targeting cancer cells using PLGA nanoparticles surface modified with monoclonal antibody.* J Control Release, 2007. *120*(1-2): p. 18-26.
40. Zhou, J., G. Romero, E. Rojas, L. Ma, S. Moya, and C. Gao, *Layer by layer chitosan/alginate coatings on poly(lactide-co-glycolide) nanoparticles for antifouling protection and Folic acid binding to achieve selective cell targeting.* J Colloid Interface Sci, 2010. *345*(2): p. 241-7.
41. Luo, R., B. Neu, and S.S. Venkatraman, *Surface functionalization of nanoparticles to control cell interactions and drug release.* Small, 2012. *8*(16): p. 2585-94.
42. Amoozgar, Z., L. Wang, T. Brandstoetter, S.S. Wallis, E.M. Wilson, and M.S. Goldberg, *Dual-layer surface coating of PLGA-based nanoparticles provides slow-release drug delivery to achieve metronomic therapy in a paclitaxel-resistant murine ovarian cancer model.* Biomacromolecules, 2014. *15*(11): p. 4187-94.
43. Duchardt, F., I.R. Ruttekolk, W.P. Verdurmen, H. Lortat-Jacob, J. Burck, H. Hufnagel, R. Fischer, M. van den Heuvel, D.W. Lowik, G.W. Vuister, A. Ulrich, M. de Waard,

and R. Brock, *A cell-penetrating peptide derived from human lactoferrin with conformation-dependent uptake efficiency.* J Biol Chem, 2009. *284*(52): p. 36099-108.

44. Oh, E., J.B. Delehanty, K.E. Sapsford, K. Susumu, R. Goswami, J.B. Blanco-Canosa, P.E. Dawson, J. Granek, M. Shoff, Q. Zhang, P.L. Goering, A. Huston, and I.L. Medintz, *Cellular uptake and fate of PEGylated gold nanoparticles is dependent on both cell-penetration peptides and particle size.* ACS Nano, 2011. *5*(8): p. 6434-48.
45. Filipe, V., A. Hawe, and W. Jiskoot, *Critical evaluation of Nanoparticle Tracking Analysis (NTA) by NanoSight for the measurement of nanoparticles and protein aggregates.* Pharm Res, 2010. *27*(5): p. 796-810.
46. Hovgaard, L. and H. Brondsted, *Dextran Hydrogels for Colon-Specific Drug-Delivery.* Journal of Controlled Release, 1995. *36*(1-2): p. 159-166.
47. Khan, S.A. and M. Schneider, *Improvement of nanoprecipitation technique for preparation of gelatin nanoparticles and potential macromolecular drug loading.* Macromol Biosci, 2013. *13*(4): p. 455-63.
48. Greß, A., Funktionalisierte Poly(2-oxyzoline): Kontrollierte Synthese, bioinspirierte Strukturbildung und Anwendungen, 2008, Mathematisch-Naturwissenschaftliche Fakultät Universität Potsdam
49. PHARMACOSMOS_A/S. *Physical Properties of Dextran*. 2016 [cited 2016 08/04/2016]; Available from: http://www.dextran.net/about-dextran/dextran-chemistry/physical-properties.aspx.
50. de Jonge, E. and M. Levi, *Effects of different plasma substitutes on blood coagulation: a comparative review.* Crit Care Med, 2001. *29*(6): p. 1261-7.
51. Korttila, K., P. Grohn, A. Gordin, S. Sundberg, H. Salo, E. Nissinen, and M.A. Mattila, *Effect of hydroxyethyl starch and dextran on plasma volume and blood hemostasis and coagulation.* J Clin Pharmacol, 1984. *24*(7): p. 273-82.
52. Lamke, L.O. and S.O. Liljedahl, *Plasma volume changes after infusion of various plasma expanders.* Resuscitation, 1976. *5*(2): p. 93-102.
53. Lamke, L.O. and S.O. Liljedahl, *Plasma volume expansion after infusion of 5%, 20% and 25% albumin solutions in patients.* Resuscitation, 1976. *5*(2): p. 85-92.
54. Zhang, R.S., M.G. Tang, A. Bowyer, R. Eisenthal, and J. Hubble, *A novel pH- and ionic-strength-sensitive carboxy methyl dextran hydrogel.* Biomaterials, 2005. *26*(22): p. 4677-4683.
55. Van Thienen, T.G., K. Raemdonck, J. Demeester, and S.C. De Smedt, *Protein release from biodegradable dextran nanogels.* Langmuir, 2007. *23*(19): p. 9794-9801.
56. Van Tomme, S.R., M.J. van Steenbergen, S.C. De Smedt, C.F. van Nostrum, and W.E. Hennink, *Self-gelling hydrogels based on oppositely charged dextran microspheres.* Biomaterials, 2005. *26*(14): p. 2129-35.
57. Watanabe, T., A. Ohtsuka, N. Murase, P. Barth, and K. Gersonde, *NMR studies on water and polymer diffusion in dextran gels. Influence of potassium ions on microstructure formation and gelation mechanism.* Magnetic Resonance in Medicine, 1996. *35*(5): p. 697-705.

58. Naji, L., J. Schiller, J. Kaufmann, F. Stallmach, J. Karger, and K. Arnold, *The gel-forming behaviour of dextran in the presence of KCl: a quantitative C-13 and pulsed field gradient (PFG) NMR study.* Biophysical Chemistry, 2003. *104*(1): p. 131-140.
59. Chalasani, K.B., G.J. Russell-Jones, A.K. Jain, P.V. Diwan, and S.K. Jain, *Effective oral delivery of insulin in animal models using vitamin B12-coated dextran nanoparticles.* J Control Release, 2007. *122*(2): p. 141-50.
60. Li, Y.L., L. Zhu, Z. Liu, R. Cheng, F. Meng, J.H. Cui, S.J. Ji, and Z. Zhong, *Reversibly stabilized multifunctional dextran nanoparticles efficiently deliver doxorubicin into the nuclei of cancer cells.* Angew Chem Int Ed Engl, 2009. *48*(52): p. 9914-8.
61. Berry, C.C., S. Wells, S. Charles, and A.S. Curtis, *Dextran and albumin derivatised iron oxide nanoparticles: influence on fibroblasts in vitro.* Biomaterials, 2003. *24*(25): p. 4551-7.
62. Berry, C.C., S. Wells, S. Charles, G. Aitchison, and A.S. Curtis, *Cell response to dextran-derivatised iron oxide nanoparticles post internalisation.* Biomaterials, 2004. *25*(23): p. 5405-13.
63. Arbab, A.S., L.B. Wilson, P. Ashari, E.K. Jordan, B.K. Lewis, and J.A. Frank, *A model of lysosomal metabolism of dextran coated superparamagnetic iron oxide (SPIO) nanoparticles: implications for cellular magnetic resonance imaging.* NMR Biomed, 2005. *18*(6): p. 383-9.
64. Raemdonck, K., B. Naeye, A. Hogset, J. Demeester, and S.C. De Smedt, *Biodegradable dextran nanogels as functional carriers for the intracellular delivery of small interfering RNA.* J Control Release, 2010. *148*(1): p. e95-6.
65. Van Thienen, T.G., K. Raemdonck, J. Demeester, and S.C. De Smedt, *Protein release from biodegradable dextran nanogels.* Langmuir, 2007. *23*(19): p. 9794-801.
66. Li, J., S. Yu, P. Yao, and M. Jiang, *Lysozyme-dextran core-shell nanogels prepared via a green process.* Langmuir, 2008. *24*(7): p. 3486-92.
67. Klinger, D., E.M. Aschenbrenner, C.K. Weiss, and K. Landfester, *Enzymatically degradable nanogels by inverse miniemulsion copolymerization of acrylamide with dextran methacrylates as crosslinkers.* Polymer Chemistry, 2012. *3*(1): p. 204-216.
68. Blank, A., C. Dekker, G. Schieven, R. Sugiyama, and M. Thelen, *Human body fluid ribonucleases: detection, interrelationships and significance.* Nucleic Acids Symp Ser, 1981(10): p. 203-9.
69. Whitchurch, C.B., T. Tolker-Nielsen, P.C. Ragas, and J.S. Mattick, *Extracellular DNA required for bacterial biofilm formation.* Science, 2002. *295*(5559): p. 1487.
70. Voet, D., J.G. Voet, and C.W. Pratt, *Lehrbuch der Biochemie*. 2002: WILEY-VCH. 3-527-30519-X
71. Cherepanova, A., S. Tamkovich, D. Pyshnyi, M. Kharkova, V. Vlassov, and P. Laktionov, *Immunochemical assay for deoxyribonuclease activity in body fluids.* J Immunol Methods, 2007. *325*(1-2): p. 96-103.
72. Skalko-Basnet, N., *Biologics: the role of delivery systems in improved therapy.* Biologics, 2014. *8*: p. 107-14.

73. Gehl, J., *Drug and Gene Electrotransfer in Cancer Therapy*, in *Somatic Genome Manipulation: Advances, Methods, and Applications*, X.-Q. Li, J.D. Donnelly, and G.T. Jensen, Editors. 2015, Springer New York: New York, NY. p. 3-15.
74. de la Fuente, J.M., C.C. Berry, M.O. Riehle, and A.S. Curtis, *Nanoparticle targeting at cells.* Langmuir, 2006. *22*(7): p. 3286-93.
75. Matsumura, Y. and H. Maeda, *A new concept for macromolecular therapeutics in cancer chemotherapy: mechanism of tumoritropic accumulation of proteins and the antitumor agent smancs.* Cancer Res, 1986. *46*(12 Pt 1): p. 6387-92.
76. Kopecek, J. and R. Duncan, *Targetable Polymeric Prodrugs.* Journal of Controlled Release, 1987. *6*: p. 315-327.
77. Itoh, Y., M. Matsusaki, T. Kida, and M. Akashi, *Enzyme-responsive release of encapsulated proteins from biodegradable hollow capsules.* Biomacromolecules, 2006. *7*(10): p. 2715-2718.
78. Thornton, P.D., R.J. Mart, and R.V. Ulijn, *Enzyme-responsive polymer hydrogel particles for controlled release.* Advanced Materials, 2007. *19*(9): p. 1252-+.
79. Bodor, N. and J.W. Simpkins, *Redox delivery system for brain-specific, sustained release of dopamine.* Science, 1983. *221*(4605): p. 65-7.
80. Robinson, A.G., *DDAVP in the treatment of central diabetes insipidus.* N Engl J Med, 1976. *294*(10): p. 507-11.
81. Glazener, C.M. and J.H. Evans, *Desmopressin for nocturnal enuresis in children.* Cochrane Database Syst Rev, 2002(3): p. CD002112.
82. Schulman, S.L., A. Stokes, and P.M. Salzman, *The efficacy and safety of oral desmopressin in children with primary nocturnal enuresis.* J Urol, 2001. *166*(6): p. 2427-31.
83. Salzman, E.W., M.J. Weinstein, R.M. Weintraub, J.A. Ware, R.L. Thurer, L. Robertson, A. Donovan, T. Gaffney, V. Bertele, J. Troll, and et al., *Treatment with desmopressin acetate to reduce blood loss after cardiac surgery. A double-blind randomized trial.* N Engl J Med, 1986. *314*(22): p. 1402-6.
84. Richardson, D.W. and A.G. Robinson, *Desmopressin.* Ann Intern Med, 1985. *103*(2): p. 228-39.
85. Mannucci, P.M., *Desmopressin (DDAVP) in the treatment of bleeding disorders: the first 20 years.* Blood, 1997. *90*(7): p. 2515-21.
86. Di Mauro, F.M. and M.K. Holowaychuk, *Intravenous administration of desmopressin acetate to reverse acetylsalicylic acid-induced coagulopathy in three dogs.* J Vet Emerg Crit Care (San Antonio), 2013. *23*(4): p. 455-8.
87. Wademan, B.H. and S.D. Galvin, *Desmopressin for reducing postoperative blood loss and transfusion requirements following cardiac surgery in adults.* Interact Cardiovasc Thorac Surg, 2014. *18*(3): p. 360-70.
88. Sheridan, D.P., R.T. Card, J.C. Pinilla, S.M. Harding, D.J. Thomson, L. Gauthier, and D. Drotar, *Use of desmopressin acetate to reduce blood transfusion requirements during cardiac surgery in patients with acetylsalicylic-acid-induced platelet dysfunction.* Can J Surg, 1994. *37*(1): p. 33-6.

89. Teng, R., P.D. Mitchell, and K. Butler, *The effect of desmopressin on bleeding time and platelet aggregation in healthy volunteers administered ticagrelor.* J Clin Pharm Ther, 2014. *39*(2): p. 186-91.
90. Thews, G., E. Mutschler, and P. Vaupel, *Anatomie Physiologie Pathophysiologie des Menschen*. 5 ed. 1999: Wissenschaftliche Verlahgsgesellschaft mbH Stuttgart. 3-8047-1616-4
91. Patton, J.S. and R.M. Platz, *Penetration Enhancement for Polypeptides through Epithelia .D. Routes of Delivery - Case-Studies .2. Pulmonary Delivery of Peptides and Proteins for Systemic Action.* Advanced Drug Delivery Reviews, 1992. *8*(2-3): p. 179-196.
92. Gehr, P., M. Bachofen, and E.R. Weibel, *The normal human lung: ultrastructure and morphometric estimation of diffusion capacity.* Respir Physiol, 1978. *32*(2): p. 121-40.
93. Groneberg, D.A., C. Witt, U. Wagner, K.F. Chung, and A. Fischer, *Fundamentals of pulmonary drug delivery.* Respir Med, 2003. *97*(4): p. 382-7.
94. Sherman, M.P. and T. Ganz, *Host Defense in Pulmonary Alveoli.* Annual Review of Physiology, 1992. *54*: p. 331-350.
95. Edwards, D.A., J. Hanes, G. Caponetti, J. Hrkach, A. Ben-Jebria, M.L. Eskew, J. Mintzes, D. Deaver, N. Lotan, and R. Langer, *Large porous particles for pulmonary drug delivery.* Science, 1997. *276*(5320): p. 1868-71.
96. Hatch, T.F., *Distribution and deposition of inhaled particles in respiratory tract.* Bacteriol Rev, 1961. *25*: p. 237-40.
97. Yeates, D.B., N. Aspin, H. Levison, M.T. Jones, and A.C. Bryan, *Mucociliary tracheal transport rates in man.* Journal of Applied Physiology, 1975. *39*(3): p. 487-95.
98. Warheit, D.B. and M.A. Hartsky, *Role of alveolar macrophage chemotaxis and phagocytosis in pulmonary clearance responses to inhaled particles: comparisons among rodent species.* Microsc Res Tech, 1993. *26*(5): p. 412-22.
99. Sibille, Y. and H.Y. Reynolds, *Macrophages and polymorphonuclear neutrophils in lung defense and injury.* American Review of Respiratory Disease, 1990. *141*(2): p. 471-501.
100. Nathan, C.F., *Secretory products of macrophages.* J Clin Invest, 1987. *79*(2): p. 319-26.
101. Vollmar, A.D., T., *Immunologie - Grundlagen und Wirkstoffe*. 2005: Wissenschaftliche Verlagsgesellschaft mbH Stuttgart. 3-8047-2189-3
102. Brain, J.D., *Macrophages in the Respiratory Tract.* Comprehensive Physiology, 1985: p. 447-471.
103. Gonda, I., *The ascent of pulmonary drug delivery.* J Pharm Sci, 2000. *89*(7): p. 940-5.
104. Hussain, A., J.J. Arnold, M.A. Khan, and F. Ahsan, *Absorption enhancers in pulmonary protein delivery.* J Control Release, 2004. *94*(1): p. 15-24.
105. Duchardt, F., I.R. Ruttekolk, W.P. Verdurmen, H. Lortat-Jacob, J. Burck, H. Hufnagel, R. Fischer, M. van den Heuvel, D.W. Lowik, G.W. Vuister, A. Ulrich, M. de Waard, and R. Brock, *A cell-penetrating peptide derived from human lactoferrin with*

conformation-dependent uptake efficiency. Journal of Biological Chemistry, 2009. *284*(52): p. 36099-108.
106. Rau, J.L., *The inhalation of drugs: advantages and problems.* Respir Care, 2005. *50*(3): p. 367-82.
107. Anderson, P.J., *History of aerosol therapy: liquid nebulization to MDIs to DPIs.* Respir Care, 2005. *50*(9): p. 1139-50.
108. Rosner, F., *Moses Maimonides' treatise on asthma.* Thorax, 1981. *36*(4): p. 245-51.
109. Anderson, P.J., *Delivery options and devices for aerosolized therapeutics.* Chest, 2001. *120*(3 Suppl): p. 89S-93S.
110. Gruber-Gerardy. *Anmerkungen zur Geschichte Inhalationstherapie (Historische Höhepunkte)*. 2004 March 14t, 2016; Available from: https://www.respimat.de/respimat/geschichte.htm.
111. Elliott, H.L. and J.L. Reid, *The clinical pharmacology of a herbal asthma cigarette.* Br J Clin Pharmacol, 1980. *10*(5): p. 487-90.
112. Gansslen, M., *Über Inhalation von Insulin.* Klinische Wochenzeitschrift, 1925. *4*(2): p. 71.
113. Schreier, H., R.J. Gonzalezrothi, and A.A. Stecenko, *Pulmonary Delivery of Liposomes.* Journal of Controlled Release, 1993. *24*(1-3): p. 209-223.
114. Woolfrey, S.G., G. Taylor, I.W. Kellaway, and A. Smith, *Pulmonary absorption of liposome-encapsulated 6-carboxyfluorescein.* Journal of Controlled Release, 1988. *5*: p. 203-209.
115. Oyarzun, M.J., J.A. Clements, and A. Baritussio, *Ventilation enhances pulmonary alveolar clearance of radioactive dipalmitoyl phosphatidylcholine in liposomes.* Am Rev Respir Dis, 1980. *121*(4): p. 709-21.
116. Liu, F.Y., Z. Shao, D.O. Kildsig, and A.K. Mitra, *Pulmonary delivery of free and liposomal insulin.* Pharm Res, 1993. *10*(2): p. 228-32.
117. Vanbever, R., J.D. Mintzes, J. Wang, J. Nice, D.H. Chen, R. Batycky, R. Langer, and D.A. Edwards, *Formulation and physical characterization of large porous particles for inhalation.* Pharmaceutical Research, 1999. *16*(11): p. 1735-1742.
118. Food_and_Drug_Administration. *FDA Approves First Ever Inhaled Insulin Combination Product for Treatment of Diabetes*. 2006 04/082013 [cited 2016 02/11]; Available from: http://www.fda.gov/newsevents/newsroom/pressannouncements/2006/ucm108585.htm.
119. Morton-Eggleston, E. and E.J. Barrett, *Inhaled insulin.* BMJ, 2006. *332*(7549): p. 1043-4.
120. Food_and_Drug_Administration. *FDA approves Afrezza to treat diabetes*. 2014 06/30/2014 [cited 2016 02/11]; Available from: http://www.fda.gov/NewsEvents/Newsroom/PressAnnouncements/ucm403122.htm.
121. Palmer, E. *Sanofi and MannKind terminate Afrezza partnership*. 2016; Available from: http://www.fiercepharma.com/story/sanofi-and-mannkind-terminate-afrezza-partnership/2016-01-05.

122. Staton, T. *Sanofi tried and failed with Afrezza. Why does MannKind still think it can win?* 2016 [cited 2016 03/21/2016]; Available from: http://www.fiercepharma.com/story/sanofi-tried-and-failed-afrezza-why-does-mannkind-still-think-it-can-win/2016-02-10.
123. Smith, I.J. and M. Parry-Billings, *The inhalers of the future? A review of dry powder devices on the market today.* Pulm Pharmacol Ther, 2003. *16*(2): p. 79-95.
124. Weiss, B., U.F. Schaefer, J. Zapp, A. Lamprecht, A. Stallmach, and C.M. Lehr, *Nanoparticles made of fluorescence-labelled Poly(L-lactide-co-glycolide): preparation, stability, and biocompatibility.* J Nanosci Nanotechnol, 2006. *6*(9-10): p. 3048-56.
125. Bhattacharjee, S., *DLS and zeta potential - What they are and what they are not?* J Control Release, 2016. *235*: p. 337-51.
126. Walstra, P., V.A. Bloomfield, G.J. Wei, and R. Jenness, *Effect of chymosin action on the hydrodynamic diameter of casein micelles.* Biochim Biophys Acta, 1981. *669*(2): p. 258-9.
127. Malvern_Instruments_Ltd., *Zetasizer Nano ZS Manual*. 2007.
128. James, S.W., R.A. Lockey, D. Egan, and R.P. Tatam, *Fiber-Optic-Based Reference Beam Laser-Doppler Velocimetry.* Optics Communications, 1995. *119*(5-6): p. 460-464.
129. Peng, S.J. and R.A. Williams, *Controlled production of emulsions using a crossflow membrane part I: Droplet formation from a single pore.* Chemical Engineering Research & Design, 1998. *76*(A8): p. 894-901.
130. Jambrak, A.R., T.J. Mason, V. Lelas, Z. Herceg, and I.L. Herceg, *Effect of ultrasound treatment on solubility and foaming properties of whey protein suspensions.* Journal of Food Engineering, 2008. *86*(2): p. 281-287.
131. Chandrapala, J., B. Zisu, M. Palmer, S. Kentish, and M. Ashokkumar, *Effects of ultrasound on the thermal and structural characteristics of proteins in reconstituted whey protein concentrate.* Ultrason Sonochem, 2011. *18*(5): p. 951-7.
132. Colliex, C. and H. Kohl, *Elektronenmikroskopie: Eine anwendungsbezogene Einführung*. 1 ed. 2007: Wissenschaftliche Verlagsgesellschaft. 987-3804723993
133. International_Organization_for_Standardization *ISO 22412:2008*. 2008.
134. Esposito, S., K. Deventer, G. T'Sjoen, A. Vantilborgh, F.T. Delbeke, A.S. Goessaert, K. Everaert, and P. Van Eenoo, *Qualitative detection of desmopressin in plasma by liquid chromatography-tandem mass spectrometry.* Anal Bioanal Chem, 2012. *402*(9): p. 2789-96.
135. Arnold, R.R., M.F. Cole, and J.R. McGhee, *A bactericidal effect for human lactoferrin.* Science, 1977. *197*(4300): p. 263-5.
136. Orsi, N., *The antimicrobial activity of lactoferrin: current status and perspectives.* Biometals, 2004. *17*(3): p. 189-96.
137. Vladisavljevic, G.T., M. Shimizu, and T. Nakashima, *Preparation of monodisperse multiple emulsions at high production rates by multi-stage premix membrane emulsification.* Journal of Membrane Science, 2004. *244*(1-2): p. 97-106.

138. Sakagami, H., K. Asano, T. Yoshida, and Y. Kawazoe, *Organ distribution and toxicity of lignin.* In Vivo, 1999. *13*(1): p. 41-4.
139. Yallapu, M.M., B.K. Gupta, M. Jaggi, and S.C. Chauhan, *Fabrication of curcumin encapsulated PLGA nanoparticles for improved therapeutic effects in metastatic cancer cells.* J Colloid Interface Sci, 2010. *351*(1): p. 19-29.

Lebenslauf Daniel Primaveßy

Enthält persönliche Daten und ist nicht Bestandteil der Online-Veröffentlichung

---

-

-